

ผลลัพธ์ที่ได้จากโครงการ

1. ผลงานตีพิมพ์ในวารสารวิชาการนานาชาติ

1. Sirisriro, A., Ardseungneon, P., Vichasri-Grams, S., Grams, R., Tan-Ariya, P., Viyanant, V., Upatham, E.S. and Sobhon, P. 2002 Production and characterization of monoclonal antibody against recombinant fatty acid binding protein of *Fasciola gigantica*. *Veterinary Parasitology* 105:119-129. (Impact factor = 1.401)
2. Kruatrachue, M., Laimaek, P., Wanichanon, C., Linthong, V., Sretarugsa, P., Upatham, E.S. and Sobhon, P. 2002 Development of the nerve ganglia of abalone, *Haliotis asinina* Linnaeus. *Journal of Shellfish Research* 21:173-183. (Impact factor = 0.557)
3. Chaitheerayanon, K., Ardseungneon, P., Wanichanon, C., Vichasri-Grams, S., Grams, R., Viyanant, V., Upatham, E.S. and Sobhon, P. 2002 Production and characterization of monoclonal antibody against 28.5 kD tegumental antigen of *Fasciola gigantica*. *Acta Tropica* 84:1-8. (Impact factor = 1.045)
4. Khawsuk, W., Soonklang, N., Grams, R., Vichasri-Grams, S., Wanichanon, C., Meepool, A., Chaitheerayanon, K., Ardseungneon, P., Viyanant, V., Upatham, E.S. and Sobhon, P. 2002 Production and characterization of a monoclonal antibody against recombinant glutathione S-transferase (GST) of *Fasciola gigantica*. *Asian Pacific Journal of Allergy and Immunology* 20:257-266. (Impact factor = 0.179)
5. Manochantr, S., Sretarugsa, P., Wanichanon, C., Chavadej, J. and Sobhon, P. 2003 Classification of spermatogenic cells in *Rana tigerina* based on ultrastructure. *ScienceAsia* 29:247-260. (Impact factor = NA)
6. Weerachatanukul, W., Xu, H., Anupriwan, A., Carmona, E., Wade, M., Hermo, L., Silva da Maria, S., Rippstein, P., Sobhon, P., Sretarugsa, P. and Tanphaichitr, N. 2003 Acquisition of arylsulfatase A onto the mouse sperm surface during epididymal transit. *Biology of Reproduction* 69:1183-1192. (Impact factor = 3.646)
7. Panasophonkul, S., Sretarugsa, P., Anunruang, N., Apisawetakan, S., Saitongdee, P., Upatham, E.S., Poomtong, T., Hanna, J. P. and Sobhon, P. 2004 Serotonergic and FMRF-amidergic neurons in the nerve ganglia of *Haliotis asinina* Linnaeus. *Journal of Shellfish Research* 23:1087-1095. (Impact factor = 0.557)

8. Wanichanon, C., Laimek, P., Chitchulanon, N., Suphamungmee, W., Apisawetakan, S., Linthong, V., Sretarugsa, P., Kruatrachue, M., Upatham, E.S., Poomtong, T. and Sobhon, P. 2004 Sensory receptors on cephalic and epipodial tentacles of *Haliotis asinina* Linnaeus. *Journal of Shellfish Research* 23:1097-1106. (Impact factor = 0.557)
9. Wanichanon, C., Laimek, P., Linthong, V., Sretarugsa, P., Kruatrachue, M., Upatham, E.S., Poomtong, T. and Sobhon, P. 2004 Histology of hypobranchial glands and gills of *Haliotis asinina* Linnaeus. *Journal of Shellfish Research* 23:1107-1112. (Impact factor = 0.557)
10. Saitongdee, P., Rabintossaporn, P., Sretarugsa, P., Poomtong, T. and Sobhon, P. 2004 Aminopeptidase reactivity in the digestive tract of adult *Haliotis asinina* Linnaeus. *Journal of Shellfish Research* 23:1031-1035. (Impact factor = 0.557)
11. Meemon, K., Grams, R., Vichasri-Grams, S., Hofmann, A., Korge, G., Viyanant, V., Upatham, E.S., Habe, S. and Sobhon, P. 2004 Molecular cloning and analysis of stage and tissue specific expression of Cathepsin B encoding genes from *Fasciola gigantica*. *Molecular and Biochemical Parasitology* 136:1-10. (Impact factor = 2.803)
12. Eursitthichai, V., Viyanant, V., Vichasri-Grams, S., Sobhon, P., Tesana, S., Upatham, E.S., Hofmann, A., Korge, G. and Grams, R. 2004 Molecular cloning and characterization of a glutathione S-transferase encoding gene from *Opisthochis viverrini*. *Asian Pacific Journal of Allergy and Immunology* 22: 219-228. (Impact factor = 0.179)
13. Manochantr, S., Sretarugsa, P., Chavadej, J. and Sobhon, P. 2005 Chromatin organization and basic nuclear proteins in the male germ cells of *Rana tigerina*. *Molecular Reproduction and Development* 70:184-197. (Impact factor = 2.543)
14. Jiraungkoorskul, W., Sahaphong, S., Sobhon, P., Riengrojpitak, S. and Kangwanransan, N. 2005 Effects of praziquantel and artesunate on the tegument of adult *Schistosoma mekongi* harboured in mice. *Parasitology International* 54:177-183. (Impact factor = 1.083)
15. Meepool, A., Wanichanon, C., Viyanant, V. and Sobhon, P. 2005 Development and roles of vitelline cells in eggshell formation in *Fasciola gigantica*. *Invertebrate Reproduction and Development* (in press). (Impact factor = 0.879)

16. Tansatit, T., Sahaphong, S., Riengrojpitak, S., Viyanant, V., Upatham, E.S. and Sobhon, P. 2004 Immunolocalization of cytoskeletal components in the tegument of adult *Fasciola gigantica*. *Veterinary Parasitology* (submitted). (Impact factor = 1.401)
17. Pankao, V., Sirisriro, A., Grams, R., Vichasri-Grams, S., Meepool, A., Kangwanrangsang, N., Wanichanon, C., Ardseungneon, P., Viyanant, V., Upatham, E.S. and Sobhon, P. 2005 Classification of the parenchymal cells in *Fasciola gigantica* based on ultrastructure and their expression of fatty acid binding proteins (FABPs). *International Journal for Parasitology* (submitted). (Impact factor = 3.092)
18. Chaithirayanon, K., Grams, R., Vichasri-Grams, S., Hofmann, A., Korge, G., Viyanant, V., Upatham, E.S. and Sobhon, P. 2005 Molecular analysis of a 14-3-3 zeta class encoding gene in *Fasciola gigantica*. *Molecular and Biochemical Parasitology* (submitted). (Impact factor = 2.803)

2. การเสนอผลงานในที่ประชุมระดับนานาชาติ

1. Eursitthichai, V., Viyanant, V., Vichasri-Grams, S., Upatham, E.S., Grams, R., Sobhon, P., Tesana, S., Korge, G., Hofmann, A. 2001 Molecular cloning of protein-encoding genes from *Opisthorchis viverrini*. The 7th Chamlong-Tranakchit Harinasuta Lecture, Joint International Tropical Medicine Meeting 2001: 8-10 August 2001, Bangkok, Thailand, pp. 57.
2. Sobhon, P., Viyanant, V., Upatham, E.S., Vichasri-Grams, S., Grams, R., Ardseungneon, P., Meepool, A., Khawsuk, W., Chaiteerayanon, K., Pankao, V. and Meemon, K. 2002 Immunomicroscopic studies of the tissue sources and cellular synthesis of antigens in *Fasciola gigantica* that have immunodiagnostic and vaccine potential. 3rd Asean Microscopy Conference and 19th Annual Conference of EMST, January 30 - February 1, 2002; Chiang Mai, Thailand. pp. 33.
3. Pradittsataporn, S., Sretarugsa, P., Chavadej, J., Wanichanon, C. and Sobhon, P. 2002 Process of chromatin condensation during spermiogenesis in *Rana tigerina*. 3rd Asean Microscopy Conference and 19th Annual Conference of EMST, January 30 - February 1, 2002; Chiang Mai, Thailand. pp. 84.
4. Pankao, V., Khawsuk, W., Sirisriro, A., Grams, R., Vichasri-Grams, S., Ardseungneon, P., Meepool, A., Chaiteerayanon, K., Viyanant, V., Upatham, E.S., Tan-Ariya, P. and Sobhon, P. 2002 Localization and relative concentration of fatty acid binding proteins in *Fasciola gigantica*. 3rd Asean Microscopy Conference and 19th Annual Conference of EMST, January 30 - February 1, 2002; Chiang Mai, Thailand. pp. 216.
5. Soonklang, N., Khawsuk, W., Wanichanon, C., Meepool, A., Grams, R., Vichasri-Grams, S., Chaiteerayanon, K., Ardseungneon, P., Viyanant, V., Upatham, E.S. and

- Sobhon, P. 2002 Localization and relative concentration of glutathione S-transferase in *Fasciola gigantica*. 3rd Asean Microscopy Conference and 19th Annual Conference of EMST, January 30 - February 1, 2002; Chiang Mai, Thailand. pp. 217.
6. Meemon, K., Grams, R., Vichasri-Grams, S., Hofmann, A., Korge, G., Viyanant, V. and Sobhon, P. 2002 The expression of cathepsin L gene in the tissues of adult *F. gigantica* as detected by in situ hybridization. 3rd Asean Microscopy Conference and 19th Annual Conference of EMST, January 30 - February 1, 2002; Chiang Mai, Thailand. pp. 218.
 7. Khawsuk, W., Kangwanrangsang, N., Pankao, V., Soonklang, N., Meepool, A., Grams, R., Vichasri-Grams, S., Ardseungneon, P., Viyanant, V., Upatham, E.S. and Sobhon, P. 2002 Scanning microscopic study of damage on the tegumental surface of *F. gigantica* by monoclonal antibodies against recombinant fatty acid binding protein (FABP), and recombinant glutathione-S-transferase (GST). 3rd Asean Microscopy Conference and 19th Annual Conference of EMST, January 30 - February 1, 2002; Chiang Mai, Thailand. pp. 219.
 8. Saitongdee, P., Anupunpisit, V., Rabintossaporn, P. and Sobhon, P. 2002 Immunohistochemical localization of multiple hormones in the cerebral ganglia of a tropical abalone, *Haliotis asinina* (Linnaeus). 3rd Asean Microscopy Conference and 19th Annual Conference of EMST, January 30 - February 1, 2002; Chiang Mai, Thailand. pp. 220.
 9. Rabintossaporn, P., Saitongdee, P., Chitramwong, Y. and Sobhon, P. 2002 Aminopeptidase reactivity in the digestive tract of the adult tropical abalone, *Haliotis asinina* Linnaeus. 3rd Asean Microscopy Conference and 19th Annual Conference of EMST, January 30 - February 1, 2002; Chiang Mai, Thailand. pp. 221.
 10. Panasophonkul, S., Wanichanon, C., Sretarugsa, P., Chavadej, C., Kruatrachue, M. and Sobhon, P. 2002 Spermatogenesis and chromatin condensation in the male germ cells of a marine Oyster, *Saccostrea forskali* Gmelin. 3rd Asean Microscopy Conference and 19th Annual Conference of EMST, January 30 - February 1, 2002; Chiang Mai, Thailand. pp. 222.
 11. Wanichanon, C., Pankao, V., Sretarugsa, P., Kruatrachue, M. and Sobhon, P. 2002 Spermatogenesis and chromatin condensation in the male germ cells of the giant african snail, *Achatina fulica* Bowdich. 3rd Asean Microscopy Conference and 19th Annual Conference of EMST, January 30 - February 1, 2002; Chiang Mai, Thailand. pp. 223.
 12. Apisawetakan, S., Weerachatanukul, W., Panasophonkul, S., Sretarugsa, P., Wanichanon, C., Kruatrachue, M., Upatham, E.S. and Sobhon, P. 2002 The process of chromatin condensation during spermiogenesis in a tropical abalone, *Haliotis asinina* Linnaeus. 3rd Asean Microscopy Conference and 19th Annual Conference of EMST, January 30 - February 1, 2002; Chiang Mai, Thailand. pp.224.

13. Palasoon, R., Chavadej, J., Praditsataporn, S., Sretarugsa, P. and Sobhon, P. 2002 Spermatogenesis in the African catfish, *Clarias gariepinus*. 3rd Asean Microscopy Conference and 19th Annual Conference of EMST, January 30 - February 1, 2002; Chiang Mai, Thailand. pp. 225.
14. Suphamungmee, W., Wanichanon, C., Weerachathanukul, W., Sretarugsa, P. and Sobhon, P. 2002 Spermatogenesis and chromatin condensation in the male germ cells of a common tree shrew, *Tupaia glis*. 3rd Asean Microscopy Conference and 19th Annual Conference of EMST, January 30 - February 1, 2002; Chiang Mai, Thailand. pp. 228.
15. Eursittichai, V., Grams, R., Vichasri-Grams, S., Sobhon, P., Upatham, E.S., Tesana, S., Hofmann, A., Korge, G., Viyanant, V. 2002 Molecular cloning and characterization of glutathione-S-transferase and vitelline B egg shell precursor protein encoding genes from *Opisthorchis viverrini*. The 8th Chamlong-Tranakchit Harinasuta Lecture, Joint International Tropical Medicine Meeting 2002, 20-22 November, 2002 Bangkok, Thailand. pp. 232.
16. Ruangsittichai, J., Viyanant, V., Vichasri-Grams, S., Grams, R., Tesana, S., Korge, G., Hofmann, A., Sobhon, P. 2002 Immunoscreeing of a cDNA library and analysis of isolated excretory-secretory protein encoding genes from a liver fluke, *Opisthorchis viverrini*. The 8th Chamlong-Tranakchit Harinasuta Lecture, Joint International Tropical Medicine Meeting 2002, 20-22 November, 2002 Bangkok, Thailand. pp. 234.
17. Wanichanon, C., Laimek, P., Apisawetakan, S., Chitchulanon, N., Suphamungmee, W., Viyanant, V., Kruatrachue, M., Upatham, E.S. and Sobhon, P. 2003 Sensory receptors on cephalic and epipodial tentacles of *Haliotis asinina* Linnaeus. The 5th International Abalone Symposium, Ocean University of China, 12-17 October, 2003 Qingdao, China. pp. 148.
18. Rabintossaporn, P., Saitongdee, P., Sretarugsa, P. and Sobhon, P. 2003 Aminopeptidase reactivity in the digestive tract of an adult *Haliotis asinina* Linnaeus. The 5th International Abalone Symposium, Ocean University of China, 12-17 October, 2003 Qingdao, China. pp. 149.
19. Panasophonkul, S., Sretarugsa, P., Apisawetakan, S., Weerachathanukul, W., Upatham, E.S., Hanna P.J. and Sobhon, P. 2003 Serotonergic neurons in the nerve ganglion of *Haliotis asinina* Linnaeus. The 5th International Abalone Symposium, Ocean University of China, 12-17 October, 2003 Qingdao, China. pp. 150.
20. Saitongdee, P., Apisawetakan, S., Hanna, P.J. and Sobhon, P. 2003 Egg-laying hormone immunoreactivity in the nervous ganglia and reproductive organ of Thai abalone, *Haliotis asinina* Linnaeus. The 5th International Abalone Symposium, Ocean University of China, 12-17 October, 2003 Qingdao, China. pp. 158.
21. Suphamungmee, W., Weerachathanukul, W., Panasophonkul, S., Chitchulanon, N., Apisawetakan, S., Anunruang, N., Wanichanon, C., Sretarugsa, P., Upatham, E.S. and Sobhon, P. 2003 Detection of neurotransmitters and endocrine substances in

- the nervous and gonadal tissues of *Haliotis asinina* Linnaeus by immunoassay. The 5th International Abalone Symposium, Ocean University of China, 12-17 October, 2003 Qingdao, China. pp. 72.
22. Saitongdee, P., Pisetpaisan, K., Apisawetakan, S., Anunruang, N., Poomthong, T., Hanna P.J. and Sobhon, P. 2004 Immunolocalization of egg-laying hormone, growth hormone, and insulin-like hormone in the neural ganglia and gonads of *Haliotis asinina* (Linnaeus). The 8th Asia-Pacific Conference on Electron Microscopy (8 APEM) in conjunction with the 60th Annual Meeting of the Japanese Society of Microscopy, 7-11 June, 2004 Kanazawa, Japan. pp. 74.
 23. Anupriwan, A., Weerachatanukul, W., Xu, H., Chakrabandhul, K., Wede, M., Carmona, E., Hermo, L., Silva, SM., Sobhon, P., Tanphaichitr, N., Sretarugsa, P. 2004 Acquisition of arylsulfatase-A (AS-A) onto the mouse sperm surface during epididymal transit and its role in cumulus cell oocyte complex (COC) dispersion. The 8th Asia-Pacific Conference on Electron Microscopy (8 APEM) in conjunction with the 60th Annual Meeting of the Japanese Society of Microscopy, 7-11 June, 2004 Kanazawa, Japan. pp. 94.
 24. Wanichanon, C., Lalmeek, P., Chitchulanon, N., Linthong, V., Kruatrachue, M., Poomtong, T. and Sobhon, P. 2004 Distribution of GABAergic neurons and fibers in nervous system of *Haliotis asinina* Linnaeus. The 8th Asia-Pacific Conference on Electron Microscopy (8 APEM) in conjunction with the 60th Annual Meeting of the Japanese Society of Microscopy, 7-11 June, 2004 Kanazawa, Japan. pp. 119.
 25. Sretarugsa, P., Panasophonkul, S., Anunruang, N., Apisawetakan, S., Saitongdee, P., Upathum, E.S., Poomtong, T., Hanna, P.J. and Sobhon, P. 2004 Serotonergic and FMRF-amidergic neurons in the nerve ganglia of *Haliotis asinina* Linnaeus. The 8th Asia-Pacific Conference on Electron Microscopy (8 APEM) in conjunction with the 60th Annual Meeting of the Japanese Society of Microscopy, 7-11 June, 2004 Kanazawa, Japan. pp. 120.

3. รหัสพันธุกรรมในฐานข้อมูล NCBI 14 รายการ

Accession no AY227673: *Fasciola gigantica* cathepsin B (cat-B1) mRNA

Accession no AY227674: *Fasciola gigantica* cathepsin B (cat-B2) mRNA

Accession no AY227675: *Fasciola gigantica* cathepsin B (cat-B3) mRNA

Accession no AF112566: *Fasciola gigantica* cathepsin L (cat L 1 A) mRNA

Accession no AF239264: *Fasciola gigantica* cathepsin L (cat L 1 B) mRNA

Accession no AF239265: *Fasciola gigantica* cathepsin L (cat L 1 C) mRNA

Accession no AF239266: *Fasciola gigantica* cathepsin L (cat L 1 D) mRNA

Accession no AF239267: *Fasciola gigantica* cathepsin L (cat L 1 E) mRNA

Accession no AF239268: *Fasciola gigantica* cathepsin L (cat L 1 F) mRNA

Accession no AF419329: *Fasciola gigantica* cathepsin L (cat L 1 G) mRNA

Accession no AY428949: *Fasciola gigantica* cathepsin L (cat L 1 H) mRNA

Accession no AF112568: *Fasciola gigantica* fatty acid binding (fabp-1) mRNA

Accession no AF112567: *Fasciola gigantica* glutathione S-transferase (gst-1) mRNA

Accession no AY878648: *Fasciola gigantica* 14-3-3 protein (Fg14-3-3) mRNA

4. นักวิจัยในโครงการที่ได้รับทุนอื่นในระหว่างรับทุนส่งเสริมกลุ่มวิจัย

1. รศ. ดร. สุขศิริ วิชาศรี กรามส์ และ Dr. Hans Rudi Grams ได้รับทุนวิจัยในฐานะผู้วิจัยร่วม (Co-Principal Investigators) กับ ศ. วิฑูรย์ ไวยนันท์ ที่ปรึกษาโครงการ 3 เรื่อง คือ

1.1 เรื่อง Diagnosis and Vaccination: A combined study to detect and prevent infections with *Fasciola gigantica* (tropical liver fluke) by DNA-based technology
ทุนอุดหนุนจากงบประมาณแผ่นดิน ผ่านมหาวิทยาลัยธรรมศาสตร์ จำนวนเงิน 3,049,200.00 บาท ระยะเวลาการวิจัย พ.ศ. 2544-46

1.2 เรื่อง *Opisthorchis viverrini*: Molecular cloning of antigens encoding genes and immunological analysis of encoded proteins for diagnosis of opisthorchiasis
ทุนอุดหนุนจากงบประมาณแผ่นดิน ผ่านมหาวิทยาลัยธรรมศาสตร์ จำนวนเงิน 3,937,116.00 บาท ระยะเวลาการวิจัย พ.ศ. 2545-47

1.3 เรื่อง การใช้กระบวนการแบบบูรณาการเพื่อการวินิจฉัย และผลิตวัคซีนสำหรับควบคุมโรคพยาธิใบไม้ในตับคนและสัตว์เลี้ยงในประเทศไทย
ทุนอุดหนุนจากโครงการส่งเสริมการเพิ่มสมรรถนะ และขีดความสามารถในการ แข่งขันระหว่างประเทศ ทบวงมหาวิทยาลัย จำนวนเงิน 4,080,000.00 บาท ระยะเวลาการวิจัย พ.ศ. 2546-2547

2. รศ. ดร. ประพีร์ เศรษฐรักษ์ ได้รับทุนในฐานะหัวหน้าโครงการวิจัย 2 เรื่อง

2.1 เรื่อง การศึกษาการสร้างและการพัฒนาที่สมบูรณ์ของเซลล์สืบพันธุ์ของหนูพุกใหญ่
ทุนอุดหนุนจากสำนักงานกองทุนสนับสนุนการวิจัย (สกว.) จำนวนเงิน 300,000.00 บาท ระยะเวลาการวิจัย พ.ศ. 2544-45

2.2 เรื่อง Localization of Arylsulfatase-A (AS-A) in male and female reproductive tract and its role in fertilization
ทุนอุดหนุนจากสำนักงานกองทุนสนับสนุนการวิจัย (สกว.) จำนวนเงิน 300,000.00 บาท ระยะเวลาการวิจัย พ.ศ. 2545-2546

5. การผลิตบุคลากรและนักวิจัย

5.1 นักวิจัยรุ่นใหม่ที่ได้รับทุนพัฒนาศักยภาพการทำงานของอาจารย์รุ่นใหม่ของ สกว.-สกอ. ที่อยู่ภายใต้การดูแล (mentorship) ของหัวหน้าโครงการ จำนวน 6 คน คือ

ผศ. ดร. พรจันท์ สายทองดี	ม.มหิดล
ผศ. ดร. อุราพร วงศ์วีชรานนท์	ม.สงขลานครินทร์
ผศ. ดร. ประเสริฐ มีรัตน์	ม.บูรพา
ดร. เสมอ ถาน้อย	ม.นเรศวร
ดร. สุทิสสา ถาน้อย	ม.นเรศวร
ดร. วรณีย์ จีระอังกูรสกุล	ม.มหิดล

5.2 นักศึกษาระดับบัณฑิตที่จบการศึกษาจากโครงการ

5.2.1 ระดับปริญญาโท 5 คน

น.ส. พรรณี ระบิลทศพร
นาย ธรรงค์ พลະศุณย์
น.ส. นันทวรรณ ศูนย์กลาง
น.ส. ณัฐพิรา จิตต์จุฬานนท์
น.ส. นฤมล อนันต์เรือง

5.2.2 ระดับปริญญาเอก 5 คน

น.ส. สมใจ อภิเศกตกานต์
นาย ไกร มีมล
นาย อาดุลย์ มีพูล
น.ส. อารยา อนุไพรวรรณ
น.ส. กุลธิดา ชัยธีระยานนท์

6. ผลลัพธ์ที่ได้ซึ่งมีโอกาสนำไปประยุกต์ในเชิงพาณิชย์หรือเชิงสาธารณะในอนาคต

6.1 ในโครงการที่ศึกษา “พยาธิชีววิทยาการสังเคราะห์และวิเคราะห์คุณลักษณะของแอนติเจนและยีนของพยาธิใบไม้ตับ *Fasciola gigantica*” มี cDNA ที่สังเคราะห์และเก็บรักษาไว้ได้ 4 กลุ่ม คือ Cathepsin B1, B2, B3, Cathepsin L1A, L1B, L1C, L1D, L1E, L1F, L1G, L1H, Fatty Acid Binding Protein (FABP), Glutathione S-transferase (GST) (ดูข้อมูลจากฐานข้อมูล NCBI ที่แนบมา) cDNA บางตัว (GST, CAT L1A) ได้ถูก expressed เป็น recombinant proteins แล้ว โดยระบบ prokaryotic cells (*E. coli*) และที่เห็ด (Cat B, FABP) กำลังพยายาม express ใน

eukaryotic cells (Yeast) เมื่อเสร็จสิ้นโครงการนี้แล้วหวังว่าจะได้นำ cDNA clones ต่าง ๆ เหล่านี้และ recombinant proteins ที่ได้ไปทดสอบประสิทธิภาพการเป็น vaccines ในสัตว์ใหญ่ (วัว, ควาย) นอกจากนั้นยังได้ผลิตและเก็บรักษาเซลล์ hybridoma ที่ผลิต monoclonal antibodies ต่อ Cat L, GST และ FABP กับต่อแอนติเจนจากชั้นผิวที่ molecular weight 28.5 kDa monoclonal antibodies และ recombinant proteins ที่ผลิตได้จะถูกนำไปพัฒนาชุดตรวจสอบการติดเชื้อต่อไปซึ่งจำเป็นต้องขอทุนสนับสนุนจากองค์การให้ทุนวิจัย เช่น สกว. ต่อ หรือจากองค์กรภาคเอกชนที่สนใจทั้งนี้เพื่อให้เกิดความต่อเนื่องของงานซึ่งจะสามารถนำไปประยุกต์ใช้ในภาคสนามโดยความร่วมมือกับสถาบันผลิตสัตว์และสุขภาพสัตว์ กรมปศุสัตว์ ต่อไป

- 6.2 ในโครงการที่ศึกษา "การควบคุมกระบวนการสร้างและหลังเซลล์สืบพันธุ์โดยประสาทฮอริโมนในหอยเป่าฮื้อ" สามารถสังเคราะห์และเก็บรักษา cDNA ของ Abalone egg laying hormone (aELH) ไว้ได้ ซึ่งสามารถ express เป็น recombinant ELH ได้แล้ว ขณะนี้กำลังทำการทดสอบประสิทธิภาพในการกระตุ้นการหลังเซลล์สืบพันธุ์จากหอยพ่อแม่พันธุ์ โดยประสานงานกับกลุ่มวิจัยของ นายธนศ พุ่มทอง ศูนย์วิจัยและพัฒนาประมงชายฝั่งประจวบคีรีขันธ์ กรมประมง ต. คลองวาฬ จ.ประจวบคีรีขันธ์ เมื่อได้ผลแล้วก็น่าจะพัฒนาเป็นชุดน้ำยาที่สามารถนำไปฉีดกระตุ้นการตกไข่และปล่อยอสุจิจากหอยเป่าฮื้อแม่พันธุ์และพ่อพันธุ์ได้ ส่วนการศึกษาเกี่ยวกับสารสื่อประสาท GABA (γ -aminobutyric acid) และโมเลกุลที่เกี่ยวข้องที่พบว่ากระจายอยู่ทั่วไปใน neurosecretory cells ของปมประสาท ในเซลล์รับรู้สัมผัสที่หน่วยรับซึ่งอยู่ในหนวด (tentacles) และในเนื้อเยื่อของอวัยวะสืบพันธุ์โดยเฉพาะรังไข่ นั้น น่าจะนำไปใช้ประโยชน์ในการกระตุ้นเพื่อเพิ่มประสิทธิภาพการลงเกาะและการกลายสภาพ (settlement, metamorphosis) และการอยู่รอด (survival) ของตัวอ่อนหอยเป่าฮื้อ อันจะเป็นประโยชน์ในการเพิ่มผลผลิตหอยในการเพาะเลี้ยงเชิงพาณิชย์อย่างมาก ซึ่งต้องร่วมงานวิจัยและการทดสอบกับคณะวิจัยจากกรมประมงดังกล่าวมาแล้วต่อไป เมื่อได้ผลแล้วก็จะนำไปใช้ประโยชน์โดยเฉพาะการนำวิธีนี้เผยแพร่สู่เกษตรกรผู้เพาะเลี้ยงหอยเป่าฮื้อโดยผ่านศูนย์วิจัยและพัฒนาประมงฯต่อไป ซึ่งจำเป็นต้องมีการขอทุนทำวิจัยไม่ให้ขาดตอน เพื่อจะได้พัฒนาวิธีที่เหมาะสมที่สุดในการเคลือบสารดังกล่าวลงบนแผ่นพลาสติกที่ล่อให้หอยตัวอ่อนลงเกาะ แล้วนำเอาไปใช้เพิ่มผลผลิตเพื่อการเพาะเลี้ยงเชิงพาณิชย์ต่อไป

ภาคผนวก

ผลงานตีพิมพ์ในวารสารวิชาการนานาชาติ



ELSEVIER

Veterinary Parasitology 105 (2002) 119–129

veterinary
parasitology

www.elsevier.com/locate/vetpar

Production and characterization of a monoclonal antibody against recombinant fatty acid binding protein of *Fasciola gigantica*

A. Sirisriro^a, R. Grams^d, S. Vichasri-Grams^b, P. Ardseungneon^b,
V. Pankao^c, A. Meepool^c, K. Chaithirayanon^c, V. Viyanant^{b,d},
P. Tan-Ariya^a, E.S. Upatham^b, P. Sobhon^{c,*}

^a Faculty of Science, Department of Microbiology, Mahidol University, RamaVI Road, Bangkok 10400, Thailand

^b Faculty of Science, Department of Biology, Mahidol University, RamaVI Road, Bangkok 10400, Thailand

^c Faculty of Science, Department of Anatomy, Mahidol University, RamaVI Road, Bangkok 10400, Thailand

^d Faculty of Allied Health Science, Thammasat University, Phahonyothin Road,
Klongluang, Pathumthani 12120, Thailand

Received 7 August 2001; received in revised form 30 November 2001; accepted 14 December 2001

Abstract

In *Fasciola* parasites fatty acid binding proteins (FABPs) are the carrier proteins that help in the uptake of fatty acids from the hosts' fluids. Attempts have been made to utilize both native and recombinant FABP (rFABP) for immunodiagnosis and vaccine development for fasciolosis. In this study, we have produced a number of monoclonal antibodies (MoAbs) against rFABP of *Fasciola gigantica*. These MoAbs were initially screened against rFABP by ELISA and then tested for their specificities by immunoblotting. Five stable clones were selected and characterized further: four of them were of the isotype IgG₁ while one clone was IgG_{2a}. All the MoAbs reacted with rFABP which has a molecular weight (MW) of 20 kD and with at least two isoforms of native proteins at MW 14.5 kD that were present in the tegumental antigen (TA) and crude worm extracts, and the excretion–secretion materials. Immunoperoxidase staining of frozen sections of adult parasites by using these MoAbs as primary antibodies indicated that FABP were present in high concentration in the parenchymal cells and reproductive tissues, in low concentration in the tegument and caecal epithelium. All MoAbs cross-reacted with a 14.5 kD antigen present in the whole body (WB) extract of *Schistosoma mansoni*, while no cross-reactivities were detected with antigens from *Eurytrema pancreaticum* and *Paramphistomum* spp. © 2002 Elsevier Science B.V. All rights reserved.

Keywords: *Fasciola gigantica*; Fatty acid binding protein; Monoclonal antibody; Localization; Cross-reaction; Immunology

*Corresponding author. Tel.: +66-2-245-5198; fax: +66-2-247-9880.
E-mail address: sepso@mahidol.ac.th (P. Sobhon).

0304-4017/02/\$ – see front matter © 2002 Elsevier Science B.V. All rights reserved.
PII: S0304-4017(02)00007-9

1. Introduction

Trematode parasites are unable to synthesize de novo most of their lipids particularly long chain fatty acids and cholesterol (Meyer et al., 1970). Therefore, they have to depend on fatty acid binding proteins (FABPs) for the uptake and transport of these molecules from the host. Phylogenetically, parasite FABPs appear to be related to those appearing in vertebrate tissues including heart, mammary gland, muscle, with about 30% identity at the amino acid level, although no clear functional relationships have been established (Esteves et al., 1997; Moser et al., 1991). Recently, *Fasciola hepatica* FABP (Fh12) and *Schistosoma mansoni* FABP (Sm15) have been shown to elicit a strong cross-protective immunity (Hillyer, 1985; Hillyer et al., 1988a). Mice vaccinated with purified Fh12 prior to challenging with *S. mansoni* cercariae displayed a 77% reduction in the worm burden (Hillyer et al., 1988b). In addition, Fh12 was found to be expressed in *F. hepatica* early after excystment through to the adult stage (Rodríguez-Pérez et al., 1992). However, due to the limitation in obtaining sufficient quantity of native FABP as antigen for vaccination, attempts to produce recombinant FABP (rFABP) of *F. hepatica* (Fh15) have been made. This recombinant protein has been shown to induce a significant level of resistance in hosts to challenges with *F. hepatica* (Muro et al., 1997) and *S. bovis* (Abane et al., 2000).

In comparison to *F. hepatica*, there have only been few studies on the cloning and vaccine potential of *F. gigantica* FABP (Estuningsih et al., 1997; Smooker et al., 1997). Since a large amount of the highly purified native FABP is difficult to obtain, in the present investigation we have generated recombinant *F. gigantica* FABP by molecular cloning, and attempted to produce and characterize monoclonal antibodies (MoAbs) against this protein. These MoAbs were used to immunolocalize FABP in *F. gigantica* tissues, and their cross-reactivities with other trematode parasite antigens were tested in order to probe for their possible applications in immunodiagnosis and vaccine development.

2. Materials and methods

2.1. Parasite samples

Adult *F. gigantica* were removed from the bile ducts and gall bladders of condemned bovine livers at local slaughterhouses. Other trematode parasites collected from the same group of cattle for a cross-reaction study included *Paramphistomum* spp. from the rumen and *Eurytrema pancreaticum* from the pancreas. *S. mansoni* were collected for the cross-reaction study from mice infected with cercariae 8 weeks earlier. All parasite specimens were washed three times with Hank's balanced salt (HBS) solution containing 100 U/ml penicillin and 100 mg/ml streptomycin to remove all traces of blood, bile and contaminating microorganisms.

2.2. Excretory–secretory (ES) antigens of adult *F. gigantica*

The ES antigens were prepared by incubating freshly collected, living adult parasites in HBS (Gibco, USA) at room temperature for 3 h. The parasite eggs in the culture medium

were removed by centrifugation at $5000\times g$ for 20 min at 4 °C. The supernatant was dialysed using Spectra/Por 1 dialysis membrane (Thomas Scientific, USA) with molecular weight (MW) cut off at 6–8 kDa, in 0.01 M PBS, pH 7.2 at 4 °C for 24 h, lyophilized, and kept at –20 °C until used.

2.3. Tegumental antigens (TA) of adult *F. gigantica*

TA antigen was obtained by extraction of live adult parasites with 1% Triton X-100 in Tris–HCl buffer, pH 8, for 30 min at room temperature. The extracting solution was collected and centrifuged at $5000\times g$ for 20 min at 4 °C to remove the parasite eggs which may be released during the extraction. The supernatant containing TA antigen was collected and dialysed using Spectra/Por 1 membrane in 0.01 M phosphate buffer saline (PBS), pH 7.2 at 4 °C for 24 h, before it was lyophilized and kept at –20 °C until used.

2.4. Whole body (WB) antigens of parasites

Whole adult parasites (*F. gigantica* and other trematodes) were homogenized in 0.01 M PBS, pH 7.2 and extracted overnight with continuous rotation at 4 °C. The suspensions were centrifuged at $5000\times g$, 4 °C, for 20 min and the supernatants were collected and stored at –70 °C until used in subsequent experiments.

The protein contents of all fractions were determined by modified Lowry's method (Lowry et al., 1951).

2.5. Preparation of *F. gigantica* rFABP

A 399 bp cDNA fragment encoding an FABP of *F. gigantica* was cloned by RT-PCR (Grams et al., 2000). The fragment was subsequently cut by *Bam*HI and *Sal*I restriction enzymes from pBluescript SK(-) (Stratagene) and subcloned in the bacterial expression vector pQE30 (QIAGEN). The cloning procedure resulted in the addition of 19 amino acids at the N-terminus including a six-residue histidine stretch for purification. At the C-terminus, another 14 amino acids were added to the rFABP. The calculated MW of rFABP is 18.5 kDa. Upon induction by IPTG (1 mM) rFABP was detected by SDS–PAGE analysis in the insoluble protein fraction. It was, therefore, purified by Ni-NTA chromatography under denaturing conditions in 6 M urea following the instructions of the manufacturer (QIAexpressionist, QIAGEN). The eluted protein fractions were analyzed by SDS–PAGE, and FABP-containing fractions were combined and dialyzed against PBS buffer.

2.6. Production of MoAbs against *F. gigantica* rFABP

BALB/c mice were immunized subcutaneously with *F. gigantica* rFABP in complete Freund's adjuvant at a dose of 10 µg in 100 µl per mouse. The second injection of a similar dose of the recombinant protein in incomplete Freund's adjuvant was given 3 weeks later. A final boost of 20 µg of protein in 100 µl PBS was given intravenously 2 weeks later. Hybridomas were produced by fusion of spleen cells from BALB/c mice immunized with

F. gigantica rFABP and mouse myeloma cells (P3/x63-Ag8). The hybridoma cells that grew successfully in culture were cloned by limiting dilution methods. Only the hybridoma clones that produced high titers of antibodies against rFABP, as screened by indirect ELISA, were selected. The antibody isotypes were determined by ELISA using the Mouse MonoAb-ID kit (ZYMED Laboratories, USA).

2.7. Immunoblotting

Immunoblotting was performed as described previously by Viyanant et al. (1993). Briefly, rFABP, TA, ES, and WB antigens were separated in 12.5% SDS-PAGE and blotted onto a nitrocellulose membrane. As positive controls, the antigenic bands in each fraction were detected by cattle-infected sera (CIS) obtained from the pooled sera of naturally infected animals. Strips containing similar antigenic fractions were also screened by MoAbs. For negative controls, the culture fluid (CF) and normal mouse serum (NMS) were used as probes. Cattle antibodies that reacted with the antigenic molecules were detected by peroxidase-conjugated rabbit anti-bovine immunoglobulin, whereas the monoclonal antibody-antigen complexes were detected by peroxidase-conjugated rabbit anti-mouse IgG. The reaction was visualized by further incubation in 3,3'-diaminobenzidine (3,3'-DAB) and H₂O₂.

2.8. Immunolocalization of FABP

The five MoAbs were used for an analysis of the distribution, and relative concentration of FABP in the frozen and acetone-fixed sections of adult *F. gigantica* by immunoperoxidase/3,3'-DAB staining. Endogenous peroxidase activity was destroyed by pretreating the tissue sections with 3% H₂O₂. The positive reaction was demonstrated by avidin-biotin-peroxidase technique as previously described by Viyanant et al. (1993). CIS diluted at 1:50 and 10% fetal calf serum were used as positive and negative controls, respectively.

3. Results

3.1. Monoclonal antibodies

Five clones of MoAbs against rFABP of *F. gigantica*, namely 3D4-12, 3D8-1, 3D8-8, 5C5-1 and 6F3-2, were produced. Four of them, 3D4-12, 3D8-1, 3D8-8 and 5C5-1 were found to be IgG₁, while only 6F3-2 was IgG_{2a}. All MoAbs were κ light chain. Clone 6F3-2 had the highest titer (up to 2.02 in ELISA OD reading at 492 nm with the cut off point at 0.5).

3.2. Immunoblotting

The immunoblotting experiment indicated that all MoAbs reacted with a single band of rFABP which has a MW of 20 kD (Fig. 1A). However, when tested against WB TA and ES antigens from adult *F. gigantica*, these MoAbs reacted with native FABP which appeared as a close double band at MW 14.5 kD (Figs. 1B and 2A). When similar antigenic fractions were analysed with polyclonal antibodies against native FABP (kindly given by

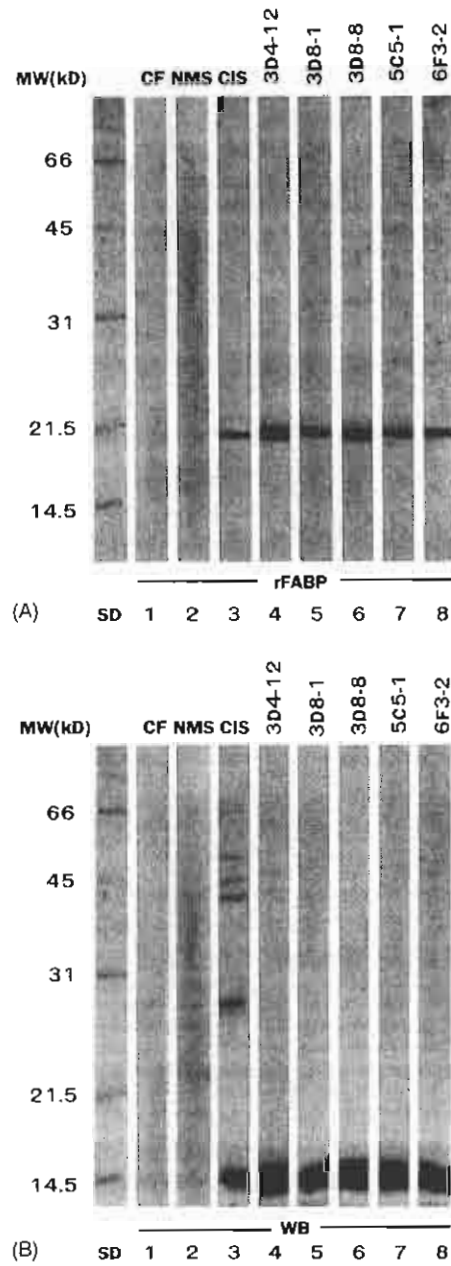


Fig. 1. (A) Immunoblotting patterns of rFABP reacted with myeloma CF (lane 1), NMS (lane 2), CIS (lane 3), MoAb 3D4-12 (lane 4), 3D8-1 (lane 5), 3D8-6 (lane 6), 5C5-1 (lane 7) and 6F3-2 (lane 8). SD is the lane containing standard MWs. (B) Immunoblotting patterns of *F. gigantica* WB antigens reacted with myeloma CF (lane 1), NMS (lane 2), CIS (lane 3), MoAb 3D4-12 (lane 4), 3D8-1 (lane 5), 3D8-6 (lane 6), 5C5-1 (lane 7) and 6F3-2 (lane 8).

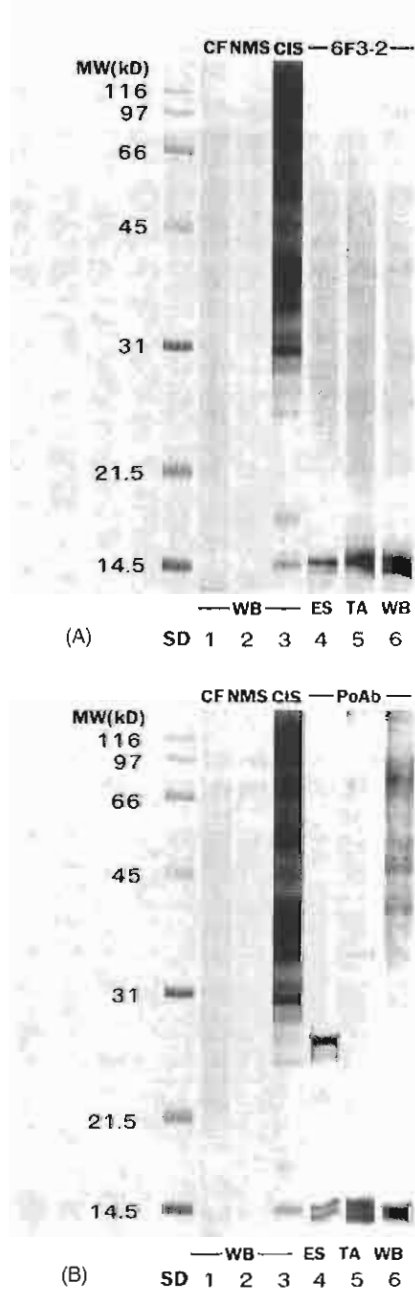


Fig. 2. (A) Immunoblotting patterns of *F. gigantica* WB antigens reacted with myeloma CF (lane 1), NMS (lane 2), CIS (lane 3), ES (lane 4), TA (lane 5) and WB (lane 6) antigens blotted with MoAb clone 6F3-2. Other clones of MoAb showed similar pattern and were not shown. (B) Immunoblotting pattern of WB antigens with CF (lane 1), NMS (lane 2), CIS (lane 3), ES (lane 4), TA (lane 5) and WB (lane 6) antigens with polyclonal antibodies against native FABP.

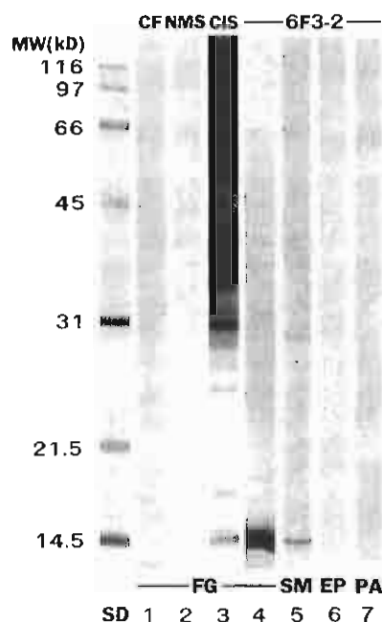


Fig. 3. Immunoblotting patterns of WB antigens from *F. gigantica* (lane 4), *S. mansoni* (lane 5), *E. pancreaticum* (lane 6) and *Paramphistomum* spp. (lane 7) with MoAb 6F3-2. The controls show WB antigen reacted with myeloma CF (lane 1), NMS (lane 2) and CIS (lane 3). Other clones of MoAb showed similar pattern and were not shown.

Dr. Terry Spithill, Monash University, Australia), the identical double band was observed at MW 14.5 kD (Fig. 2B) which confirmed that the proteins detected by MoAb were FABP. However, in contrast to MoAb, the polyclonal antibodies also reacted with bands in ES and WB at higher MW which could be due to impurities in the native FABP preparation used for immunization.

When tested against WB antigens from three other trematode parasites (*S. mansoni*, *Paramphistomum* spp. and *E. pancreaticum*), all MoAbs showed a strong cross-reaction with a *S. mansoni* antigen at MW 14.5 kD, while no cross-reactions were detected in WB antigens from other parasites (Fig. 3).

3.3. Immunolocalization

All MoAbs showed similar immunoperoxidase staining characteristics as represented by MoAb 6F3-2 (Fig. 4) which exhibited the strongest reaction. The sites and intensities of the brownish reaction products indicated the location and relative concentration of FABP which were bound to MoAb. The highest intensity was observed in the cytoplasm of parenchymal cells and their processes (Fig. 4A–C). However, while most parenchymal cells (Pc_1) were intensely stained, some parenchymal cells (Pc_2 , Pc_3) were only moderately or lightly stained (Fig. 4B and C). The testicular and ovarian tissues were also moderately stained with the early stage germ cells on the periphery of the gonadal follicles appeared more intensely

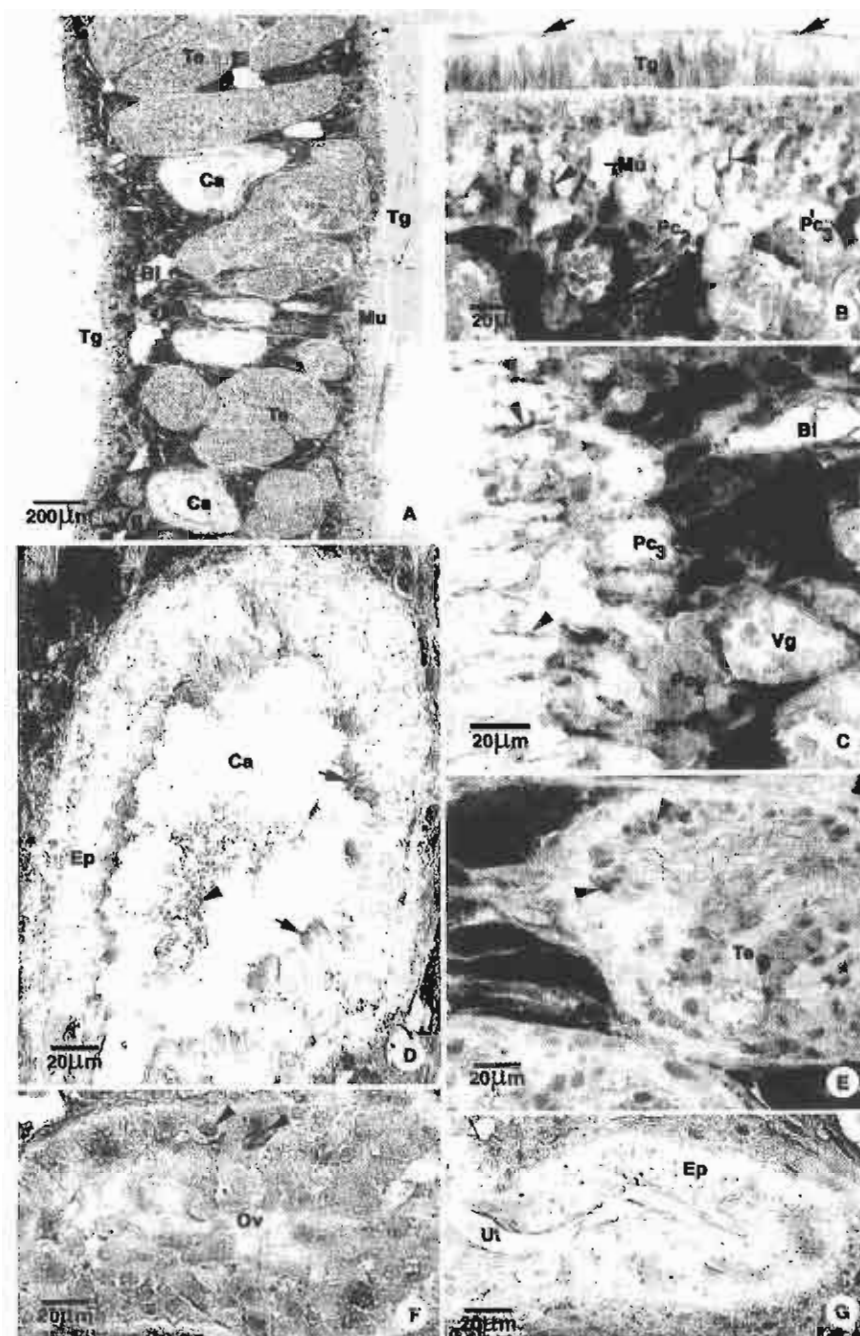


Fig. 4.

stained than the late stage cells in the center (Fig. 4E and F). The basal part and the surface of tegument were moderately stained (Fig. 4B). Most cytoplasm of the caecal epithelium was lightly stained, whilst the apical cytoplasm and lamellae were intensely stained (Fig. 4D). The uterine epithelium was only lightly stained (Fig. 4G).

4. Discussion

In this study, we could produce MoAbs specific to rFABP. These MoAbs reacted with the native *F. gigantica* FABP at MW 14.5 kD represented as closely aligned double bands in immunoblots of WB and tegumental (TA) extracts, and the excretion–secretion material of the adult parasites. Smooker et al. (1997) could also identify two isoforms of native *F. gigantica* FABP with similar MW. In contrast, it has been shown by many studies that *F. hepatica* has at least three isoforms of the cytoplasmic FABP family (Rodriguez-Perez et al., 1992; Chic, 1994; Bozas and Spithill, 1996). Their MWs range between 14 and 16 kD with 127–133 amino acids in length (Hillyer, 1985; Hillyer et al., 1987; Veerkamp et al., 1991; Rodriguez-Perez et al., 1992). In comparison, homologous protein in *S. mansoni* has a MW about 12 kD (Hillyer et al., 1988a) and exhibited cross-reactivity with *F. hepatica* FABP as well as cross-protection for both species of parasites (Hillyer et al., 1988b). Analysis of cDNAs indicated that FABP in the two species showed 44% identity (Moser et al., 1991; Rodriguez-Perez et al., 1992). Our MoAb could detect only two isoforms of the *F. gigantica* FABP family which may possess similar epitopes. These two isoforms were also detected by polyclonal antibodies against native FABP. In comparison to the native FABP, rFABP that reacted with all MoAbs has a higher MW of 20 kD. The higher MW of rFABP is due to the addition of 31 amino acids for cloning and purification purposes as mentioned in Section 2.

The immunolocalization experiment demonstrated that FABP has a wide distribution in almost all tissues of the parasites. However, it has the highest concentration in one type of parenchymal cells which forms the major stroma or general packing tissue between epithelia lining the tegument, digestive, reproductive and urinary tracts; whereas two other




Fig. 4. Light micrographs of *F. gigantica* frozen sections stained by immunoperoxidase technique, using MoAb as primary antibody and biotinylated rabbit antimouse IgG as secondary antibody. (Only sections stained with MoAb 6F3-2 were shown.) (A) A low magnification micrograph of the cross-section of an adult parasite's body, showing intense staining in parenchymal cells (Pc) which form the general packing tissue between the Tg and other organs (testis: Te; bladder: Bl; caecum: Ca; muscle: Mu). (B) A high magnification micrograph, showing intensely stained processes of parenchymal cells (arrow heads) running between muscle cells (Mu) towards the Tg, which is only lightly stained except at the surface membrane (arrows) and the basal cytoplasm which appears more intensely stained. Parenchymal cells showed variation in staining from the highest to the lowest intensities in Pc₁, Pc₂ and Pc₃. (C–E) Higher magnification micrographs of the interior of the adult parasites' bodies, showing in (C) intensely stained type 1 parenchymal cells (Pc₁) and their processes (arrow heads), and less intensely stained types 2 and 3 parenchymal cells (Pc₂, Pc₃). Vitelline cells (Vg) are not stained. In (D), most of the cytoplasm of caecal epithelium (Ep) is lightly stained, while the apical cytoplasm and lamellae (arrows) and content of the caecal lumen (Ca—arrow head) are intensely stained. In (E) and (F), the testicular (Te) and ovarian (Ov) cells exhibit moderate staining, especially those lying on the periphery of the gonadal follicles (arrow heads). In (G), the uterine epithelium (Ut-Ep) is only lightly stained.

types of parenchymal cells exhibit less staining intensity and thus probably contained a lower concentration of FABP. In contrast, the relative concentration of FABP in the caecal epithelium and tegument which were exposed to the hosts' fluid and thus thought to be involved in the initial uptake of fatty acids was quite low. It is possible that after the uptake through these two kinds of epithelia, fatty acids and cholesterol could be concentrated and stored in the first type of parenchymal cells which acts as the intermediary in supplying these building block molecules to other kinds of cells that they maintain close contact. Some of the latter, such as the tegument, may require a significant quantity of lipids for the synthesis of the surface membrane which has a high rate of turn over for the parasite's homeostasis and protection (Hanna, 1980).

In addition to *F. gigantica* native FABP, these MoAbs also recognized similar-sized antigens in *S. mansoni*, while no cross-reactions were detected against antigens from other trematode parasites, including *Paramphistomum* spp. and *Eurytrema* spp. As has been reported, the strong cross-reaction and cross-protection between the FABP of *Fasciola* and *Schistosoma* are due to the high degree of conservation of 43% amino acid sequence identity (Smooker et al., 1997). In fact, FABP is considered to be one of the most promising vaccine candidates that could confer dual protection against fasciolosis and schistosomiasis (Casanueva et al., 2001). Vaccination against FABP may interfere with the processes of fatty acid and cholesterol uptakes and thus damage the structural integrity of many tissues, especially the surface membrane of the tegument, which have high need of these molecules for their building blocks. Furthermore, because of their specificities to only *Fasciola* and *Schistosoma*, these MoAbs may be good candidates for immunodiagnosis which will be further investigated.

Acknowledgements

This work was supported by the Thailand Research Fund (Senior Research Scholar Fellowship to Prasert Sobhon) and the National Center for Genetic Engineering and Biotechnology, NSTDA (Grant No. BT-B-06-2B-14-004 to Vitoon Viyanant).

References

- Abane, J.L., Oleaga, A., Ramajo, V., Casanueva, P., Arellana, J.L., Hillyer, G.V., Muro, A., 2000. Vaccination of mice against *Schistosoma bovis* with a recombinant fatty acid binding protein from *Fasciola hepatica*. *Vet. Parasitol.* 91, 33–42.
- Bozas, S.E., Spithill, T.W., 1996. Identification of 3-hydroxyproline residues in several proteins of *Fasciola hepatica*. *Exp. Parasitol.* 82, 69–72.
- Casanueva, R., Hillyer, G.V., Ramajo, V., Oleaga, A., Espinoza, E.Y., Muro, A., 2001. Immunoprophylaxis against *Fasciola hepatica* in rabbits using a recombinant Fh15 fatty acid binding protein. *J. Parasitol.* 87, 697–700.
- Chiez, R.M., 1994. Accession No. A44638. Submitted to the Protein Sequence Database, August 1994.
- Esteves, A., Joseph, L., Paulino, M., Ehrlich, R., 1997. Remarks on the phylogeny and structure of fatty acid binding proteins from parasitic platyhelminths. *Int. J. Parasitol.* 27, 1013–1023.
- Estuningsih, S.E., Smooker, P.M., Wiedosari, E., Widjajanti, S., Vaiano, S., Partoutomo, S., Spithill, T.W., 1997. Evaluation of antigens of *Fasciola gigantica* as vaccines against tropical fasciolosis in cattle. *Int. J. Parasitol.* 27, 1419–1428.

- Grains, R., Vichasri-Grains, S., Sobhon, P., Upatham, E.S., Viyanant, V., 2000. Molecular cloning and characterization of antigen encoding genes from *Fasciola gigantica*. In: Sirisinha, S., Chaiyaroj, S.C., Tapchaisri, P. (Eds.), International Proceedings of the Second Congress of the Federation of Immunological Societies of Asia-Oceania, Bangkok, Thailand, January 23–27. Monduzzi Editore, Bologna, Italy, pp. 39–43.
- Hanna, R.E., 1980. *Fasciola hepatica*: glycocalyx replacement in the juvenile as a possible mechanism for protection against host immunity. *Exp. Parasitol.* 50, 103–114.
- Hillyer, G.V., 1985. Induction of immunity in mice to *Fasciola hepatica* with a *Fasciola*/*Schistosoma* cross-reactive defined immunity antigen. *Am. J. Trop. Med. Hyg.* 34, 1127–1131.
- Hillyer, G.V., Haroun, E.T., Hernandez, A., De Galanes, M.S., 1987. Acquired resistance to *Fasciola hepatica* in cattle using a purified adult worm antigen. *Am. J. Trop. Med. Hyg.* 37, 363–369.
- Hillyer, G.V., De Galanes, M.S., Garcia Rosa, M.I., Montealegre, F., 1988a. Acquired immunity in schistosomiasis with purified *Fasciola hepatica* cross-reactive antigens. *Vet. Parasitol.* 29, 265–280.
- Hillyer, G.V., Garcia Rosa, M.I., Alicea, H., Hernandez, A., 1988b. Successful vaccination against murine *Schistosoma mansoni* infection with a purified 12 kD *Fasciola hepatica* cross-reactive antigen. *Am. J. Trop. Med. Hyg.* 38, 103–110.
- Lowry, O.H., Rosenbrough, N.J., Farr, S.L., Randal, R.J., 1951. Measurement of protein with the folin phenol reagent. *J. Biol. Chem.* 193, 265–275.
- Meyer, F., Myer, H., Ruefing, E., 1970. Lipid metabolism in the parasitic and free-living flatworms, *Schistosoma mansoni* and *Dugesia dorotocephala*. *Biochim. Biophys. Acta* 210, 257–266.
- Moser, D., Tendler, M., Griffiths, G., Klinkert, M.Q., 1991. A 14 kD *Schistosoma mansoni* polypeptide is homologous to a gene family of fatty acid binding proteins. *J. Biol. Chem.* 266, 8447–8454.
- Muro, A., Ramajo, V., Lopez, J., Simon, F., Hillyer, G.V., 1997. *Fasciola hepatica*: vaccination of rabbits with native and recombinant antigens related to fatty acid binding proteins. *Vet. Parasitol.* 69, 219–229.
- Rodriguez-Perez, J., Rodriguez-Medina, J.R., Garcia-Blanco, M.A., Hillyer, G.V., 1992. *Fasciola hepatica*: molecular cloning, nucleotide sequence, and expression of a gene encoding a polypeptide homologous to a *Schistosoma mansoni* fatty acid binding protein. *Exp. Parasitol.* 74, 400–407.
- Smooker, P.M., Hickford, D.E., Vajano, S.A., Spithill, T.W., 1997. Isolation, cloning and expression of fatty acid binding proteins from *Fasciola gigantica*. *Exp. Parasitol.* 85, 89–91.
- Veerkaup, J.H., Peeters, R.A., Maatman, R.G., 1991. Structural and functional features of different types of cytoplasmic fatty acid binding proteins. *Biochim. Biophys. Acta* 1081, 1–24.
- Viyanant, V., Chaijanadana, O., Upatham, E.S., Sobhon, P., Kruatrachue, M., Ahmed, S., Ardseungnoen, P., 1993. Monoclonal antibodies against *Schistosoma mekongi* surface tegumental antigens. *Southeast Asian J. Trop. Med. Pub. Hlth.* 24, 484–488.

DEVELOPMENT OF THE NERVE GANGLIA OF ABALONE, *HALIOTIS ASININA* LINNAEUS

M. KRUATRACHUE,¹ P. LAIMEK,² C. WANICHANON,² V. LINTHONG,² P. SRETARUGSA,²
E. S. UPATHAM,³ AND P. SOBHON²

¹Department of Biology, Faculty of Science, Mahidol University, Bangkok 10400, Thailand;

²Department of Anatomy, Faculty of Science, Mahidol University, Bangkok 10400, Thailand;

³Department of Biology, Faculty of Science, Mahidol University, Bangkok 10400 and Department of Medical Science, Faculty of Science, Burapha University, Chonburi 20131, Thailand

ABSTRACT The development of cells in the ganglia during various ages of the abalone, *Haliotis asinina*, was studied. There were three types of neurosecretory cells (NS₁₋₃), four types of neurons (NR₁₋₄) and three types of neuroglia (NG₁₋₃). In the cerebral ganglia, NS₁ and NR₁ (giant neurons) first appeared in 1-month-old abalone while NS₂ and NS₃ first appeared in 3-month-old and 4-month-old abalone, respectively. These cells increased in number in 5- and 10-month-old abalone, reaching a maximum number at 12 months, and thereafter remained constant. In the pleuropedal ganglia, NS₁ and NR₁ first appeared in 1-month-old abalone, while NS₂ and NS₃ first appeared in 2-month-old and 4-month-old abalone, respectively. They increased in number in 4- and 7-month-old abalone, reaching a maximum at 11 months, and thereafter remained constant. In the visceral ganglia, NS₁ and NR₁ first appeared in 2-month-old abalone while NS₂ and NS₃ appeared later in 3-month-old and 5-month-old abalone, respectively. They increased in number at 4 months, reaching a maximum number at 11 months, and thereafter remained constant. NR₂, NR₃, NR₄ and NG were present in all ganglia early in development from one month onwards, and their numbers increased rapidly with age.

KEY WORDS: development, nerve ganglia, abalone, *Haliotis asinina*

INTRODUCTION

During neurogenesis of gastropods, the central ganglia of gastropods arise by proliferation and later delamination and/or invagination of the ectoderm. Cell division continues in the peripheral proliferative zones throughout embryogenesis, and post-mitotic cells then migrate inwardly to join the central ganglia which are formed nearby (Jacob 1984). Gangliogenesis in gastropods progresses from anterior to posterior with the cerebral ganglia developing first, followed by the pedal ganglia and then the more posterior ganglia of the abdominal loop (Kerkut & Walker 1975). The pattern of neurogenesis in the gastropod central nervous system resembles the proliferation of cells in the neural tube and the migration of the neural crest and ectodermal placode cells in the vertebrate nervous system but differs from the pattern described for other invertebrates (Jacob 1984).

Although the nervous systems of more derived species of gastropods as well as the development of neurons and individual transmitter systems have been studied (Lever et al. 1965; Coggeshall 1967; Kerkut & Walker 1975; Van Minnen & Sokolove 1984; Roubos et al. 1988; Carroll & Kempf 1994; Kruatrachue et al. 1994; Kempf et al. 1997; Marois & Carew 1997), the nervous development of prosobranchs has not been investigated in detail. Most studies of ganglia development in gastropods were conducted on opisthobranchs and pulmonates. In pulmonates, variation in morphology and lobulization of the ganglia is related to age and development (Kerkut & Walker 1975). Roubos et al. (1988) studied the development of neuroendocrine centers of *Lymnaea stagnalis* (Linnaeus) and found that the dorsal bodies and light green cells were already present in snails of 1 mm in shell length and that the caudo-dorsal cells first appeared in snails of 3 mm in shell length. The dorsal bodies and caudo-dorsal cells increased in number and size with increasing shell length. In *Achatina fulica* (Bowdich), the size of the ganglia and the number of nerve cells in the ganglia increased with increasing age. The prominent nerve cells in the ganglia were large cells and giant cells. The large cells were already present in all ganglia of the newly hatched snails, while the giant cells first appeared in 1-month-old snails. The

neurosecretory cells in the cerebral ganglia of *A. fulica* first appeared in 2-month-old snails and increased in number and size with increasing age, reaching a maximum number in 8-month-old snails and thereafter remained constant in 9- to 12-month old snails (Kruatrachue et al. 1994).

In general, the number of nerve cells in the ganglia of gastropods increases with age (Kerkut & Walker 1975; Lever et al. 1965; Coggeshall 1967). Coggeshall (1967) studied the opisthobranch snail, *Aplysia californica* (Cooper), and found that, during its maturation, the number of nerve cells in the ganglia increased by 40% and that the greatest number of large neurosecretory cells occurred in full grown animals. In the stylommatophoran snail, *Limax maximus* (Linnaeus), the morphology of the dorsal body cells also changed during maturation (Van Minnen & Sokolove 1984). The neurosecretory cells were small and released little secretory product in the immature and early male-phase animals. In contrast, these cells became larger and released large amounts of secretory product in the later female-phase animals (Van Minnen & Sokolove 1984). To the best of our knowledge, there is little information on the development of ganglia in prosobranch snails. Hence, the aim of the present investigation was to study the development of nerve ganglia of *Haliotis asinina* (Linnaeus), a common abalone species found along the coastal waters of Thailand.

MATERIALS AND METHODS

Ten adult *H. asinina* (average shell length 66.58 mm) (five males and five females) were obtained from the Marine Biological Station, Chulalongkorn University, Chonburi Province, Thailand. They were relaxed with 5% MgCl₂ for 3-4 hours prior to dissection. Dissections of the nervous system were done under an Olympus stereoscopic binocular microscope with a fiber optic dissecting light and drawings were made with the aid of a camera lucida.

To study the histological development of the nervous system of *H. asinina*, adult abalone and those from 1 to 12 months old were obtained. Ten animals from each age class were examined. They were relaxed and the cerebral, pleuropedal and visceral ganglia were dissected out and fixed in Bouin's fluid in 0.14 M NaCl for

24 hours, and washed with 70% ethyl alcohol. Then, they were dehydrated through a graded series of ethanol, cleared in dioxane, infiltrated and embedded in paraffin. Serial frontal sections of 5 μm thickness were cut and alternating sections were stained with hematoxylin and eosin, chrome-hematoxylin-phloxine (Gomori 1941) and paraldehyde-fuchsin (Gomori 1950). Sections were examined under an Olympus Vanox light microscope. Measurements (width, length and thickness) of the ganglia were taken from the median frontal sections (10 sections per ganglion; 10 animals for each age group). Neurons and neurosecretory cells in all ganglia were identified based on their histological characteristics (cell size and shape, nuclear size and shape) and staining affinities (Upatham et al. 1998; Kruatrachue et al. 1999; Thongkukiatkul et al. 2000). In addition, the numbers of cells in each ganglion of each age group were counted. For each animal, the cell count was done on the median frontal sections (10 sections per ganglion). The cell type and number were scored as follows:

Neurosecretory Cell (per section)		Neuron (per section)	
(-)	= 0 cell	(-)	= 0 cell
(+)	= 1-5 cells	(+)	= 1-10 cells
(++)	= 6-10 cells	(++)	= 11-20 cells
(+++)	= 11-15 cells	(+++)	= 21-30 cells
(++++)	= >15 cells	(++++)	= >30 cells

RESULTS

Figure 1 shows a diagrammatic drawing of the gross anatomy of adult *H. asinina*. The nervous system consists of a pair of cerebral ganglia, a pleuropedal ganglion and a visceral ganglion.

Figure 2 shows the frontal sections of the cerebral (Fig. 2A), pleuropedal (Fig. 2B) and visceral ganglia (Fig. 2C) in adult *H. asinina*. There are 10 types of nerve cells in all ganglia of *H. asinina* (Figs. 2D, 3A), i.e., three types of neurosecretory cells (NS_{1-3}), four types of neurons (NR_{1-4}) and three types of neuroglia (NG_{1-3}) (Upatham et al. 1998; Kruatrachue et al. 1999; Thongkukiatkul et al. 2000). The NS cells were identified using special stains, i.e. chrome-hematoxylin-phloxine (Gomori 1941) and paraldehyde-fuchsin (Gomori, 1950).

The shape, size, and type of cells and their number in ganglia during various ages of developing abalone are summarized in Tables 1, 2 and 3.

Cerebral Ganglia

In 1-month-old abalone, the cerebral ganglion appeared as an elongated bean shape whose size was approximately $121 \times 471 \times 100 \mu\text{m}$ (Fig. 3B). Most of the ventral, dorsal and lateral parts of the ganglia had a thick cortex that contained 3-4 cell layers, while the medial part contained only 0-1 cell layers (Table 1). NS_1 cells first appeared in 1-month-old abalone; there were 1-2 cells per section. These cells were concentrated in the dorsal horn of the ganglion (Table 1). Most types of neurons (NR_{1-4}) were present, but NR_2 were the most numerous. NR_3 and NR_4 were moderate in number, while the NR_1 or the giant neurons were rarely found but when present were usually located in the dorsal horn similar to NS cells (Table 1). All types of NG were present but in a small number.

At 2-4 months, the ganglia appeared bean shape similar to those in 1-month-old abalone. The number of cell layers increased with age. The number of NS cells increased to about 2-5 cells per section (Table 1). Most of these were NS_1 , while NS_2 were ob-

served in 3-month-old and NS_3 in 4-month-old abalone. Most NS cells were concentrated in the dorso-lateral and dorso-medial, ventral and ventro-medial parts of the ganglia (Table 1). NR cells were similar in type and number to those in 1-month-old abalone. NG cells increased in number from one month onwards.

At 5 months, the size of the ganglion increased to $203 \times 632 \times 200 \mu\text{m}$ (Table 1). From 5 months onwards, the ganglion assumed a sickle shape (Fig. 3C). The number of cell layers in the cortex increased, especially in the ventral and dorsal parts. The number of NS cells increased to about 10 cells per section, and although all types of NS were scattered in all parts of the ganglia, most were still concentrated in the dorsal and ventral horns (Table 1). The number of NR increased with age, and the NR_1 count was approximately 11-20 cells per section (Table 1). They were present in the dorsal and ventral areas. At this age, the number of NG slightly increased.

From 6 to 10 months, the ganglia appeared sickle shaped but were larger and more elongated than those of 5-month-old abalone. The cortex in all areas thickened and the quantities and distribution of NS and NR cells were similar to those of 5-month-old abalone (Table 1).

At 11 months, the cerebral ganglia increased in size to about $377 \times 810 \times 300 \mu\text{m}$ (Fig. 3D). Other appearances were similar to those of 5- to 10-month-old abalone. However, the numbers of NS and NR_1 cells increased (Table 1). NG also increased with increasing age. When abalone were 12 months old, their ganglia ($377 \times 901 \times 325 \mu\text{m}$ in size) were fully developed and appeared similar in all aspects to those of the adult abalone (Fig. 2A).

Pleuropedal Ganglia

In 1-month-old abalone, the pleuropedal ganglion appeared butterfly-shaped and about $189 \times 418 \times 150 \mu\text{m}$ in size (Fig. 4A). In the ventral and lateral parts of the ganglia, the cortex was thick and contained 2-5 cell layers (Table 2). The remaining parts of cortex were relatively thin. There were only about 1-2 NS cells per section. These cells were confined to the dorsal sulcus of the ganglion; most of them being NS_1 (Table 2). There were all types of NR, but a few NR_1 and NR_4 were present in the dorso-medial part (Table 2). All types of NG cells were found in the ganglion at this age.

At 2-3 months, the size of the ganglia increased from $273 \times 497 \times 155$ to $289 \times 522 \times 170 \mu\text{m}$, but the shape was not altered (Fig. 4B). The number of cell layers in the cortex, NS and NR cells appeared to increase, and most cells were found in all parts of the cortex. However, NR cells were concentrated in the dorsal and dorso-lateral parts, while NS cells were concentrated in the dorso-medial and lateral sulci (Table 2).

At 4-6 months, the pleuropedal ganglia was still butterfly-shaped but increased in size from $337 \times 556 \times 200 \mu\text{m}$ to approximately $488 \times 707 \times 250 \mu\text{m}$ (Fig. 4B), and the cortex became much thicker. The number of NS cells (mostly NS_1) increased to about 20 cells per section and a larger number were found in the dorso-lateral and ventro-lateral parts (Table 2). NR cells increased in number with increasing age and were found in the ventro-medial, ventro-lateral and ventral sulci (Table 2).

At 7 months, the ganglia were H-shaped and increased in size to about $544 \times 1615 \times 315 \mu\text{m}$ (Fig. 4C). The number of cell layers increased and NS cell (mostly NS_1) number was about 30-40 cells per section; these cells were distributed in all areas (Table 2). NR cells (mostly NR_1) increased in number in comparison to earlier stages. From 8 to 10 months, pleuropedal ganglia were similar in shape to those of 7-month-old abalone (Table 2).

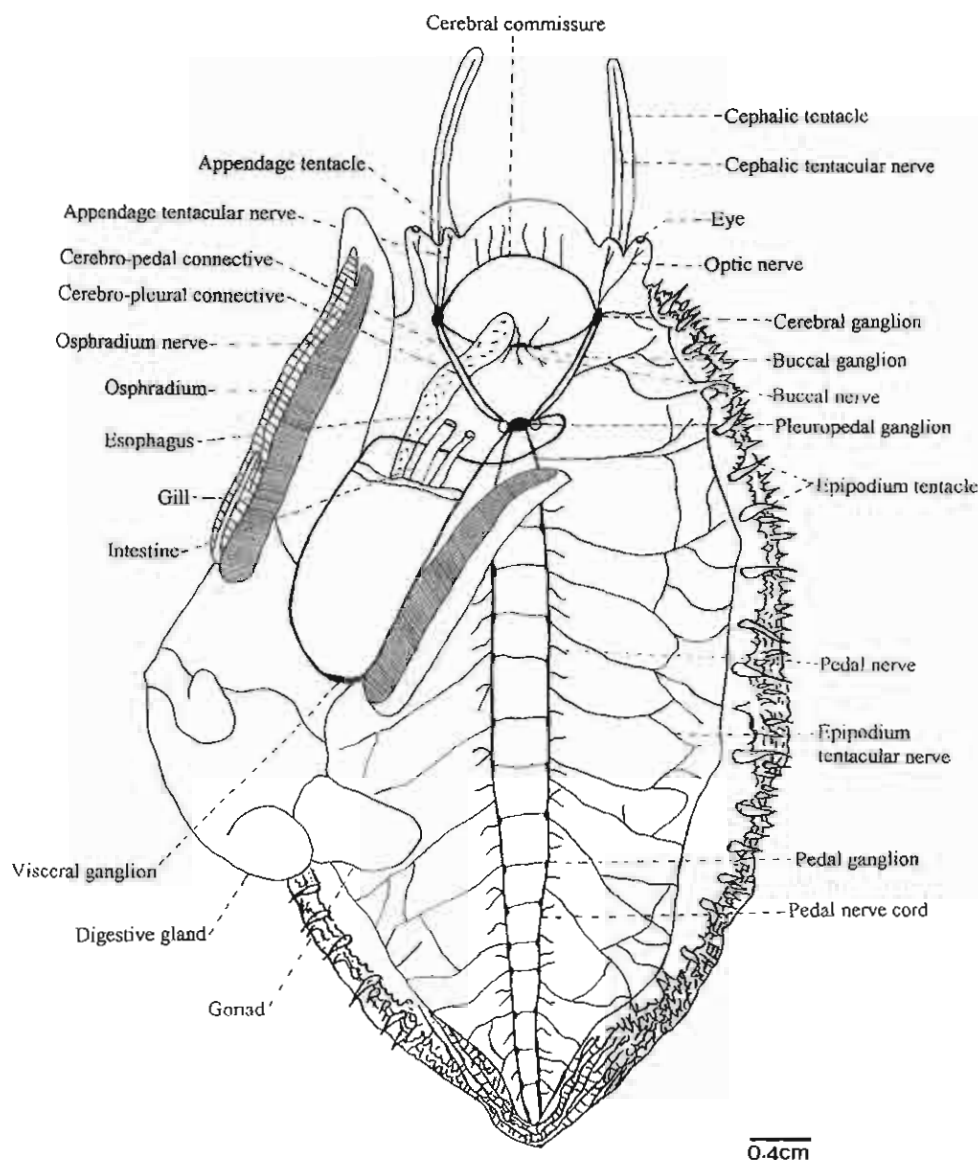


Figure 1. Diagrammatic drawing of the gross anatomy of adult abalone showing the ganglia and their peripheral nerves (modified from Crofts, 1929).

At 11 months, the ganglia increased in size to $589 \times 2508 \times 470 \mu\text{m}$; the ventral and dorsal horns were elongated (Fig. 4D). The number of cell layers in the cortex increased. The number of NS cells was about 60 cells per section (Table 2). NR cells and NG cells were distributed in all areas; their numbers increased with increasing age. At 12 months, the pleuropedal ganglia ($589 \times 2543 \times 500 \mu\text{m}$ in size) were fully developed and appeared similar to those of the adult abalone (Fig. 2B).

Visceral Ganglia

In 1-month-old abalone, the visceral ganglion was as small as $37 \times 72 \times 30 \mu\text{m}$ and bean-shaped (Fig. 5A). The cortex had only one layer of cells (Table 3). NS cells and NR_1 cells had not yet appeared. In contrast, the remaining types of NR (NR_{2-4}) were present but still few in number (Table 3). All types of NG were observed.

From 3 months onwards, the ganglion was dumbbell-shaped (Figs. 5B–5D) and its size increased with increasing age (Table 3). The cortex was thicker, especially the lateral part. NS_1 cells first appeared in 2-month-old abalone, and their number was about 1–2 cells per section (Table 3). They were present in the left lateral, left latero-dorsal and left latero-ventral parts. There were all types of NR, but NR_1 and NR_3 were rarely observed.

At 3–10 months, the visceral ganglion increased in size from $118 \times 488 \times 50 \mu\text{m}$ to about $160 \times 770 \times 110 \mu\text{m}$ (Fig. 5B). The number of cell layers in the cortex increased. The number of NS cells increased to about 20 cells per section, and they were distributed in the right lateral part (Table 3). NR cells were similar in number and distribution to those at 3 months (Table 3).

At 11 months, the ganglion ($160 \times 889 \times 110 \mu\text{m}$) increased in length, but still had a similar width to that of 10-month old abalone (Fig. 5C). NS cells (mostly NS_1) increased in number and were

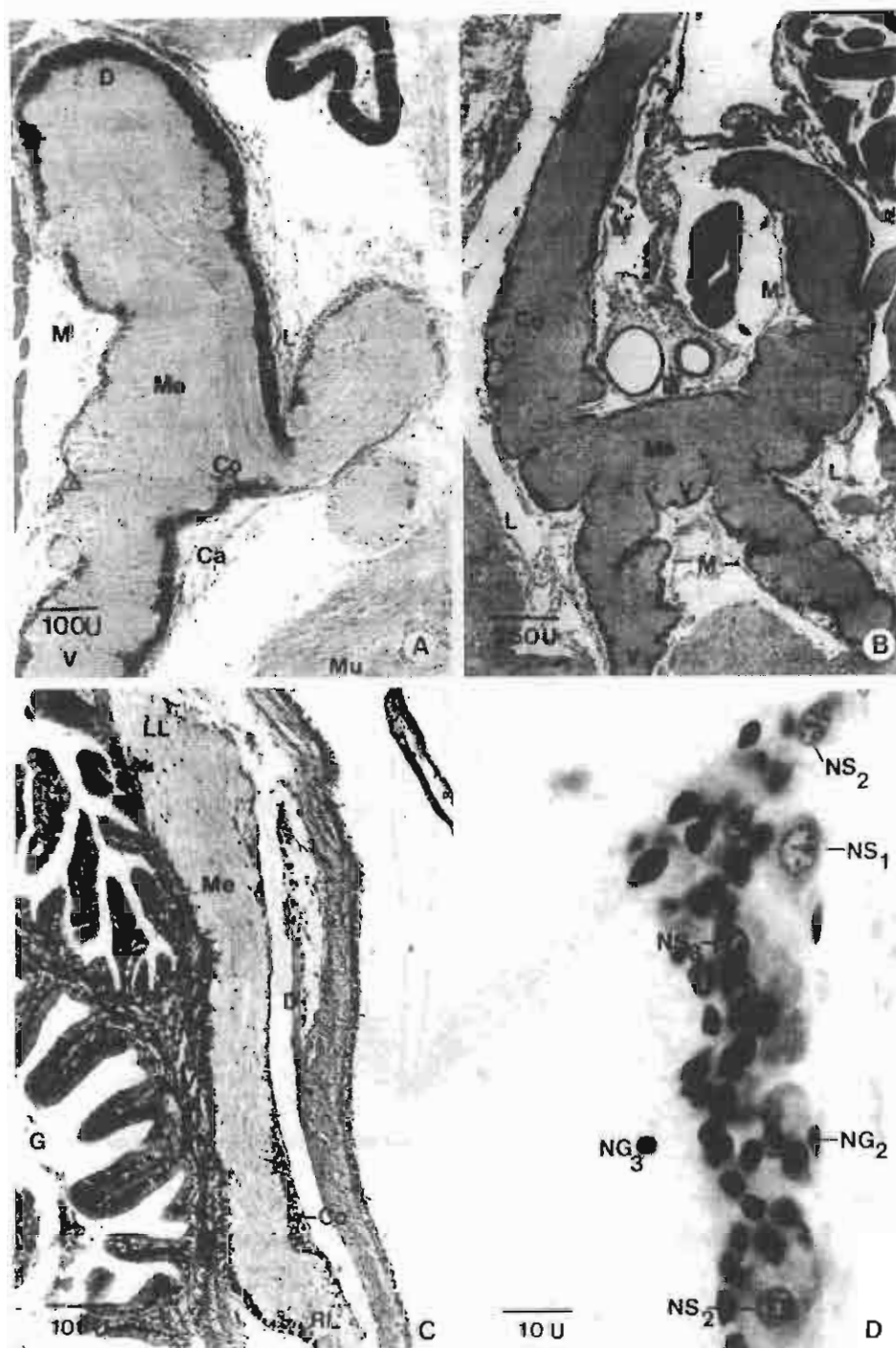


Figure 2. Photomicrographs of the frontal sections of ganglia of *H. asinina*. (A) A low-power micrograph of a cerebral ganglion, showing thick cell layers on the ventral (V) and dorsal (D) sides. Ca-capillary, Co-cortex, L-lateral, M-medial, Me-medulla, Mu-muscle. (B) A low-power micrograph of a pleuropedal ganglion showing thick cell layers on the dorsal (D) and lateral (L) sides. Co-cortex, M-medial, Me-medulla, V-ventral. (C) A low-power micrograph of a visceral ganglion showing thick cell layers on the ventral side. LL-left lateral, RL-right lateral, G-gill, Co-cortex, Me-medulla. (D) A high-power micrograph of a pleuropedal ganglion showing various types of nerve cells in the cortex region. NG₂-type 2 neuroglia, NG₃-type 3 neuroglia, NS₁-type 1 neurosecretory cell, NS₂-type 2 neurosecretory cell, NS₃-type 3 neurosecretory cell.

distributed in all areas of the ganglia (Table 3), but were concentrated mostly in the right lateral part (Fig. 5D). At 12 months, the ganglion ($165 \times 939 \times 150 \mu\text{m}$ in size) appeared similar to those of adult abalone (Fig. 2C).

DISCUSSION

During postembryonic development of the nervous system of gastropods, the nerve cells and neurosecretory cells increase in size

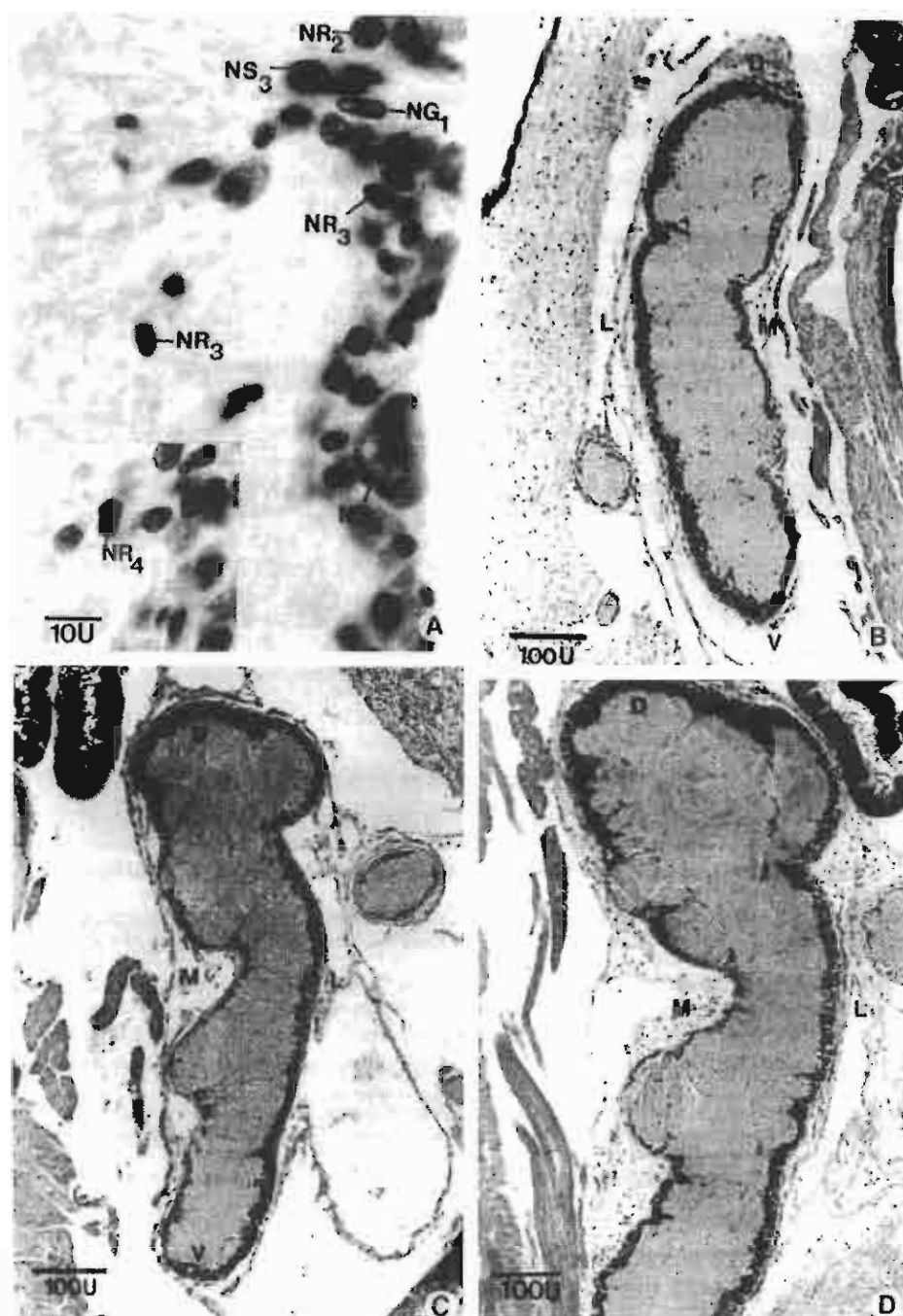


Figure 3. (A) High-power micrograph of cerebral ganglia showing type 1 neuroglia (NG_1), types 1-4 neurons (NR_{1-4}) and type 3 neurosecretory cell (NS_3). (B) Frontal sections of cerebral ganglia in 1- to 4-month-old abalone that appeared bean-shaped. (C) In 5- to 10-month-old abalone, the ganglion appeared as a sickle shape. (D) In 11-month-old abalone, the ganglion greatly increased in size. D-dorsal, L-lateral, M-medial, V-ventral

and number (Bullock & Horridge 1995), for example, the neuroendocrine cells of *L. stagnalis* increase in number and size with increasing shell length (Roubos et al. 1988). In addition, Lever et al. (1965) showed the same result in the cerebral and parietal ganglia of *Biomphalaria glabrata* (Say). Similarly, Kruttschue et al. (1994) reported that the number and size of neurosecretory cells in the cerebral ganglia of *A. fulica* increased with increasing age.

A similar trend was observed in *H. ussima* in the present study. Furthermore, our histological study indicates that the cerebral, pleuropedal and visceral ganglia appeared as definite organs with specific shapes in 1-month-old abalone. Later there were changes in the size but not so much shape of these ganglia; and the numbers of neurons and neurosecretory cells in all ganglia markedly increased with increasing age.

TABLE 1.
Key events during the development of a cerebral ganglion in *H. asinina*.

Month	Shape	Size (μm) W \times L \times T	Average Number of Cell Layers			Average Number of NS/ Section	Location of NS	Relative Number of NS ^a			CH-P	PF	Relative Number of NR ^b				Location of NR ₁
			Ventral (V)	Dorsal (D)	Medial (M)	Lateral (L)		NS ₁	NS ₂	NS ₃			NR ₁	NR ₂	NR ₃	NR ₄	
1	Bean shape	121 \times 471 \times 100	4	3	0-1	2-3	1-2	+	-	-	-	-	+	+++	++	++	D
2	Bean shape	182 \times 607 \times 100	5	4	0-3	1-3	2-5	+	-	-	-	-	+	++++	++	++	D,DM
3	Bean shape	182 \times 644 \times 110	5	4	0-3	1-3	2-5	+	+	-	-	-	+	++++	++	++	D,DM,V
4	Bean shape	154 \times 648 \times 150	6	7	0-3	2-4	10	+	+	+	-	-	+	++++	+++	++	D,DM,V
5	Sickle shape	203 \times 632 \times 200	6	7-8	0-3	1-4	20	++	++	+	+	+	++	++++	+++	++	D,DM,DL,VV M,VL
6	Sickle shape	203 \times 637 \times 213	4-5	6-8	0-3	1-3	20	++	++	+	+	+	++	++++	+++	++	Same
7	Sickle shape	206 \times 808 \times 220	4-5	5-7	1-2	1-3	20	++	++	+	+	+	++	++++	+++	++	Same
8	Sickle shape	273 \times 735 \times 240	4-5	5-7	0-3	1-3	20	++	++	+	+	+	++	++++	+++	++	Same
9	Sickle shape	286 \times 699 \times 250	4-5	5-7	0-3	1-5	20	++	++	+	+	+	++	++++	+++	++	Same
10	Sickle shape	294 \times 787 \times 280	4	6	0-3	1-4	30	+++	+++	++	+	+	+++	++++	++++	++	Same
11	Sickle shape	377 \times 810 \times 300	4	5-7	1-3	1-4	30-40	+++	+++	++	+	+	+++	++++	++++	++	Same
12	Highly elongated, convoluted	377 \times 901 \times 325	4-6	5-7	1-3	1-5	30-40	+++	+++	++	+	+	+++	++++	++++	++	Same

^a 1-+ = 0 cell/section, ++ = 1-5 cells/section, +++ = 6-10 cells/section, (++++ = 11-15 cells/section, (+++++) = >15 cells/section.

^b 1-+ = 0 cell/section, ++ = 1-10 cells/section, +++ = 11-20 cells/section, (++++ = 21-30 cells/section, (+++++) = >30 cells/section.

n = 10 animals per month; 100 sections per ganglion.

W = width; L = length; T = thickness.

(CH-P = chromo-hematexylin-phloxine, PF = paraldeyde-fuchsin, NR = neuron, NS = neurosecretory cell).

TABLE 2.
Key events during the development of a pleuropedal ganglion in *H. asinina*.

Month	Shape	Size (μm) W \times L	Average Number of Cell Layers				Average Number of NS/Section	Location of NS	Relative Number of NS ^a			CH-P	PF	Relative Number of NR ^b				Location of NR ^b
			Ventral (V)	Dorsal (D)	Medial (M)	Lateral (L)			NS ₁	NS ₂	NS ₃			NR ₁	NR ₂	NR ₃	NR ₄	
1	Butterfly shape	189 \times 418 \times 150	2-4	0-3	1-3	0-5	1-2	DS	+	-	-	-	-	+	+++	++	++	DM
2	Butterfly shape	273 \times 497 \times 125	2-4	1-5	1-2	1-5	2-3	DS, DM, LS	+	+	-	+	-	+	+++	++	++	DM
3	Butterfly shape	289 \times 525 \times 70	4	1-5	1-3	2-4	2-3	DS, DM, LS	+	+	-	+	-	+	+++	++	++	DM, DL, D
4	Butterfly shape	337 \times 556 \times 200	5	2-5	2-3	2-7	20	DS, DM, LS, DL, VL	++	+	+	+	+	++	+++	---	++	DM, DL, D, V
5	Butterfly shape	455 \times 572 \times 230	5	2-5	2-3	1-7	20	DS, DM, LS, DL, VL, V	++	++	+	+	+	++	++++	+++	++	Same M, VL, VS
6	Butterfly shape	488 \times 707 \times 280	5	2-5	2-3	1-7	20	DS, DM, LS, DL, VL, V, D	++	++	+	+	+	++	++++	+++	++	Same
7	H shape	544 \times 1,015 \times 315	4-6	2-5	5	3-10	30-40	In all areas	+++	++	++	+	+	+++	++++	++++	++	Same
8	H shape	546 \times 1,052 \times 340	3-5	5	2-3	4-7	30-40	In all areas	+++	++	++	+	+	++	++++	++++	++	Same
9	H shape	572 \times 1,061 \times 390	4-5	2-5	3-4	1-8	30-40	In all areas	+++	+++	++	+	+	++	++++	++++	++	Same
10	H shape	580 \times 1,100 \times 430	4-5	2-5	3-4	2-7	30-50	In all areas	++++	+++	++	+	+	+++	++++	++++	++	Same
11	Highly elongated, enlarged similar	580 \times 2,408 \times 470	3-6	4-6	5	3-10	60	In all areas	++++	++++	+++	+	+	+++	++++	++++	+++	In all areas
12	H shape, similar	589 \times 2,543 \times 261	5	5-6	3-4	7	60	In all areas	++++	++++	+++	+	+	+++	++++	++++	+++	In all areas

(-) = 0 cells/section, (+) = 1-5 cells/section, (++) = 6-10 cells/section, (+++) = 11-15 cells/section, (++++) = >15 cells/section.

^a (i) = 0 cells/section, (i+) = 1-10 cells/section, (i++) = 11-20 cells/section, (i+++) = 21-30 cells/section, (i++++) = >30 cells/section.

^b (i) = 0 cells/section, (i+) = 1-10 cells/section, (i++) = 11-20 cells/section, (i+++) = 21-30 cells/section, (i++++) = >30 cells/section.

W = width, L = length, T = thickness.

CH-P = choline-hematoxylin-phenylethylamine, PF = parafaldehyde-toluidine, NR = neuron, NS = neurosecretory cell.

TABLE 3.
Key events during the development of a visceral ganglion in *H. asinina*.

Month	Shape	Size (μm) $W \times L \times T$	Average Number of Cell Layers				Average Number of NS/ Section	Location of NS	Relative Number of NS ^a			Relative Number of NR ^b				Location of NR ₁		
									NS ₁	NS ₂	NS ₃	CH-P	PF	NR ₁	NR ₂		NR ₃	NR ₄
			Ventral (V)	Dorsal (D)	Medial (M)	Lateral (L)												
1	Bean shape	$37 \times 72 \times 30$	1	0-1	1	1-2	-	-	-	-	-	-	-	++	++	+	-	
2	Bean shape	$48 \times 74 \times 35$	1-2	1-2	1	1-3	1-2	LL	+	-	-	-	-	+	++	++	+	LL.LLV
3	Dumbbell shape	$118 \times 488 \times 50$	1-2	1-2	1	1-4	2-3	LL.LLV,LLD	+	+	-	-	-	+	++	++	+	LL.LLV
4	Dumbbell shape	$123 \times 494 \times 55$	1-2	1-2	1	2	10	LL.LLV,LLD	+	+	-	-	-	+	++	++	+	LL.LLV, LLD
5	Dumbbell shape	$151 \times 607 \times 65$	1-2	1-2	1	1-3	10	LL.LLV,LLD, RL	++	+	+	-	-	+	++	++	+	LL.LLV, LLD,RL
6	Dumbbell shape	$155 \times 923 \times 65$	1-3	1-2	1-3	1-3	10	Same	++	+	+	+	+	++	++	++	+	Same
7	Dumbbell shape	$168 \times 640 \times 80$	1-3	1-2	1-2	1-3	10	Same	++	+	+	+	+	++	++	++	+	Same
8	Dumbbell shape	$161 \times 640 \times 90$	1-3	1-2	1	1-3	10	Same	++	+	+	+	+	++	++	++	+	Same
9	Dumbbell shape	$160 \times 700 \times 110$	1-3	1-2	1-2	1-3	10	In all areas	++	+	+	+	+	++	+++	++	+	Same
10	Dumbbell shape	$160 \times 770 \times 110$	1-3	1-2	1-2	1-3	20	In all areas	+++	+	+	+	+	++	+++	++	+	Same
11	Dumbbell shape	$160 \times 889 \times 110$	1-3	1-2	1-2	1-3	20	In all areas	+++	+	+	+	+	++	+++	+++	++	In all areas
12	Dumbbell shape	$165 \times 939 \times 150$	1-3	1-2	1-2	1-3	20	In all areas	+++	++	+	+	+	++	+++	+++	++	In all areas

^a (-) = 0 cells/section, (+) = 1-5 cells/section, (++) = 6-10 cells/section, (+++) = 11-15 cells/section, (++++) = >15 cells/section

^b (-) = 0 cells/section, (+) = 1-10 cells/section, (++) = 11-20 cells/section, (+++) = 21-30 cells/section, (++++) = >30 cells/section

n = 10 animals per month; 100 sections per ganglion

W = width; L = length; T = thickness

CH-P = chrome hematoxylin-phloxine, PF = paraldehyde-fuchsin, NR = neuron, NS = neurosecretory cell

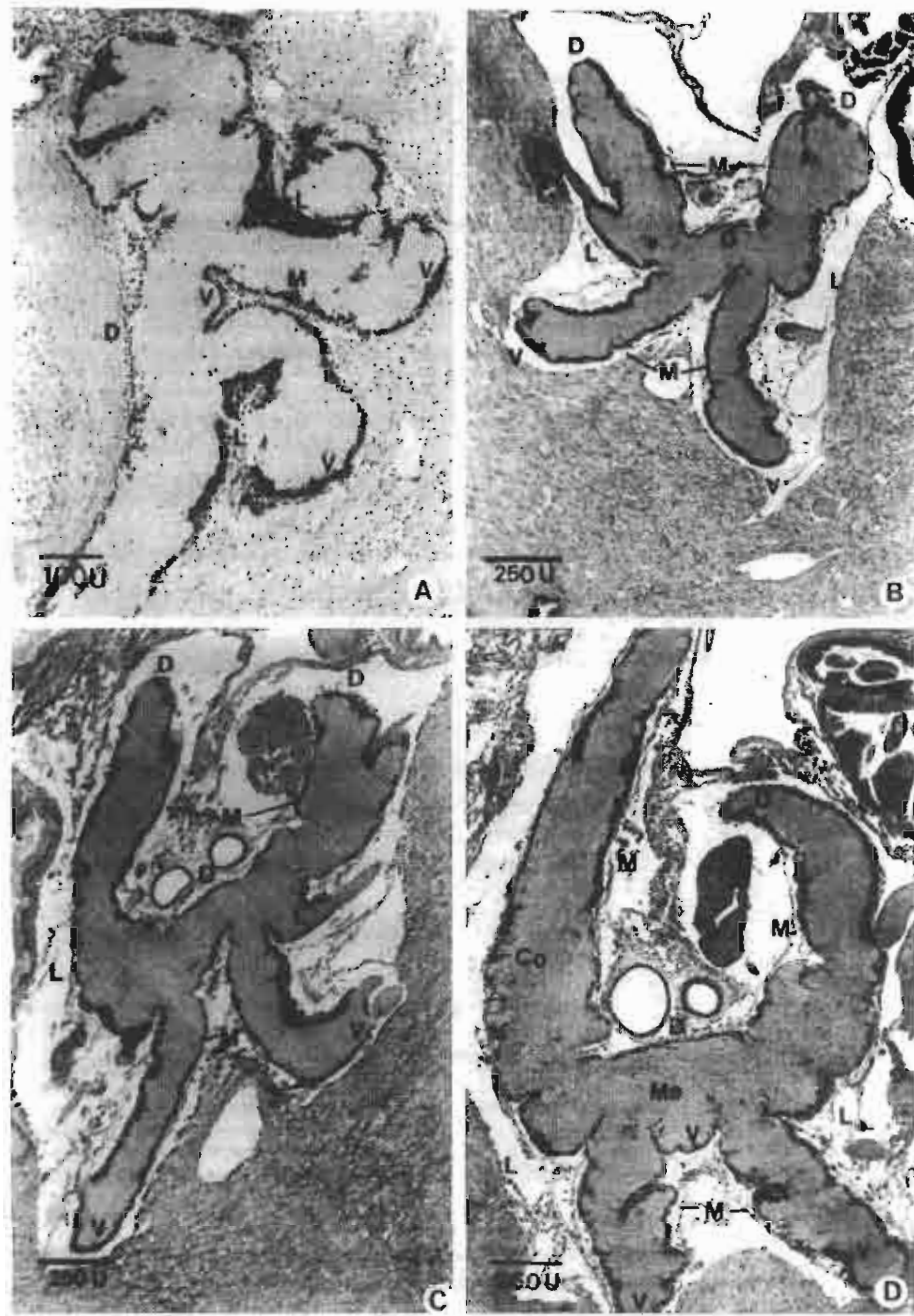


Figure 4. Low-power micrographs of frontal sections of pleuropedal ganglia. (A) In 1- to 2-month-old abalone, the pleuropedal ganglion had a butterfly shape. (B) In 3- to 6-month-old abalone, the ganglion still had a butterfly shape. (C) In 7- to 10-month-old abalone, the ganglion had an H shape. (D) In 11-month-old abalone, the ganglion was larger in size but still had an H shape. Co-cortex, D-dorsal, L-lateral, M-medial, Me-medulla, V-ventral

There have been many reports on the functions of neurosecretory cells in the cerebral ganglia of snails. It has been found that some snails have factors that stimulate growth rate (Geraerts & Algera 1976) and shell regeneration (Dillaman et al. 1976). Thongkukiatkul et al. (1998) reported that neurosecretory cells in the cerebral ganglia of *H. asinina* were positively stained with anti-human GH and anti-human insulin. In this study, it was observed that the neurosecretory cells in the cerebral ganglia first appeared in 1-month-old abalone and increased in number with

increasing age. A large number of neurosecretory cells were found in 5- and 10-month-old abalone that are assumed to be juvenile and pre-adult stages, respectively. They formed maximum numbers that were observed and appeared adult-like in 12-month-old abalone that reached the adult stage. It seems, therefore, that the increase in the number of NS cells is correlated with the increase in abalone growth.

Similar studies of other species of gastropods suggest that the number and staining properties of neuroendocrine cells in pleu-

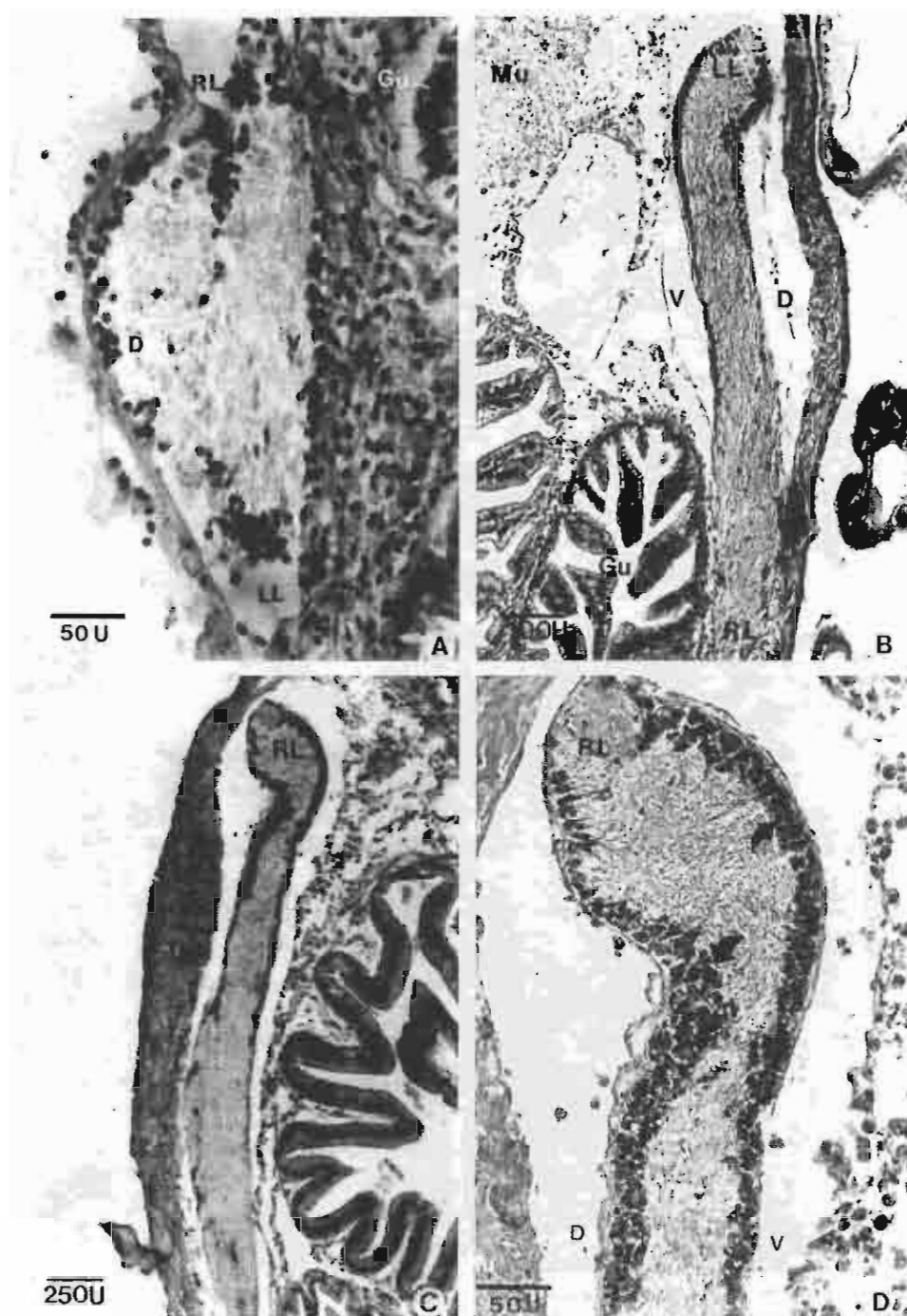


Figure 5. Frontal sections of visceral ganglia. (A) In 1- to 2-month-old abalone, the visceral ganglion was small and had a bean shape. (B) In 3- to 10-month-old abalone, the ganglion was large and assumed a dumbbell shape. (C) In 11-month-old abalone, the ganglion increased only in length. (D) High magnification of (C) showing thick cortex containing all types of nerve cells (arrows). D-dorsal, Gu-gut, LL- left lateral, RL- right lateral, Mu-muscle, V-ventral

ropedal and visceral ganglia are related to the gonadal maturation (Coggeshall 1967; Dogterom et al. 1983; Van Minnen & Sokolove 1984; Smith 1967). In our study it was observed that the neurosecretory cells in the pleuropedal and visceral ganglia first appeared in 1-month old abalone. The number of neurosecretory cells in the pleuropedal ganglia increased in 4- and 7-month-old

abalone, while in the visceral ganglia it increased in 4-month-old abalone. They reached a maximum number in 11-month-old abalone. The development of these neurosecretory cells may correlate with the development of the reproductive organs. Thongkukiatkul et al. (1998) reported that neurosecretory cells in the pleuropedal and visceral ganglia of *H. asinina* were stained by anti-human LH.

while only those in the pleuropedal ganglion were stained by anti-human FSH.

It was reported that early spermatocytes and spermatids of *H. asinina* appeared at 4 months, and early oocytes (OC₁₋₃) at 6–7 months (Sobhon et al. 1999), while fully mature spermatozoa appeared in the gonads as early as 6–7 months. At this age, there were already a large number of neurosecretory cells in the visceral and pleuropedal ganglia of the abalone. Moreover, Sobhon et al. (1999) showed that a large number of mature oocytes of the reproductive cycle of *H. asinina* occurred at 10 to 11 months, the age at which the neurosecretory cells in the pleuropedal and visceral ganglia reached a maximum number and appeared adult-like. Our observations were supported by Yahata (1973) who demonstrated that the pleuropedal and visceral ganglia might produce and release factors that could induce spawning.

In the present study, the number of giant neurons (NR₁) increased following the development of the ganglia. In the cerebral ganglia, they increased in number in 5- and 10-month-old abalone that were assumed to be the juvenile and pre-adult stages. They reached a maximum number and appeared adult-like in 12-month-old abalone. NR₁ first appeared in the dorsal horn of the pleuope-

dal ganglia, later they were regularly found in both dorsal and ventral horns. Thus, NR₁ may proliferate relatively later than the other types of neurons (NR₂₋₄) that are abundant at an early age. This may be related to active movement due to muscular activity exhibited by abalone, as they become older.

NR₁ were more abundant in the pleuropedal ganglia than in the cerebral ganglia of *H. asinina* (Upatham et al. 1998). These cells are very large, multipolar and pyramidal in shape. Compared with the classification of neurons in the nervous system of higher vertebrates, NR₁ are similar to such large motor cells as the ventral horn motor cells of the spinal cord and Purkinje cells of the cerebellum in vertebrates. As such, they may be involved in controlling and coordinating motor activities, especially that of the pedal muscle.

ACKNOWLEDGMENTS

This research was supported financially by the Thailand Research Fund (Senior Research Scholar Fellowship to Prasert Sobhon) and BRG/04/2543. We thank Dr. Padermsak Jarayabhand of the Marine Biological Station, Chulalongkorn University, Chonburi Province, Thailand, for providing the abalone specimens.

LITERATURE CITED

- Bullock, T. H. & G. A. Horridge. 1965. Structure and function in the nervous system of invertebrates II. San Francisco: W. H. Freeman, pp. 1293–1369.
- Carroll, D. I. & S. C. Kempf. 1994. Changes occur in the central nervous system of the nudibranch *Bergia verrucornis* (Mollusca, Opisthobranchia) during metamorphosis. *Biol. Bull.* 186:202–212.
- Coggeshall, R. F. 1967. A light and electron microscope study of the abdominal ganglion of *Aplysia californica*. *J. Neurophysiol.* 30:1263–1287.
- Dillaman, R. M., A. S. M. Saleuddin & G. M. Jones. 1976. Neurosecretion and shell regeneration in *Helisoma duryi* (Mollusca, Pulmonata). *Can. J. Zool.* 54:1771–1778.
- Dogterom, R. E., H. Van Loenhout & W. P. M. Geraerts. 1983. Synchronous maturation of the female reproductive system and of the ovulation hormone-producing system in *Lymnaea stagnalis*. *Gen. Comp. Endocrinol.* 52:242–246.
- Geraerts, W. P. M. & L. H. Algra. 1976. The stimulating effect of the dorsal-body hormone on cell differentiation in the female accessory sex organs of the hermaphrodite freshwater snail *Lymnaea stagnalis*. *Gen. Comp. Endocrinol.* 29:109–118.
- Gomori, G. 1941. Observation with differential stains on human Islets of Langerhans. *Am. J. Pathol.* 17:395–406.
- Gomori, G. 1950. Aldehyde-fuchsin: A new stain for elastic tissue. *Am. J. Clin. Pathol.* 20:665–666.
- Jacob, M. H. 1984. Neurogenesis in *Aplysia californica* resembles nervous system formation in vertebrates. *Neuroscience* 4:1225–1239.
- Kempf, S. C., L. R. Page & A. Pires. 1997. Development of serotonin-like immunoreactivity in the embryos and larvae of nudibranch mollusks with emphasis on the structure and possible function of the apical sensory organ. *J. Comp. Neurol.* 386:507–528.
- Kerkut, G. A. & R. J. Walker. 1975. Nervous system. In: G. A. Kerkut and R. J. Walker, editors. *Pulmonates*. Vol. 1. London: Academic Press, pp. 165–245.
- Kruatrachue, M., V. Seebutr, J. Chivadej, P. Sretarugsa, E. S. Upatham & P. Sobhon. 1994. Development and histological characteristics of neurosecretory cells in the cerebral ganglia of *Achatina fulica* (Bowditch). *Moll. Res.* 15:29–37.
- Kruatrachue, M., A. Thongkuktakul, P. Sobhon, E. S. Upatham, C. Wanichanon, P. Sretarugsa, Y. Chitramvong & V. Linthong. 1999. The ultra-structure of neurons and neuroglia in the cerebral and pleuropedal ganglia of *Haliois asinina* Linnaeus. *Science Asia* 25:137–142.
- Lever, J., C. M. deVries & J. C. Jager. 1965. On the anatomy of the central nervous system and the location of neurosecretory cells in *Australorbis glabratus*. *Malacologia* 2:219–230.
- Marois, R. & T. J. Carew. 1997. Projection patterns and target tissues of the serotonergic cells in larval *Aplysia californica*. *J. Comp. Neurol.* 386:491–506.
- Roubos, E. W., A. Van Winkoop, C. Van der Haar & J. Van Minnen. 1988. Postembryonic development of endocrine dorsal bodies and neuroendocrine egg-laying and growth hormone producing neurons of *Lymnaea stagnalis*. *Int. J. Invertebr. Reprod. Develop.* 13:119–145.
- Smith, B. J. 1967. Correlation between neurosecretory changes and maturation of the reproductive tract of *Arion ater* (Stylommatophora, Arionidae). *Malacologia* 5(2):285–298.
- Sobhon, P., S. Apaswetakul, M. Chumoo, C. Wanichanon, V. Linthong, A. Thongkuktakul, P. Jarayabhand, M. Kruatrachue, E. S. Upatham & T. Punthong. 1999. Classification of germ cells, reproductive cycle and maturation of gonads in *Haliois asinina* Linnaeus. *Science Asia* 25:3–21.
- Thongkuktakul, A., P. Sobhon, C. Wanichanon, P. Laimek, V. Anupapsoth, P. Jarayabhand, M. Kruatrachue & E. S. Upatham. 1998. Localization of GH-, insulin, FSH, and LH-like hormones in the nerve ganglia of *Haliois asinina* Linnaeus. Changmai, Thailand: Proceedings of the Fifth International Congress on Medical and Applied Malacology, December 27–30, 1998.
- Thongkuktakul, A., E. S. Upatham, P. Sobhon, M. Kruatrachue, Y. P. Chitramvong, C. Wanichanon, T. Punthong and J. Nigamud. 2000. Histological studies of the pleuropedal ganglion, visceral ganglion and pedal cord ganglia of *Haliois asinina*. *J. Med. & Appl. Mol. Biol.* 10:111–120.
- Upatham, E. S., A. Thongkuktakul, M. Kruatrachue, C. Wanichanon, Y. P. Chitramvong, S. Sahavacharin & P. Sobhon. 1998. Classification of neurosecretory cells, neurons and neuroglia in the cerebral ganglia of *Haliois asinina* Linnaeus by light microscope. *J. Shellfish Res.* 17:737–742.
- Van Minnen, J. & G. Sokolove. 1984. Galactogen synthesis-stimulating factor in the slug, *Limax maximus*: cellular localization and partial purification. *Gen. Comp. Endocrinol.* 54:114–122.
- Yahata, T. 1973. Induced spawning of abalone (*Nordotis discus* Reeve) injected with ganglionic suspensions. *Bull. Jap. Soc. Sci. Fish.* 39:1117–1122.

Production and characterization of a monoclonal antibody against 28.5 kDa tegument antigen of *Fasciola gigantica*

Kulathida Chaithirayanon^a, Chaitip Wanichanon^a, Suksiri Vichasri-Grams^b,
Pissanee Ardseungneon^b, Rudi Grams^c, Vithoon Viyanant^{b,c}, Edward
Suchart Upatham^b, Prasert Sobhon^{a,*}

^a Department of Anatomy, Faculty of Science, Mahidol University, Rama VI Road, Bangkok 10400, Thailand

^b Department of Biology, Faculty of Science, Mahidol University, Rama VI Road, Bangkok 10400, Thailand

^c Faculty of Allied Health Science, Thammasat University, Pathumthani 12121, Thailand

Received 2 November 2001; accepted 7 May 2002

Abstract

A monoclonal antibody (MoAb) against the 28.5 kDa tegumental antigen of *Fasciola gigantica* was produced by the hybridoma technique using spleen cells from BALB/c mice immunized with the tegumental extract from adult *F. gigantica*. This MoAb was found to be of the isotype IgG₁, κ-light chain, and shown by immunoblotting to specifically react with the 28.5 kDa antigen present in the tegument, excretion–secretion material of the adult, whole-body extracts of newly excysted juveniles, 5-week-old juvenile and adult parasites. It did not cross-react with antigens from other trematode parasites, including *Schistosoma mansoni*, *Eurytrema pancreaticum* and *Paramphistomum* spp. Immunolocalization of this antigen by indirect immunofluorescence indicated that it was present as a major component of the adult tegument, particularly in its outer rim, tegumental cells, and their processes. Furthermore, the epithelium linings of the oral sucker, buccal tube, pharynx, caecal bifurcation, both male and female genital canals, which were the continuation of the tegumental-type epithelium, were also positively stained with this MoAb. A similar pattern of immunolocalization, but with weaker staining intensity, was observed in newly excysted, 5- and 7-week-old juveniles. Thus this antigen is expressed in all developmental stages of the parasite, and it could be a strong candidate for immunodiagnosis and vaccine development. © 2002 Elsevier Science B.V. All rights reserved.

Keywords: *Fasciola gigantica*; Tegument; 28.5 kDa antigen; Monoclonal antibody

1. Introduction

Up to now the main source of potential immunodiagnostic antigens in fasciolosis are the metabolic antigens released in the excretion–

* Corresponding author. Tel.: +662-245-5198; fax: +662-247-9880

E-mail address: sepsob@mahidol.ac.th (P. Sobhon).

secretion (ES) material of adult parasites (Rivera-Marrero et al., 1988; Fagbemi, 1995; Fagbemi and Guobadia, 1995; Fagbemi et al., 1995; Rodriguez-Perez and Hillyer, 1995; Sampaio-Silva et al., 1996; Fagbemi et al., 1997; Intapan et al., 1998). Most notable are the cysteine proteases against which monoclonal antibodies (MoAbs) have been produced by a number of investigators (Yamasaki et al., 1989; Fagbemi, 1995; Fagbemi and Guobadia, 1995; Viyanant et al., 1997a). Since these proteases are universal enzymes found in most parasites, MoAb against them showed high cross-reaction, and hence were not considered to be trematode-specific (Coles and Rubano, 1988) even though they showed some potential as a vaccine candidate (Estuningsih et al., 1997).

Another source of immunodiagnostic antigens is the tegumental proteins. Poopyruchapong et al. (1990) have shown that the tegumental (TA) antigens of *Opisthorchis viverrini* were highly specie-specific, and could give a satisfactory result in immunodiagnosis. Several other studies have also demonstrated common as well as specie-specific protein antigens in the tegument and surface of different stages in the life cycle of *Schistosoma* (Rogers et al., 1988; Goes et al., 1989). MoAbs have also been raised against antigens present in the tegumental syncytium and the glycocalyx of juvenile *Fasciola hepatica* and because of their high specificities they could be used for specific immunolocalization studies (Hanna and Trudgett, 1983). Krailas et al. (1999) have produced an MoAb against a 66 kDa surface TA of adult *Fasciola gigantica*. This antigen could be detected as a circulating antigen in the blood of cattle experimentally and naturally infected with *F. gigantica*. Therefore, tegument antigens are considered to be more specie- and genus-specific, and could be used for rapid immunodiagnosis even at an early stage of infection (Viyanant et al., 1997b). In this study, we have produced an MoAb specific for a 28.5 kDa TA of *F. gigantica*. Due to its prevalence in the tegument and high specificity, this antigen may have high potential for immunodiagnosis and vaccine development.

2. Material and methods

2.1. Preparation of antigens

Adult *F. gigantica* were collected from the bile ducts and gall bladders of cattle killed at local slaughterhouses. Other trematode parasites, namely *Eurythrema pancreaticum* and *Paramphistomum* spp., were collected from the same cattle for cross-reaction studies. Adult *Schistosoma mansoni* were obtained from mice 8 weeks after infection with cercariae. All parasite samples were washed three times with Hank's balanced salt solution (HBS) to remove all traces of contaminating blood and bile.

2.1.1. Whole body (WB) antigens of adult and juvenile parasites

Whole adult parasites (all species) were homogenized in 0.01 M phosphate buffer saline (PBS), pH 7.2, and extracted overnight with continuous rotation at 4 °C. The suspensions were centrifuged at 5000 × g, 4 °C, for 20 min to get rid of the eggs and the supernatants were collected. Protein concentrations were determined by Lowry's method (Lowry et al., 1951). These extracts were stored at –70 °C until use in subsequent experiments.

In addition, whole body extracts were prepared from newly excysted juveniles (NEJ) and 5-week-old juveniles (JP) collected from mice prior infected with *F. gigantica* metacercariae.

2.1.2. TA antigens of adult *F. gigantica*

To obtain TA antigens, adult worms were extracted with a non-ionic detergent (1% Triton X-100 in 0.05 M Tris buffer, pH 8.0, 0.01 M EDTA, 0.15 M NaCl) for 20 min at room temperature. Shedding of the tegument was monitored under a light microscope and at the end of extraction the supernatant was collected and devoided of contaminating eggs by centrifugation at 5000 × g for 20 min. The supernatant that contained soluble TA antigens was collected and dialyzed against 0.01 M PBS overnight at 4 °C, using Spectra/Por 1 dialysis membrane (Thomas Scientific) with molecular weight cut off at 6–8 kDa. The protein concentration was determined

by Lowry's method, and the protein solution was stored at -70°C until use in later experiments.

2.1.3. Excretory–secretory (ES) antigens of adult *F. gigantica*

ES antigens were prepared by incubating newly collected, living adult *F. gigantica* in PBS for 3 h at room temperature. After incubation, the culture medium was centrifuged at $5000 \times g$ for 20 min at 4°C to remove the parasites' eggs from the culture medium. The supernatant was then filtered through $0.22\ \mu\text{m}$ Millipore filter. The protein concentration was measured by Lowry's method and the protein solution was stored at -70°C until further use.

2.2. Production and screening of MoAbs

Female BALB/c mice were immunized by subcutaneous injections of $30\ \mu\text{g}$ TA antigen of *F. gigantica* in complete Freund's adjuvant. The second injection of the same dose of extracted proteins in incomplete Freund's adjuvant was given 3 weeks later. The final boost was given by intravenous injection with $60\ \mu\text{g}$ of this antigen in $100\ \mu\text{l}$ PBS, 2 weeks later. To produce hybridomas, spleen cells from BALB/c mice immunized with TA antigen were fused with myeloma cells (P3-X63-Ag8.653). The MoAbs produced by the hybridoma clones were screened by indirect ELISA. A peroxidase-conjugated rabbit anti-mouse immunoglobulin (DAKO, Denmark) at dilution 1:1000 and *O*-phenylenediamine (OPD) were used for enzymatic detection. The optical density was measured at 492 nm in an ELISA reader (Titertek Multiscan Flow Laboratories Pty Ltd., Australia). The specific MoAb class and subclass were determined by an enzyme immunoassay using the Mouse Typer Sub-Isotyping Kit (Bio-Rad).

2.3. Immunoblotting and detection

ES, TA, WB, NEJ and JP antigens of *F. gigantica* were separated in a 12.5% SDS-PAGE according to Laemmli (1970) and transferred onto nitrocellulose membranes for immunodetection by selected positive monoclones. Peroxidase-conju-

gated rabbit anti-mouse IgG at dilution 1:1000 and diaminobenzidine (DAB; Sigma) were used for enzymatic detection of the 28.5 kDa antigen. Serum of a naturally infected cow (CIS) and fetal calf serum (FCS) were used as positive and negative controls. For the detection of CIS-antigen complex, a peroxidase-conjugated rabbit anti-cow IgG was used as the secondary antibody.

In the cross-reaction study, WB antigens from *F. gigantica* and other trematode parasites were separated and analyzed with MoAb as described above.

2.4. Immunofluorescence

The distribution of the 28.5 kDa antigen in the tissues of various developmental stages of *F. gigantica* was detected by indirect immunofluorescence using the specific MoAb (6E9-1E) identified in the immunoblotting experiment. Consecutive frozen sections of each stage of the parasite including, metacercariae, 5- and 7-week-old juveniles obtained from metacercaria-infected mice, and adult, were fixed with acetone at -10°C for 10 min. After washing with 10 mM PBS, pH 7.4, for 5 min, the sections were incubated with 0.1% glycine in 10 mM PBS, and subsequently in 4% BSA in 10 mM PBS to block nonspecific binding, for 15 and 30 min, respectively. Finally, the sections were incubated with the specific MoAbs for 60 min at room temperature. The sections were rinsed three times with 10 mM PBS, pH 7.4, for 5 min each, and treated with fluorescein isothiocyanate (FITC)-conjugated goat anti-mouse IgG, diluted to 1:100 with 0.05% Tween-PBS, for 30 min at room temperature. The treated sections were rinsed thoroughly with PBS and mounted on glass slides in glycerol–PBS (9:1), and then examined under a Nikon HB 10101 AF fluorescence microscope.

3. Results

3.1. MoAbs against 28.5 kDa TA

Three hybridoma clones (6E9-1E, 8B11-2B and 8E5-1A) were found by ELISA and by immuno-

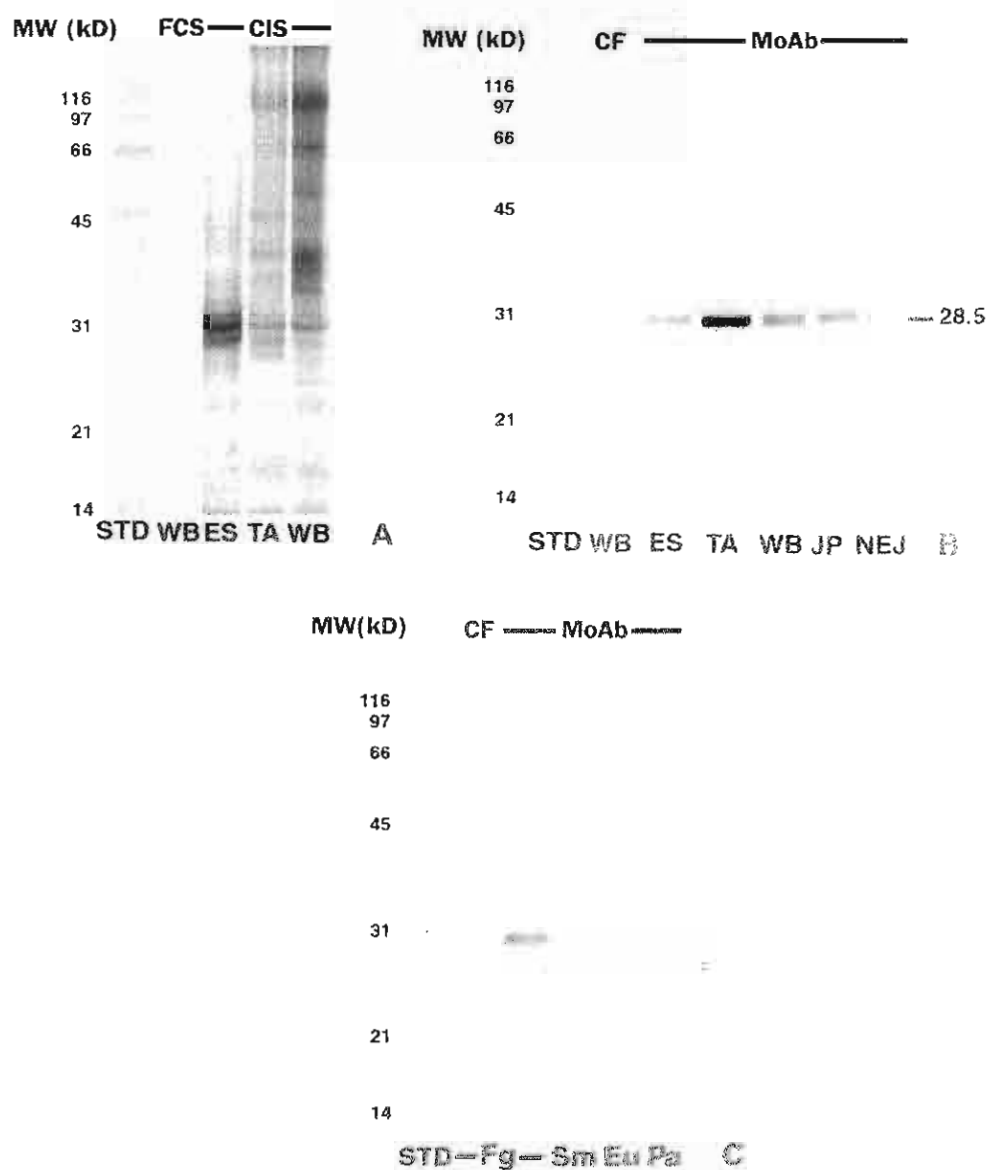


Fig. 1. (A) Immunoblots of adult *F. gigantica* WB, ES and TA antigens with FCS and CIS. STD lane contains the standard molecular weights. (B) Immunoblots of ES, TA, WB antigens of adult *F. gigantica*, 5-week-old juvenile (JP) and NEJ with MoAb clone 6E9-1F. Only the 28.5 kDa antigen was detected in each fraction of the antigens. Molecular weight marker is shown in lane 1 (STD). Lane 2 is WB antigens blotted with the hybridoma culture fluid (CF) as a control. (C) Immunoblot analysis of the cross-reactivities of MoAb 6E9-1F with WB antigens from *F. gigantica* (Fg), *S. mansoni* (Sm), *Eurytrema* spp. (Eu) and *Paramphistomum* spp. (Pa). The 28.5 kDa antigen could be detected only in *F. gigantica* and no cross-reaction of MoAb was observed in other lanes. Lane 1 contained standard molecular weights and lane 2 contained *F. gigantica* WB antigens blotted with CF.

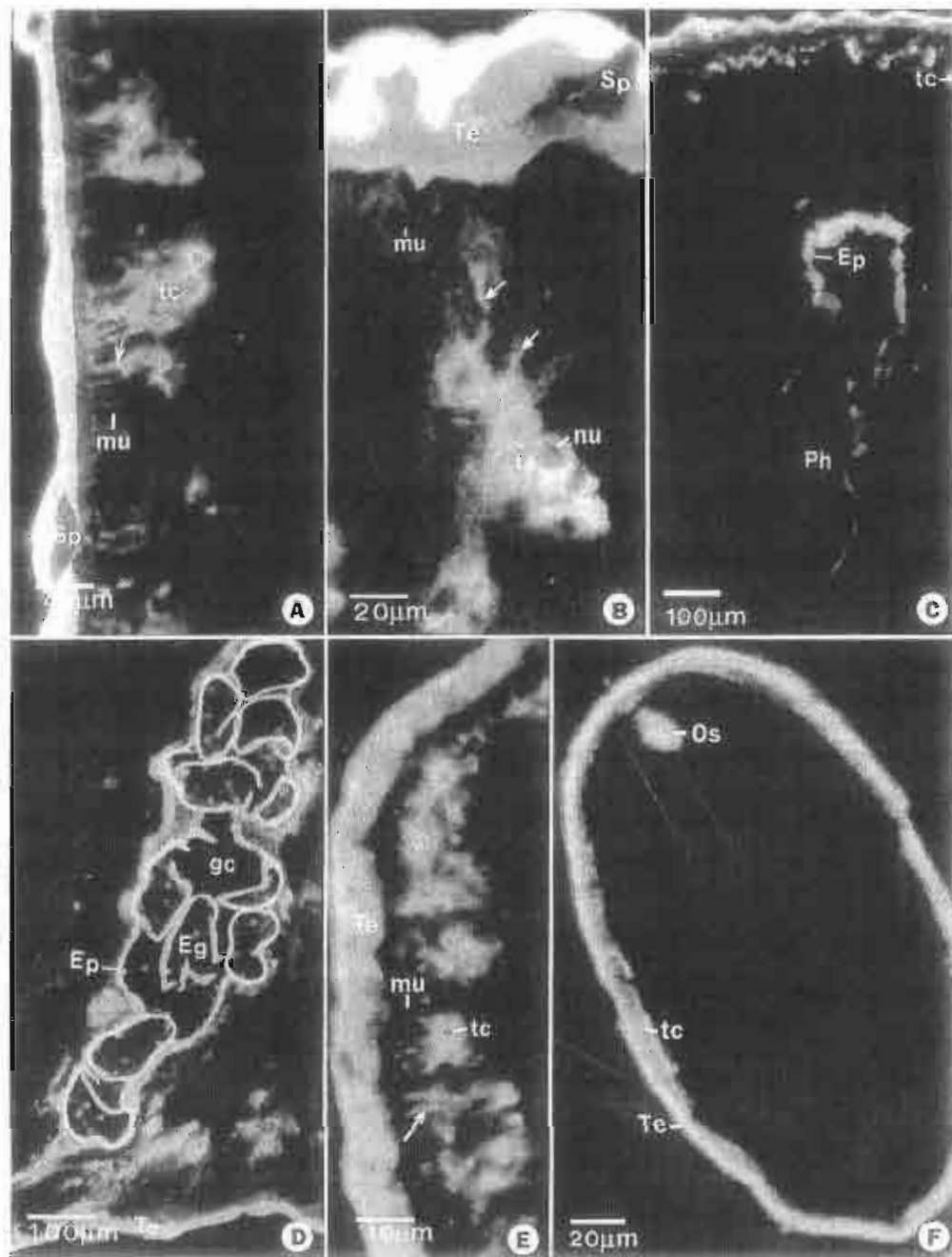


Fig. 2.

blotting to produce antibodies which have specificity against the 28.5 kDa TA. Among these clones, MoAb 6E9-1E has the highest titer and tested to be of IgG₁ isotype. Hence, it is the only clone used in subsequent experiments.

Antigens in the TA and WB fractions of adult *F. gigantica* that were detected in immunoblots by the serum of a CIS were clustered at four regions, i.e. 116–97, 66–40, 31–26 and 17–14 kDa, while the ES fractions had major bands at 45, 31–26 and 17–14 kDa (Fig. 1A). In immunoblots of ES, TA and WB antigens, MoAb 6E9-1E detected only a single 28.5 kDa antigen in the ES, TA and WB fractions (Fig. 1B, lane 3–5). The observed staining intensity of the band ranged from that in TA, WB to ES, respectively. Since each lane contained 10 µg of protein and the duration of staining was identical, it could be surmised that this antigen was highly concentrated in the tegument, and might be partially released into ES which had a lower concentration.

Furthermore, it was found that this antigen could also be detected in the whole body fractions of newly excysted juvenile (Fig. 1B, lane 7) and 5-week-old parasites (Fig. 1B, lane 6), but with much lower intensity when compared to the TA fraction of the adult parasites.

3.2. Cross-reactions with other trematodes' antigens

In immunoblots with WB fractions of *F. gigantica* and other parasites, including *S. mansoni*, *E. pancreaticum* and *Paramphistomum* spp., using MoAb 6E9-1E as probe, the 28.5 kDa antigen

could be detected only in *F. gigantica* and not in the other parasites (Fig. 1C).

3.3. Immunolocalization of the 28.5 kDa antigens

In indirect immunofluorescence staining of frozen sections of adult *F. gigantica* with MoAb 6E9-1E as primary antibody, a high intensity of fluorescence was observed in the tegument especially at its outer rim, the tegument cells and their processes (Fig. 2A and B). In addition, this MoAb also stained the epithelium linings of the oral sucker, the digestive tract proximal to the caecal bifurcation, and both male and female genital canals (Fig. 2C and D). A similar pattern and intensity of immunofluorescence was observed in 7- and 5-week-old parasites (Fig. 2E). In comparison, the newly excysted juvenile exhibited only weak staining in the tegument which appeared as a thin line and in the scanty cytoplasm of tegument cells (Fig. 2F).

4. Discussion

In this study, we produced a specific MoAb against a 28.5 kDa TA of *F. gigantica*. The isotype of this MoAb is IgG₁, κ-light chain. Immunolocalization studies indicated that this antigen is a major antigen in the tegument and the cytoplasm of the tegumental cells of all stages of the parasite. In the adult parasite, this antigen is highly concentrated in the outer rim of the tegument.

Recent ultrastructural studies of the tegument of adult *F. gigantica* by our group showed that the tegumental granules, which contribute to the

Fig. 2. Immunofluorescence staining of frozen sections of the adult (A–D), 5-week-old juvenile (E) and newly excysted juvenile (F) of *F. gigantica*, using MoAb clone 6E9-1E as primary antibody and FITC-conjugated goat anti-mouse IgG as secondary antibody. The magnifications are indicated by micrometer bars (µm). (A, B) Low- and high-power magnifications showing intense staining of the adult tegument (Te), particularly at its outer rim, and the cytoplasm of tegumental cells (tc) and their processes (arrows), while the tegument cells' nuclei (nu), the tegumental spines (sp) and nearby muscle cells (mu) and stromal cells are not stained. (C) Cross-section of the pharynx (Ph) showing strong staining at the outer portion of its epithelium (Ep). (D) Cross-section of the female genital canal (gc) showing intense fluorescence in its epithelium (Ep), while the eggshell (Eg) shows non-specific yellow-orange fluorescence. (E) High magnification of the tegument of a 5-week-old juvenile, showing bright staining of the tegument (Te) and the cytoplasm of tegumental cells (tc) that lie in rows underneath the muscle layers (mu), and their numerous processes (arrows) running between muscle cells to join with the tegument (Te). (F) High magnification of the newly excysted juvenile showing positive staining in the tegument which appears as a thin line (Te) and cytoplasm of the tegumental cell (tc). The epithelial lining of the oral sucker (Os) is also stained.

formation of the surface membrane, are produced in the tegumental cells and are transported via the cells' processes to be concentrated in the outer rim of the tegument underneath the surface membrane (Sobhon et al., 2000). From the similarity between the staining pattern of MoAb and the concentration of the tegumental granules in the outer rim of the tegument, it is possible that the 28.5 kDa antigen may be part of the tegumental granules and the surface membrane. This suggestion has to be confirmed by immunoelectron microscopy, which is currently being carried out in our laboratory. In addition to the tegument, the epithelial linings of the adult genital canals and digestive tract from the oral sucker to the caecal bifurcation were also intensely stained by this MoAb, while the caecal epithelium distal to the bifurcation was not stained. This implies that the epithelial cells of the former also expressed this antigen whilst those of the caecal epithelium did not. Histological examination revealed that the epithelium of the genital canal and the anterior part of the digestive tract proximal to the bifurcation, consists of a syncytial layer with similar characteristics as that of the tegument (Sriburee, 2000).

The 28.5 kDa antigen could also be detected by MoAb in the ES material of the adult parasites. This implies that the antigen may be a surface antigen that is released from the tegument together with other tegument proteins (Viyanant et al., 1997b; Krailas et al., 1999) and metabolic enzymes such as proteases which are released from the caecum (Viyanant et al., 1997a). The release of the former may occur as a result of the continuous renewal of the surface membrane and associated glycocalyx as reported to normally occur in trematode parasites that inhabit the bile like *F. hepatica* (Hanna, 1980; Duffus and Franks, 1981). This is one of the mechanisms that trematode parasites may use to prevent the attachment of antibodies and immune effector cells of the host to their surfaces (Fairweather et al., 1999).

Apart from its strong presence in adult parasites, the 28.5 kDa antigen was also detected in the newly excysted and juvenile parasites as shown in both immunoblotting and immunofluorescence experiments. This suggests that it may be a key

component of the tegument and/or surface membrane that is expressed early in the younger stages. Furthermore, this antigen is specific to *F. gigantica* since no cross-reactivities were detected with antigens of other trematode parasites. Hence, it could be considered as a strong candidate antigen for immunodiagnosis since it is more specific than other reported metabolic antigens.

Acknowledgements

This work was supported by the Thailand Research Fund (Senior Research Scholar grant to Prasert Sobhon) and the National Center for Genetic Engineering and Biotechnology, NSTDA (Grant No. BT-B-06-2B-14-004 to Vithoon Viyanant).

References

- Coles, G.C., Rubano, D., 1988. Antigenicity of a proteolytic enzyme of *Fasciola hepatica*. J. Helminthol. 62, 257–260.
- Duffus, W.P.H., Franks, D., 1981. The interaction in vitro between bovine immunoglobulin and juvenile *Fasciola hepatica*. Parasitology 82, 1–10.
- Estuningsih, S.E., Smooker, P.M., Wiedowari, E., Widjajanti, S., Vaziano, S., Partoutomo, S., Spithill, T.W., 1997. Evaluation of antigens of *Fasciola gigantica* as vaccine against tropical fasciolosis in cattle. Int. J. Parasitol. 27, 1419–1428.
- Faghemi, B.O., 1995. Development and characterization of a monoclonal antibody reactive with a 28 kDa protease of *Fasciola gigantica*. Vet. Parasitol. 57, 351–356.
- Faghemi, B.O., Guobadia, E.E., 1995. Immunodiagnosis of fasciolosis in ruminants using a 28-kDa cysteine protease of *Fasciola gigantica* adult worms. Vet. Parasitol. 57, 309–318.
- Faghemi, B.O., Obaristagbon, L.O., Mbulu, J.V., 1995. Detection of circulating antigen in sera of *Fasciola gigantica*-infected cattle with antibodies reactive with a *Fasciola*-specific 88 kDa antigen. Vet. Parasitol. 58, 235–246.
- Faghemi, B.O., Aderibigbe, O.A., Guobadia, E.E., 1997. The use of monoclonal antibody for the immunodiagnosis of *Fasciola gigantica* infection in cattle. Vet. Parasitol. 69, 231–240.
- Fairweather, I., Threlkeld, L.T., Hanna, R.E.B., 1999. Development of *Fasciola hepatica* in the mammalian host. In: Dalton, J.P. (Ed.), Fasciolosis. CABI Publishing, Wallingford, UK, pp. 47–111.
- Goes, A.M., Rocha, R.S., Gazzinelli, G., Dougherty, B.L., 1989. Production and characterization of human monoclonal

- antibodies against *Schistosoma mansoni*. *Parasite Immunol.* 11, 695–711.
- Hanna, R.E.B., 1980. *Fasciola hepatica*: glycocalyx replacement in the juvenile as a possible mechanism for protection against host immunity. *Exp. Parasitol.* 50, 103–114.
- Hanna, R.E.B., Trudgett, A.G., 1983. *Fasciola hepatica*: development of monoclonal antibodies and their use to characterize a glycocalyx antigen in migrating flukes. *Parasite Immunol.* 5, 409–425.
- Intapun, P.M., Maleewong, W., Wongkham, C., Tomanakarn, K., Leamviteevanich, K., Pipitgool, V., Sukolapong, V., 1998. Excretory-secretory antigenic components of adult *Fasciola gigantica* recognized by infected human sera. *Southeast Asian J. Trop. Med. Public Health* 29, 579–583.
- Krailas, D., Viyanant, V., Ardseungnoen, P., Sobhon, P., Upatham, E.S., Keawjam, R., 1999. Identification of circulating antibodies in fasciolosis and localization of 66 kDa antigenic target using monoclonal antibodies. *Asian Pac. J. Allergy Immunol.* 17, 53–58.
- Laemmli, U.K., 1970. Cleavage of structural proteins during the assembly of the head of bacteriophage. *Nature* 227, 680–685.
- Lowry, O.H., Rosebrough, N.J., Farr, A.L., Randal, R.J., 1951. Protein measurement with the folin phenol reagent. *J. Biol. Chem.* 193, 265–275.
- Poopyruchapong, N., Viyanant, V., Upatham, E.S., Srivatana-kul, P., 1990. Diagnosis of opisthorchiasis by enzyme-linked immunosorbent assay using partially purified antigens. *Asian Pac. J. Allergy Immunol.* 8, 27–231.
- Rivera-Marrero, C.A., Santiago, N., Hillyer, G.V., 1988. Evaluation of immunodiagnostic antigens in the excretory-secretory products of *Fasciola hepatica*. *J. Parasitol.* 74, 646–652.
- Rodriguez-Perez, J., Hillyer, G.V., 1995. Detection of excretory-secretory circulating antigens in sheep infected with *Fasciola hepatica* and with *Schistosoma mansoni*. *Vet. Parasitol.* 56, 57–66.
- Rogers, M.V., Davern, K.M., Smythe, J.A., Mitchell, G.F., 1988. Immunoblotting analysis of the major integral membrane protein antigens of *Schistosoma japonicum*. *Mol. Biochem. Parasitol.* 29, 77–88.
- Sampaio-Silva, M.L., Da-Costa, J.M., Da-Costa, A.M., Pires, M.A., Lopes, S.A., Castro, A.M., Monjour, L., 1996. Antigenic components of excretory-secretory products of adult *Fasciola hepatica* recognized in human infections. *Am. J. Trop. Med. Hyg.* 54, 146–148.
- Sobhon, P., Dangprasert, T., Chuanchaiyakul, S., Meepool, A., Khawsuk, W., Wanichanon, C., Viyanant, V., Upatham, E.S., 2000. *Fasciola gigantica*: ultrastructure of the adult tegument. *Sci. Asia* 26, 137–148.
- Sriburee, S., 2000. Characterization of epithelial cells and the expression of cathepsin L gene in the digestive tract of *Fasciola gigantica*. M. Sc. Thesis. Mahidol University, Bangkok, Thailand.
- Viyanant, V., Upatham, E.S., Sobhon, P., Krailas, D., Ardseungnoen, P., Anatawara, S., 1997. Development and characterization of monoclonal antibodies against excretory-secretory antigens of *Fasciola gigantica*. *Southeast Asian J. Trop. Med. Public Health* 28, 128–133.
- Viyanant, V., Krailas, D., Sobhon, P., Upatham, E.S., Kusamran, T., Chompoochan, T., Thammasart, S., Prasittirat, P., 1997. Diagnosis of cattle fasciolosis by the detection of a circulating antigen using a monoclonal antibody. *Asian Pac. J. Allergy Immunol.* 15, 153–159.
- Yamasaki, H., Aoki, T., Oya, H., 1989. A cysteine protease from the liver fluke *Fasciola* spp.: purification, characterization, localization and application to immunodiagnosis. *Jpn. J. Parasitol.* 38, 373–384.

Production and Characterization of a Monoclonal Antibody against Recombinant Glutathione S-Transferase (GST) of *Fasciola gigantica*

Witoon Khawsuk¹, Nantawan Soonklang⁴, Rudi Grams³, Suksiri Vichasri-Grams², Chaitip Wanichanon¹, Ardool Meepool¹, Kulathida Chaithirayanon¹, Pissanee Ardseungneon², Vithoon Viyanant^{2,3}, Suchart Edward Upathum⁵ and Prasert Sobhon¹

Glutathione-S-transferases (GSTs) are a family of multifunctional enzymes that occur in most forms of life and are considered to serve in the intracellular detoxification of oxygen free radicals, which may be generated by mutagens, carcinogens, other noxious chemical substances and even from ordinary metabolic reactions. GSTs are also proposed to play similar roles in helminthes, especially in protecting the parasites by inactivating the reactive oxygen free radicals and nitric oxide generated by the hosts' immune effector cells.^{1,2,3} In mammals, a number of cytosolic GSTs have been shown to belong to four homologous multigene families designated α , μ , π and θ . The GST isoenzymes within each class have a high level of sequence conservation but can be distinguished by the difference in molecular weights, isoelectric points, immunological properties and specific substrate affinities.⁴ In *F. hepatica*,^{1,5} *S. mansoni*^{6,7} and *S. japonicum*^{8,9,10} GST isozymes in the α class and the even more abundant μ classes have

SUMMARY A monoclonal antibody (MoAb) against a recombinant glutathione S-transferase (rGST) of *F. gigantica* was produced in BALB/c mice. Reactivity and specificity of this monoclonal antibody was assessed by ELISA and immunoblotting. Six stable clones, namely 3A3, 3B2, 3C6, 4A6, 4B1 and 4D6 were obtained. All these MoAb reacted with rGST and native GST at a molecular weight of 28 kDa and found to be IgG₁, κ -light chain isotypes. These MoAb cross-reacted with *Schistosoma mansoni* and *Schistosoma japonicum* antigens at molecular weights of 28 and 26 kDa, respectively, but no cross-reactions were detected with antigens of *Eurytrema* and *Paramphistomum* spp. The localization of GST in metacercaria, 7-week-old juvenile and adult *F. gigantica* was performed by immunofluorescence technique, using MoAb as well as polyclonal antibody (PoAb) to the native protein as probes. In general, all clones of MoAb gave similar results and the pattern was quite similar to staining by PoAb. The fluorescence was intense, which implied the presence of a high concentration of GST in the parenchymal tissue in all stages of the parasite. However, the parenchymal cells were not evenly stained which implied the existence of subpopulations of this cell type with regard to GST production and storage. In addition, in adult and juvenile stages a moderate fluorescence was present in the basal layer of the tegument, while light fluorescence was observed in the caecal epithelium, cells in the ovary, testis and vitelline gland of the adult. In the metacercaria stage, in addition to parenchymal tissue, the tegument and tegumental cells were stained relatively more intense with MoAb and PoAb than in other stages.

been characterized, and they show similarities in molecular masses and cross-reaction. In immunolocalization studies, GSTs were detected in all developmental stages of *S. mansoni*,⁷ except in the intra-uterine immature eggs. The antigen was reported to be present in the tegument, protonephridial cells, sub-

tegumental parenchyma of male and

From the ¹Department of Anatomy, ²Department of Biology, Faculty of Science, Mahidol University, Bangkok, Thailand, ³Department of Medical Technology, ⁴Faculty of Allied Health Sciences, ⁵Department of Preclinical Science, Faculty of Medicine, Thammasat University, Pathumthani, Thailand, ⁶Department of Medical Science, ⁷Faculty of Science, Burapha University, Chonburi, Thailand
Correspondence: Prasert Sobhon

female, and the dorsal tubercles of male tegument. Immature germinal cells in both sexes and the ootype in the female genital system were also found to contain GSTs. In adult *S. japonicum*¹⁰ the enzyme was detected in parenchymal cells but not on the surface nor within the tegument matrix or caecal epithelium. In comparison, in *F. hepatica* GST isoenzymes were specifically confined to parenchyma, caecal epithelium¹ and the inner zone of the tegument syncytium,⁵ while they were detected only in the parenchyma and excretory ducts of the newly excysted juvenile parasites.⁷ A similar study has not yet been performed in *F. gigantica*. As a result of their highly vital role in protecting the parasites from attacks by hosts' immune effector cells, GSTs have been proposed as one of the ideal targets for immunological intervention in a variety of host-parasite systems, especially infections by *Schistosoma* and *Fasciola* spp.^{11,12,13} The isolation and purification of GST from native source is a difficult and laborious process, hence recombinant protein has been synthesized by molecular cloning.^{5,14} In the present study, a monoclonal antibody against recombinant *F. gigantica* GST was produced, characterized, used for probing the distribution of GST in this parasite's tissues at various stages of the life cycle. The cross reactivities with other trematode parasite antigens were tested in order to probe for their possible applications in immunodiagnosis and vaccine development.

MATERIALS AND METHODS

Parasite samples

Adult *F. gigantica* were removed from the bile ducts and gall bladders of condemned bovine livers at slaughterhouses. Other trematode parasites collected from the same group of cattle for cross reaction studies included *Paramphisto-*

mum spp. from the rumen and *Eurytrema pancreaticum* from the pancreas. *S. mansoni* and *S. japonicum* were collected from mice infected with cercariae 8 weeks earlier. All parasite specimens were washed three times with Hank's balanced salt solution (HBS) containing 100 U/ml penicillin and 100 mg/ml streptomycin to remove all traces of blood, bile and contaminating microorganisms.

The metacercariae were obtained from infected *Lymnae ollula* snails. The snails were infected with miracidia and allowed to develop sporocysts and cercariae. The cercariae were shed from the snails and settled on 5" x 5" cellophane sheets, on which cercariae encysted themselves and developed into metacercariae. At day 45 metacercariae were examined under the stereomicroscope, brushed from the cellophane papers and washed several times with 0.85% normal saline and kept at 4°C until use.

Seven-week-old juveniles were obtained from infected male Swiss albino mice, each of which was orally infected with 20 metacercariae. The juveniles were collected from the liver in the seventh week after the infection, and washed several times with 0.85% normal saline before being used further.

Excretory-secretory antigen (ES) of adult *F. gigantica*

The ES-antigen was prepared by incubating freshly collected, living adult parasites in Hank's balanced salt solution (Gibco, USA) containing 10 mM phenylmethylsulfonyl fluoride (PMSF) and 10 mM EDTA at room temperature for 3 hours. The parasite eggs in the culture medium were removed by centrifugation at 5,000 x g for 20 minutes at 4°C. The supernatant was dialyzed in 0.01M PBS, pH 7.2 at 4°C for 24 hours using Spectra/Por 1 dialysis membrane (Thomas Sci-

entific, USA) with molecular weight cut-off at 6 to 8 kDa. Then it was lyophilized, and kept at -20°C until use.

Tegumental antigen (TA) of adult *F. gigantica*

TA was obtained by extraction from live adult parasites with 1% Triton X-100 in Tris-HCl buffer, pH 8, for 30 minutes at room temperature. The extracting solution was collected and centrifuged at 5,000 x g for 20 minutes at 4°C to remove the parasite eggs which might be released during the extraction. The supernatant containing TA was collected and dialyzed in 0.01 M phosphate buffered saline (PBS), pH 7.2, at 4°C for 24 hours using Spectra/Por 1 membrane before it was lyophilized and kept at -20°C until use.

Whole body antigen (WB) of parasites

Whole adult parasites (*F. gigantica* and other trematodes) were homogenized in 0.01 M PBS, pH 7.2, which contained 0.5% Triton X-100, 10 mM PMSF and 10 mM EDTA, and extracted overnight with continuous rotation at 4°C. The suspensions were centrifuged at 5,000 x g, 4°C, for 20 minutes and the supernatants were collected, lyophilized, and stored at -20°C until use.

The protein contents of all fractions were determined by modified Lowry's method.¹⁵

Preparation of *F. gigantica* rGST

A 657 bp cDNA fragment encoding a GST of *F. gigantica* was cloned by RT-PCR.¹⁴ It was reamplified by PCR to introduce a *Nde* I recognition sequence at the 5' end of the fragment. The reamplified GST DNA fragment was inserted in pBluescript SK(-) (Stratagene) and, after sequence verification, isolated

from the vector by digestion with the restriction endonucleases *Nde* I and *Bam*HI. Subsequently, it was subcloned into the *Nde* I and *Bam*HI sites of the expression vector pET-21a (Novagene). The subcloning procedure ensured that the expressed recombinant GST contained no additional amino acids as both start and stop codons were provided by the inserted DNA. Upon induction by IPTG (1 mM) rGST was detected by SDS-PAGE analysis in the soluble protein fraction. It was, thereafter, purified by affinity using the Redi-Pack GST purification Module (Pharmacia) following the protocol of the manufacturer.

Production of monoclonal antibodies (MoAb) against *F. gigantea* rGST

BALB/c mice were immunized subcutaneously with *F. gigantea* rGST in complete Freund's adjuvant at a dose of 25 µg in 100 µl per mouse. The second injection with a similar dose of the recombinant protein in incomplete Freund's adjuvant was given 3 weeks later. A final boost of 25 µg of protein in 100 µl PBS was given intravenously 2 weeks later. Hybridomas were produced by fusion of spleen cells from BALB/c mice immunized with *F. gigantea* rGST and mouse myeloma cells (P3/x63-Ag8). The hybridoma cells that grew successfully in the culture were monocloned by the limiting dilution method. Only the hybridoma clones that produced high titers of antibodies against rGST, as screened by indirect ELISA, were selected for immunoblotting. The antibody isotypes were determined by ELISA using the Mouse MonoAb-ID kit (ZYMED Laboratories, USA).

Immunoblotting

Immunoblotting was performed as described previously.¹⁰ Briefly, rGST, TA, ES, and WB an-

tigens were separated in 12.5% SDS-PAGE and blotted onto nitrocellulose membranes. As positive controls, the antigenic bands in each fraction were detected by immune sera of naturally infected cattle (CIS). Strips containing similar antigenic fractions were also screened by MoAbs and PoAb (rabbit anti *F. gigantea* GST- a gift from Dr. Terry Spithill, Monash University, Australia). For negative controls, culture fluid (CF) and normal mouse serum (NMS) were used. Antigenic molecules that reacted with CIS were detected by peroxidase-conjugated rabbit anti-bovine immunoglobulin, whereas the MoAb-antigen and PoAb-antigen complexes were detected by peroxidase-conjugated rabbit anti-mouse- and goat anti-rabbit IgG, respectively. The reaction was visualized by further incubation in 3,3' diaminobenzidine (DAB) and H₂O₂.

Immunolocalization of GST

Consecutive frozen sections of *F. gigantea* at each developmental stages (metacercaria, 7-week-old juvenile and adult) were cut in a cryostat and fixed with acetone at -10°C for 10 minutes. After washing with 10 mM PBS, pH 7.4, for 5 minutes, the sections were incubated with 0.1% glycine in 10 mM PBS, and subsequently with 4% BSA in 10 mM PBS to block nonspecific binding for 15 and 30 minutes, respectively. Thereafter, the sections were incubated with the MoAb or PoAb for 1 hour at room temperature and then rinsed 3 times with 10 mM PBS, pH 7.4, for 5 minutes each. They were finally incubated with fluorescein isothiocyanate (FITC)-conjugated goat anti-mouse (for MoAb) or goat anti-rabbit (for PoAb) IgG for 30 minutes at room temperature. Finally, the treated sections were rinsed thoroughly with PBS, mounted in glycerol-PBS (9:1), and then observed under a Nikon HB 10101 AF fluorescence microscope.

RESULTS

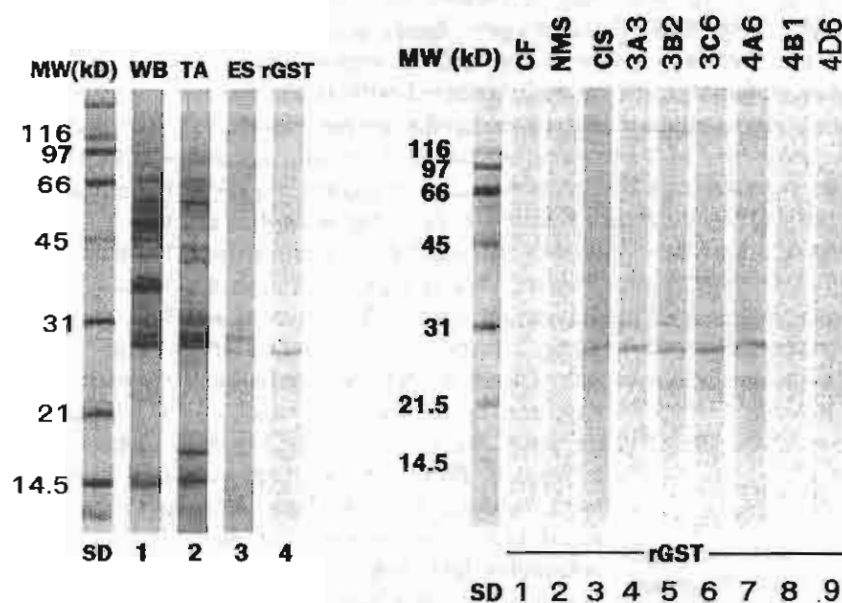
Characterization of *F. gigantea* antigens by SDS-PAGE

F. gigantea proteins in the WB and the TA fractions were similar in appearance, and appeared to be highly complex and consisting of a vast number of bands ranging in molecular weights (MW) from below 14.5 kDa to more than 116 kDa (Fig. 1A). The major protein bands of the WB fraction which showed intense staining were at 66, 52, 37, 28 and 14.5 kDa while minor bands were found at 57, 45, 42 and 29 kDa. The tegumental antigens showed major bands at 57, 43, 41, 29, 28, 18 and 14.5 kDa. In contrast to the TA and WB, the ES fraction showed much fewer bands with the two most predominant ones at MW of 28 and 29 kDa; in addition a few light bands at high MW of 66, 64 and 58 and low MW of 14.5 kDa. The rGST appeared as a single band at 28 kDa (lane 4, Fig. 1A).

Monoclonal antibodies against rGST

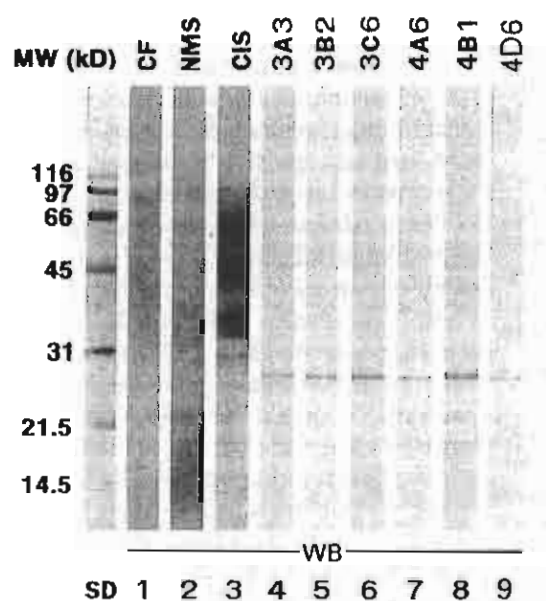
Six stable clones of MoAb, designated 3A3, 3B2, 3C6, 4A6, 4B1, 4D6 were selected and expanded in culture flasks to obtain large volume of MoAb which were then gathered for further experiments. All MoAb exhibited specific binding to the rGST band of 28 kDa, although with varying intensities (Fig. 1B). The immunoglobulin classes and sub-isotypes of all MoAb selected were found to be kappa-IgG₁.

When tested by WB from the adult *F. gigantea*, all MoAb reacted with a single native band at 28 kDa, which also reacted with PoAb (Fig. 1C; 2A). When tested against WB, TA and ES fractions all MoAbs exhibited similar patterns as illustrated by the reaction of clone



A

B



C

Fig. 1 (A) Coomassie blue stained 12.5% SDS-PAGE of *F. gigantica* antigens: lane 1-whole body fraction (WB); lane 2-tegument fraction (TA); lane 3-excretory-secretory fraction (ES); lane 4-recombinant GST (rGST). (B) Immunoblotting patterns of rGST reacted with myeloma culture fluid-CF (lane 1), normal mouse serum-NMS (lane 2), cattle infected serum-CIS (lane 3), MoAb 3A3 (lane 4), 3B2 (lane 5), 3C6 (lane 6), 4A6 (lane 7), 4B1 (lane 8) and 4D6 (lane 9). (C) Immunoblotting patterns of *F. gigantica* WB antigens reacted with myeloma CF (lane 1), NMS (lane 2), CIS (lane 3), MoAb 3A3 (lane 4), 3B2 (lane 5), 3C6 (lane 6), 4A6 (lane 7), 4B1 (lane 8) and 4D6 (lane 9). SD = standard molecular weights.

3A3, which reacted intensely with a single band in ES and WB at MW 28 kDa (Fig. 2A). In contrast, this band appeared very light in the TA fraction. When PoAb against native GST was tested against the WB, TA and ES fractions from adult *F. gigantica*, the PoAb also reacted with the native protein at 28 kDa which appeared as a doublet (Fig. 2A). In addition, there was another positive band at 24 kDa in WB against TA which was also detected by PoAb (lanes 8, 9, Fig. 2A). In the cross-reactivity study, the MoAb specifically reacted with a single protein band at MW 28 kDa of *S. mansoni* and 26 kDa of *S. japonicum*. In contrast, no positive band was detected when MoAb were reacted against the crude worm extracts from *Eurytrema* and *Paramphistomum* spp. (Fig. 2B).

Immunolocalization and distribution of GST

Since all MoAbs exhibited similar staining patterns, the data obtained from clone 3A3 were used as the representative of the group.

The most intense immunostaining by MoAb in the adult tissues was observed in the parenchyma (Fig. 3B, C). Moderate staining was observed in the middle and basal layer of the tegument, the tegument cell's cytoplasm and their processes, light staining appeared in the caecal epithelium, cells of the vitelline gland, ovary and testis, whereas the tegumental spines and muscle were not stained (Fig. 3B-E). The negative control experiment using myeloma culture fluid and normal mouse serum did not give positive staining, but yellowish autofluorescence appeared in the vitelline glands in a granulated pattern which may correspond to vitelline granules (Fig. 3A). The positive control experiment using PoAb showed very intense staining in the parenchyma tissue (Fig. 4B), moderate staining in cells

of the vitelline gland (Fig. 4B), the tegument and the processes of tegumental cells running between negatively stained muscle cells (Fig. 4B, E). Cells of the testis, ovary and caecal epithelium exhibited moderate to weak staining (Fig. 4B-D).

Similar to adults, immunostaining of the juvenile worm with MoAb and PoAb was found to be intense in the parenchymal tissue, but moderate in the tegument, and light in the caecal epithelium (Fig. 3F; 4G). The negative control experiment using myeloma culture fluid did not exhibit any positive staining (Fig. 3A, 4F).

In metacercariae and newly excysted juvenile worms (NEJ), GST was localized by MoAb and PoAb in similar tissues. However, the tegument was relatively more intensely stained than in other stages and appeared as a narrow intense fluorescent layer around the parasites underneath the innermost layer of the cyst wall (Fig. 3H, 4I). Intense staining was clearly also observed in the cytoplasm of parenchymal and tegument cells, while their nuclei remained unstained (Fig. 3H, 4I). In contrast, caecal epithelium appeared to be lightly stained in comparison to that of adult and juvenile stages (Fig. 3H, 4I). Nonspecific weak autofluorescence appeared in the inner cyst wall, and stronger yellowish autofluorescence was also observed in the outer cyst wall, while the tissues in metacercariae (Fig. 3G) and NEJ (Fig. 4H) remained negative.

DISCUSSION

Characterization of monoclonal antibodies to rGST of *F. gigantica*

GST of adult *F. hepatica* have been purified and shown to consist of a mixture of at least three to five isoenzymes of MW 23-26.5 kDa, all of which showed N-terminal sequence variations.^{1,5} This heteroge-

neity of *F. hepatica* GSTs was also reflected in the cloning and characterization of several cDNA encoding GST that showed a 59-89% identity at nucleotide levels and a 71-89% identity at the amino acid level.¹⁷ In the present report, MoAb against *F. gigantica* rGST could detect only a single band of the SDS-PAGE separated-ES and WB antigens which might reflect the identification of only one isotype in these two antigen fractions, while PoAb could detect up to three isotypes (lanes 8, 9, Fig. 2A). In contrast to PoAb, the stain of the GST band detected by MoAb was very weak in the TA fraction, which might be due to the low concentration of this particular GST isotype in the tegument as confirmed by the immunofluorescence experiment. The presence of GST at a rather high concentration in ES material may be due to the need to detoxify oxidants generated from chemicals or host immune cells external to the parasites, thus this oxidant scavenging enzyme may be needed on the surface of the parasite though the secretory pathways are not yet known.¹⁸ Tang *et al.*¹⁹ reported that GST have been found in the ES materials of several genera of parasites, including *Dictyocaulus viviparus*, *Onchocerca volvulus* and *Brugia* spp., a lymphatic filarial nematode. Cervi *et al.*²⁰ identified glutathione S-transferase as an ES protein in *F. hepatica* adults, and it has been suggested that there is a low but continuous release of this enzyme into the ES.^{21,22}

It has been established that cross-protection exists between *Fasciola* and *Schistosoma* species in many hosts. Hillyer *et al.*²³ and Christensen *et al.*¹² showed that *F. hepatica* infections in mice induced significant resistance to subsequent challenges with *S. mansoni*. Conversely, mice infected with *S. mansoni* showed significant resistance to the subsequent challenge with *F. hepatica*.¹³ Furthermore, GSTs of *F. hepatica* (FhGSTs),

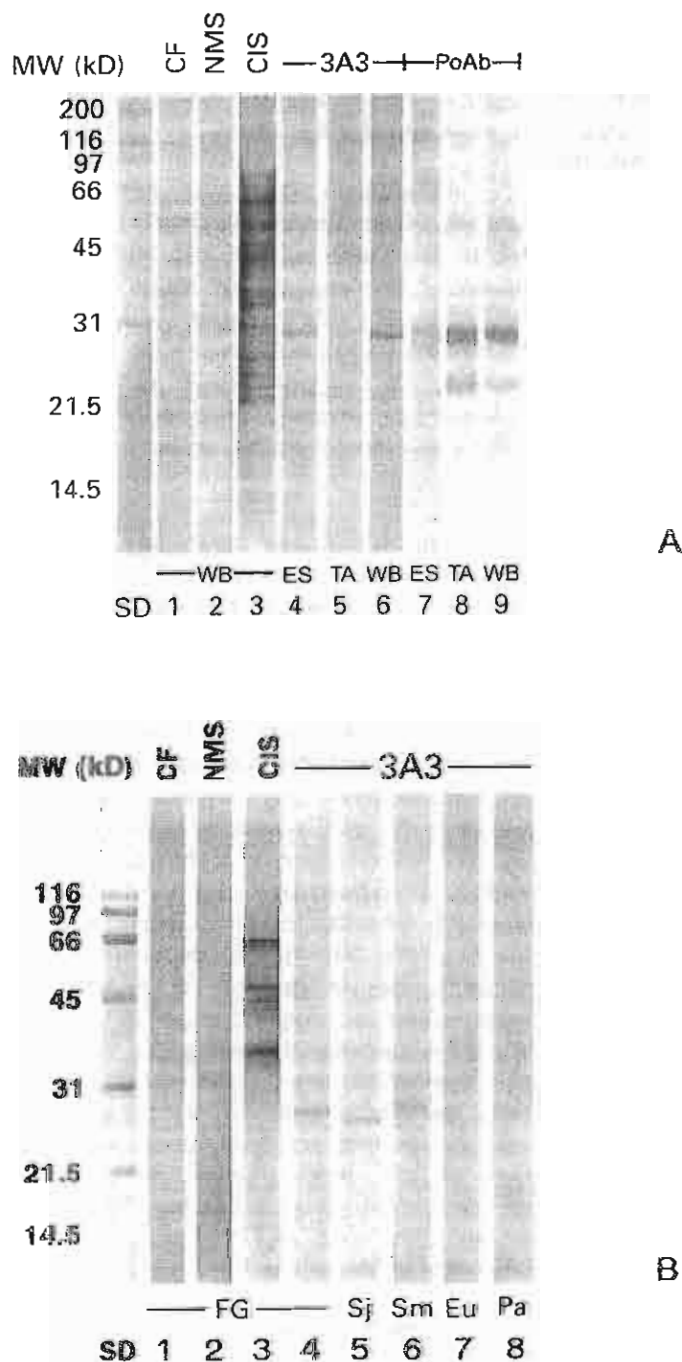


Fig. 2 (A) Immunoblotting patterns of *F. gigantica* WB antigens reacted with myeloma CF (lane 1), NMS (lane 2), CIS (lane 3); ES, TA and WB probed with MoAb clone 3A3 (lanes 4, 5, 6) and PoAb (lanes 7, 8, 9). (B) Immunoblotting patterns of WB from *F. gigantica* (lane 4), *S. japonicum* (lane 5), *S. mansoni* (lane 6), *E. pancreaticum* (lane 7) and *Paramphistomum* spp. (lane 8) probed with MoAb 3A3. Lanes 1, 2 and 3 show WB patterns of SDS-PAGE separated-antigen of *F. gigantica* reacted with myeloma CF, NMS and CIS, respectively. Other clones of MoAb showed similar patterns (data not shown). SD = standard molecular weights.

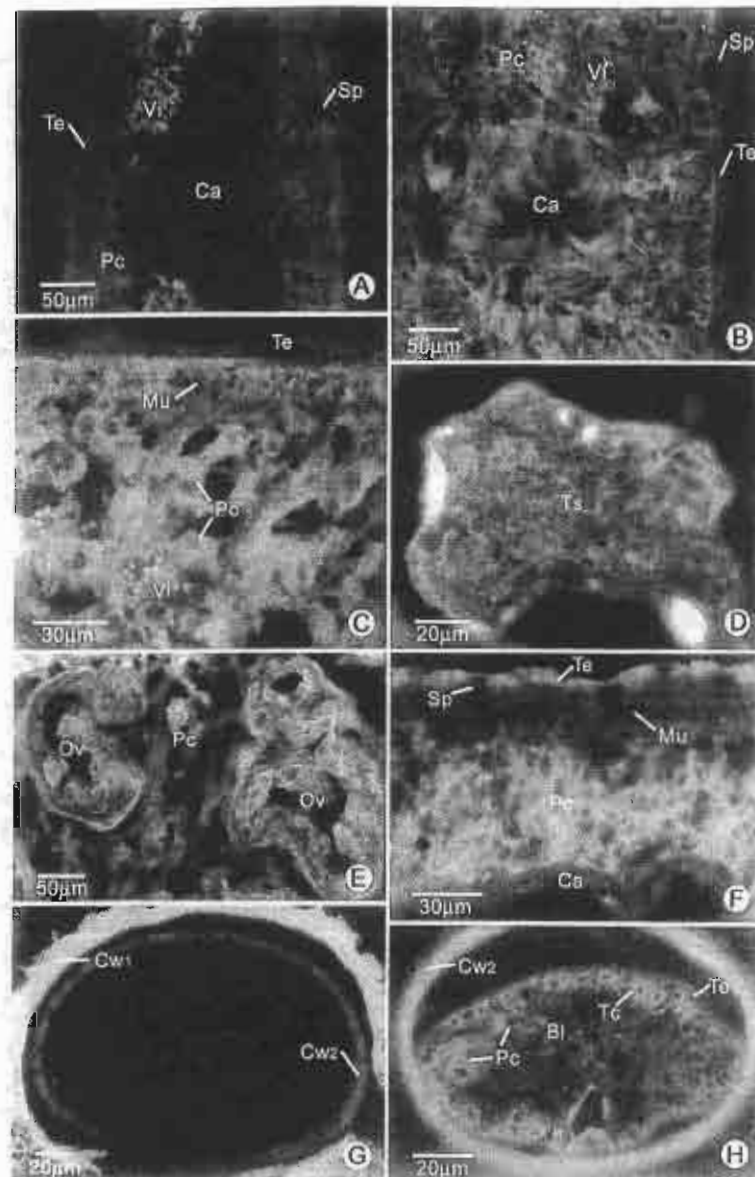


Fig. 3 Light micrographs of *F. gigantica* frozen sections stained by immunofluorescence technique, using MoAb as primary antibody and FITC-conjugated goat anti-mouse IgG as secondary antibody. (A) A control section of an adult parasite, using myeloma CF in place of primary antibody, showing granulated autofluorescence in vitelline cells (Vi). (B) Low magnification micrograph of an adult parasite, showing intense staining in parenchyma (Pc), moderate staining in tegument (Te), light staining in caecum (Ca) and vitellaria (Vi). (C) High magnification micrograph, showing intensely stained parenchymal cells (Pc), moderately stained tegument (Te), and lightly stained vitellaria (Vi). Note the intensely stained processes of parenchymal cells between unstained muscle cells (Mu). (D) A high magnification micrograph showing light staining of testicular cells (Ts). (E) A high magnification micrograph showing light staining of cells in the ovary (Ov). (F) Micrograph of a 7-week-old juvenile section, showing intense staining in parenchyma (Pc), moderate staining in tegument (Te), and light staining in the caecum (Ca). (G) Control section of metacercaria, using myeloma CF in place of primary antibody, showing yellow autofluorescence in the outer cyst wall (Cw1) and non-specific staining of the inner cyst wall (Cw2) while the metacercarial tissues are unstained. (H) Micrograph of a metacercarial section, showing intense staining in parenchyma (Pc) and tegumental cell (Tc). (Bl, bladder).

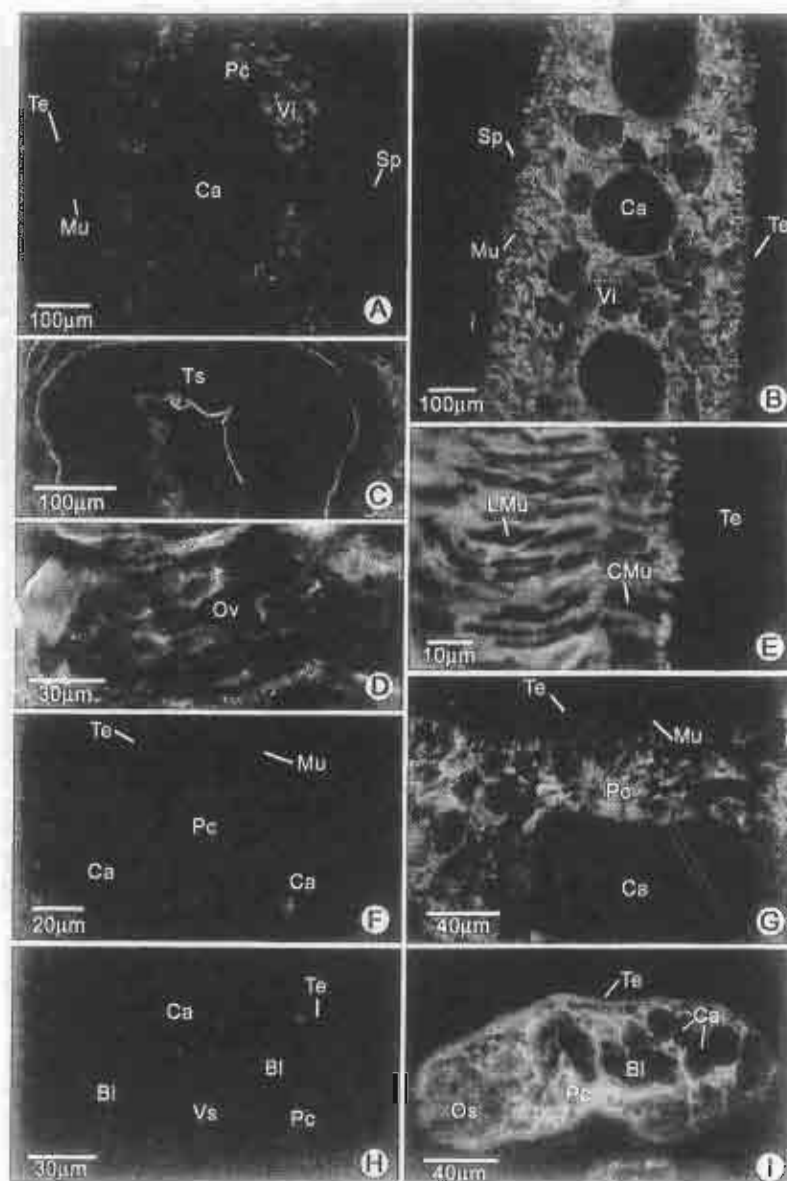


Fig. 4 Light micrographs of *F. gigantica* frozen sections stained by immunofluorescence technique, using PoAb (rabbit anti-native GST) as primary antibody and FITC-conjugated goat anti-rabbit IgG as secondary antibody. (A) Control section of an adult parasite, using myeloma CF in place of primary antibody, showing autofluorescence in vitelline cells (Vi). (B) Low magnification micrograph of an adult section, showing intense staining in parenchyma (Pc), and light staining in tegument (Te) caecum (Ca) and vitellaria (Vi). (C) A micrograph showing light staining of cells in the testis (Ts). (D) A high magnification micrograph showing light staining of cells in the ovary (Ov). (E) High magnification micrograph, showing intensely stained parenchymal cells and their processes running between muscle layers (LMu) towards the tegument (Te), and lightly stained tegument (Te). (F) Control section of a 7-week-old juvenile, showing no staining. (G) A micrograph of a 7-week-old juvenile, showing intense staining in parenchyma (Pc), light staining in tegument (Te) and caecum (Ca). (H) Control section of NEJ. (I) A section of metacercaria, showing intense staining in parenchyma (Pc), fairly intense staining in tegument (Te), and light staining in caecum (Ca). (CMu, circular muscle; LMu, longitudinal muscle; Os, oral sucker; Sp, spine; Vs, ventral sucker).

S. mansoni (Sm28) and *S. japonicum* (Sj26) were shown to have cross protection in experimentally vaccinated laboratory animals, including mice and hamsters.²⁴ It was also found that the putative gene encoding FhGSTs has 54 and 58% homology to Sj26 and Sm28 genes, respectively.^{8,25} In the present study, the crude antigens of *F. gigantica*, *S. mansoni*, *S. japonicum*, *Eurytrema* spp. and *Paramphistomum* spp. separated by SDS-PAGE were immunoblotted with MoAbs against rGST, and the result showed that only a 28 kDa antigen of *S. mansoni* and a 26 kDa antigen of *S. japonicum* reacted specifically with these monoclonal antibodies. This indicated a high degree of cross-reactivity between *S. mansoni*, *S. japonicum* and *F. gigantica* GSTs, at least for this single isotype. In contrast, no cross reaction was found with antigens from even closely related trematode parasites, i.e. *Eurythema* and *Paramphistomum* spp. Hence, it is possible that these MoAb could be used for immunodiagnosis of fasciolosis and schistosomiasis which will be studied further.

Localization of GST

In the present study, GST expressed in various stages in the life cycle of *F. gigantica* were localized by indirect immunofluorescence using PoAb against native GST and MoAb against rGST as probes. In general, the results showed that the pattern of immunostaining by PoAb was very similar but more intense than staining by MoAb. From the fluorescence intensity it could be surmised that GST has the highest concentration in the parenchymal tissue in all stages of the parasite. Moreover, in the adult parasite GST was also detected at a moderate concentration in the middle and basal cytoplasm of the tegument. GST was present in low amount in cells of the vitelline gland, ovary, testis and the caecal epithelium. In juvenile para-

sites parenchymal tissue also showed a high concentration of GST, while the enzyme was present in a rather low concentration in the tegument and caecal epithelium. In contrast, GST was detected in a relatively high concentration in the tegument and tegumental cells of the metacercarial stage, in addition to parenchymal tissue. Since the MoAb that was produced in the present study could detect only one isotype the immunolabeling pattern may not be the complete picture of all native GSTs. However, its staining is in general agreement with other reports on *F. hepatica*^{2,5} which showed the existence of GST in the parenchymal cells and their cytoplasmic extensions in the subtegumental area, as well as in the caecum and excretory ducts of the adult and juvenile stages. However, there is still no report on GST expression and concentration in the metacercarial stage of *F. hepatica*.

For the *Schistosoma* spp., several studies have been undertaken to analyze the distribution of GST. Taylor *et al.*,⁷ using immunoelectron microscopy, detected GST (Sm28) in the tegument, protonephridial cells and subtegumental cells of *S. mansoni*. Holy *et al.*,²⁶ using immunofluorescence technique, could detect SmGST only in the parenchyma, while Porchet *et al.*²⁷ could also detect the enzyme in the genital organs. Gobert *et al.*¹⁰ performed the immunolocalization study of the 26 kDa and 28 kDa glutathione S-transferase within adult *S. japonicum*, and found that both proteins were localized within the parenchyma of both male and female parasites. However, there was no staining of this protein on the surface or within the tegument of either the male or female worms. The absence of GST in the caecal epithelium in *Schistosoma* spp. is in notable contrast to the positive finding of this enzyme in the caecum of *Fasciola* spp. as reported earlier^{2,5} as well

as in the present studies.

The presence of a moderate amount of GST in the tegument, in contrast to the lower amount in the caecal epithelium, may be due to the fact that this enzyme is needed for the parasite's protection from oxygen free radicals generated from the host immune cells, which are more likely to attack the tegument surface than the caecal epithelium. It is still not known how GST in the tegument is produced. Since tegumental cells provide the cytoplasmic mass for the tegument they may actually be the original source of GST, though the staining of the tegumental cells themselves was not intense except in the metacercarial and NEJ stages. Alternatively, GST may be provided by the parenchymal cells, which evidently synthesized and stored a large amount of GST. These cells branch profusely and always have the terminals of their slim processes in close contact with the tegument.²⁸ The passage of GST from parenchymal cell processes to the tegument is possible but there is still no proof for this cell to cell transfer. In addition, the abundance of GST in the parenchyma implicates that there is a very high degree of protection from oxidants' damaging effects within the parasite's body. This was supported in an experiment when the adult parasites were incubated with MoAb against rGST, and the tegument was severely damaged, but the adult parasites could still survive and regenerate the new tegument (unpublished observation). In the younger stages, especially NEJ there appeared to be a relatively much lower quantity of GST in the parenchyma than in adult as shown by immunofluorescence in this study, and by quantitation of specific activity of this enzyme (showing about x20 fold increase) in *F. hepatica*.²⁹ Hence a GST vaccine may have a higher chance of killing these young parasites. Because of its expression in all developmental stages of *F. gi-*

gantica and its moderate specificity to only *Fasciola* and *Schistosoma* species, rGST synthesized in this study could be considered as a candidate for both immunodiagnosis and vaccine development for these species, which will be studied further.

ACKNOWLEDGEMENTS

This work was supported by the Thailand Research Fund (Senior Research Scholar Fellowship to Prasert Sobhon) and the National Center for Genetic Engineering and Biotechnology, NSTDA, (Grant # BT-B-06-2B-14-004 to Vithoon Viyanant).

REFERENCES

- Brophy PM, Crowley P, Barrett J. Detoxification reactions of *Fasciola hepatica* cytosolic glutathione transferases. *Mol Biochem Parasitol* 1990; 39: 155-62.
- Creaney J, Wijffels GL, Sexton JL, Sandeman RM, Spithill TW, Parsons JC. *Fasciola hepatica*: localisation of glutathione S-transferase isoenzymes in adult and juvenile liver fluke. *Exp Parasitol* 1995; 81: 106-16.
- Spithill TW, Dalton JP. Progress in development of liver fluke vaccines. *Parasitol Today* 1998; 14: 224-8.
- Mannervik B. The isoenzyme of glutathione S-transferase. *Adv Enzymol Relat Areas Mol Biol* 1985; 57: 357-417.
- Wijffels GL, Sexton JL, Salvatore L, et al. Primary sequence heterogeneity and tissue expression of glutathione S-transferase of *Fasciola hepatica*. *Exp Parasitol* 1992; 74: 87-99.
- Balloul JM, Sondermeyer P, Dreyer D, et al. Molecular cloning of a protective antigen of schistosomes. *Nature* 1987; 326: 149-53.
- Taylor JB, Vidal A, Torpier G, et al. The glutathione transferase activity and tissue distribution of a cloned M₂₈K protective antigen of *Schistosoma mansoni*. *EMBO J* 1988; 7: 465-72.
- Smith DB, Davern KM, Board PG, Tiu WU, Garcia EG, Mitchell GF. M₂₆, 26,000 antigen of *Schistosoma japonicum* recognized by resistance WEHI 129/J mice is a parasite glutathione S-transferase. *Proc Natl Acad Sci USA* 1986; 83: 8703-7.
- Davern KM, Tiu WU, Samaras N, et al. *Schistosoma japonicum*: monoclonal antibodies to the Mr 26,000 schistosome glutathione S-transferase (Sj26) in an assay for circulating antigen in infected individuals. *Exp Parasitol* 1990; 70: 293-304.
- Gobert GN, Stenzel DJ, McManus DP. Immunolocalisation of the glutathione S-transferases, GST-26 and GST-28, within adult *Schistosoma japonicum*. *Int J Parasitol* 1998; 28: 1437-43.
- Estuningsih SE, Smooker PM, Wiedosari E, et al. Evaluation of antigens of *Fasciola gigantica* as vaccine against tropical fasciolosis in cattle. *Int J Parasitol* 1997; 27: 1419-28.
- Christensen NO, Nasen P, Frandsen F, Bjorneboe A, Monrad J. *Schistosoma mansoni* and *Fasciola hepatica*: cross resistance in mice. *Parasitol* 1978; 46: 113-20.
- Hillyer GV. Effect of *Schistosoma mansoni* infection on challenge infection with *Fasciola hepatica* in mice. *J Parasitol* 1981; 67: 731-3.
- Grams R, Vichasri-Grams S, Sobhon P, Upatham ES, Viyanant V. Molecular cloning and characterization of antigen encoding genes from *Fasciola gigantica*. In: Sirisinha S, Chaiyaroj SC, Tapechaisri P, eds. International Proceedings of the Second Congress of the Federation of Immunological Societies of Asia-Oceania, Bangkok, Thailand, January 23-27, 2000. Bologna: Monduzzi Editore, 2000; pp. 39-43.
- Lowry OH, Rosenbrough NJ, Farr SL, Randal RJ. Measurement of protein with the folin phenol reagent. *J Biol Chem* 1951; 193: 265-75.
- Viyanant V, Gajanadana O, Upatham ES, et al. Monoclonal antibodies against *Schistosoma mekongi* surface tegumental antigens. *Southeast Asian J Trop Med Public Health* 1993; 24: 484-8.
- Panaccio M, Wilson LR, Cramer SL, Wijffels GL, Spithill TW. Molecular characterization of cDNA sequence encoding glutathione S-transferase of *Fasciola hepatica*. *Exp Parasitol* 1992; 74: 232-7.
- Callahan HL, Crouch RK, James ER. Helminth antioxidant enzymes: a protective mechanism against host oxidants. *Parasitol Today* 1988; 4: 218-25.
- Tang L, Ou X, Henkle-Duhrge K, Selkirk ME. Extracellular and cytoplasmic Cu-Zn superoxide dismutases from *Brugia lymphatic filarial nematode* parasites. *Infect Immun* 1994; 62: 961-7.
- Cervi L, Rossi G, Masih DT. Potential role for excretory-secretory forms of glutathione S-transferase (GST) in *Fasciola hepatica*. *Parasitol* 1999; 119: 627-33.
- Howell MJ, Board PG, Boray JC. Glutathione S-transferases in *Fasciola hepatica*. *J Parasitol* 1988; 74: 715-8.
- Sexton JL, Milner AR, Panaccio M, et al. Glutathione S-transferase: Novel vaccine against *Fasciola hepatica* infection in sheep. *J Immunol* 1990; 145: 3905-10.
- Hillyer GV. Can we vaccinate against Schistosomes? *Fed Proc* 1976; 35: 2568-71.
- Brophy PM, Pritchard DI. Parasitic helminth glutathione S-transferases: an update on their potential as targets for immuno- and chemotherapy. *Exp Parasitol* 1994; 79: 89-96.
- Balloul JM, Grzych JM, Pierce RJ, Capron A. A purified 28,000 dalton protein from *Schistosoma mansoni* adult worms protects rats and mice against experimental schistosomiasis. *J Immunol* 1987; 138: 3448-53.
- Holy JM, O'Leary KA, Oaks JA, Tracy JW. Immunocytochemical localization of the major glutathione S-transferases in adult *Schistosoma mansoni*. *J Parasitol* 1989; 2: 181-90.
- Porchet E, McNair A, Caron A, Kusnierz JP, Zemzoumi K, Capron A. Tissue expression of the *Schistosoma mansoni* 28 kDa glutathione S-transferase. *Parasitol* 1994; 109: 565-72.
- Gallagher SSE, Threadgold LT. Electron microscope studies of *Fasciola hepatica*. II. The interrelationship of the parenchyma with other organ systems. *Parasitol* 1967; 57: 627-32.
- Piedrafita D, Spithill TW, Dalton JP, et al. Juvenile *Fasciola hepatica* are resistant to killing *in vitro* by free radicals compared with larvae of *Schistosoma mansoni*. *Parasite Immunol* 2000; 22: 287-95.

Classification of Spermatogenic Cells in *Rana tigerina* Based on Ultrastructure

Sirikul Manochantr, Prapee Sretarugsa, Chaitip Wanichanon, Jittipan Chavadej and Prasert Sobhon*

Department of Anatomy, Faculty of Science, Mahidol University, Rama VI Road, Bangkok 10400, Thailand.

* Corresponding author. Email: scpsob@mahidol.ac.th

Received 27 Sep 2002

Accepted 18 Apr 2003

ABSTRACT: Germ cells in the spermatogenetic process of *Rana tigerina* can be classified into 14 steps based on the pattern and degree of chromatin condensation as studied by transmission electron microscopy. Primary spermatogonia contain a large spherical nuclei with mostly euchromatin that consists of 2 levels of fibers with 10 and 30 nm thicknesses. Secondary spermatogonia have small heterochromatin blocks consisting of tight aggregations of 30 nm fibers on the inner surface of the nuclear envelope, as well as in the central area of the nucleus. Primary spermatocytes are divided into 6 steps. A leptotene spermatocytes contain small loosely packed chromatin clumps that are resulted from the winding of 30 nm fibers around the condensation axes, each of which is a single electron dense line. Zygotene spermatocytes contain long and increasingly thickened heterochromatin blocks, which are joined together by synaptonemal complexes. Pachytene spermatocytes show long, thick, intertwined heterochromatin blocks cords, which are parts of the complete chromosomes. These chromatin blocks become distributed in a cartwheel pattern in diplotene spermatocytes. Long and large heterochromatin blocks are separated from each other during the diakinesis step and become aligned along the equatorial region in the metaphase spermatocytes. Throughout the transformation of primary spermatocytes, the 30 nm chromatin fibers become increasingly condensed into heterochromatin blocks of various sizes, while the 10 nm fibers are decreased in quantity until they are absent entirely in the metaphase spermatocytes. Secondary spermatocytes have nuclei that contain 4-6 large blocks of heterochromatin along the inner facet of the nuclear envelope, the 30 nm fibers are loosened up and the 10 nm fibers of which start to reappear. Spermatids can be divided into 4 steps. In spermatid I, the nucleus is round and contains more dispersed 30 nm chromatin fibers that are unraveled from the more tightly packed chromatin of the secondary spermatocytes. The 30 nm chromatin fibers are uniformly packed together and increasingly condensed in spermatid II, whose nucleus is decreased in size and becoming oval-shaped. In spermatid III, the nucleus becomes elongated and it contains 30 nm chromatin fibers which are aggregated more tightly and evenly together, while 10 nm fibers disappear. In spermatid IV, the nucleus becomes highly elongated into a cylindrical shape, with a small acrosome covering the anterior pole. Its chromatin is highly condensed, but the outline of the 30 nm fibers could still be observed. In spermatozoa, the 30 nm chromatin fibers are packed so tightly together that chromatin becomes completely electron-opaque. The condensation of chromatin in *Rana* spermatozoa is, therefore, similar to the process of heterochromatinization in fully differentiated somatic cells, where 30 nm fibers coalesce together without changing their initial size.

KEYWORDS: *Rana tigerina*, spermatogenic cells, ultrastructure, chromatin organization.

INTRODUCTION

During spermatogenesis and spermiogenesis of vertebrates, the chromatin undergoes extensive molecular reorganization and condensation that renders it more compact and metabolically inert as all paternal genes are switched off, and the chromatin must be contained within the highly reduced volume of the sperm nucleus.^{1,2} Thus, the paternal genome is protected against physical damage and chemical mutagenesis during transport to the site of fertilization.³ Changes in basic proteins complexed with the

DNA are of particular interest and have long been regarded as an important contributing factor to variations in the chromatin packaging pattern.⁴ The process of chromatin condensation has been well studied in mammalian spermatozoa,⁵⁻⁷ and at least two patterns of chromatin condensation can be discerned.^{1,8} In primates including human, the fine granular chromatin substance of early spermatids is gradually replaced by coarser and denser bodies, which appear to arise by the "growing" or "aggregating" of smaller dispersed chromatin granules.^{7,9,10} The chromatin bodies increase in size and eventually

coalesce to form the compact homogenous mass of the typical chromatin in the mature spermatozoa.^{7, 11} Alternatively, in most rodents the basic nucleosomal-type, the 30 nm chromatin fibers, are transformed into larger (40-50 nm) fibers that are straight and arranged in parallel during the early acrosomal stage.¹² These fibers appear to grow larger by the lateral fusion of the smaller parallel fibers, until they reach about 100 nm in width. Later the large fibers are completely fused to form the compact chromatin.¹² While early round spermatids (Golgi and cap phases) contain a mixture of somatic types as well as testis-specific histones, these proteins are largely replaced by a set of novel transition proteins (TP) about midway through spermiogenesis (acrosomal stage),³ when the chromatin appears as 40-50 nm straight parallel fibers.¹² Shortly thereafter (maturation stage), the transition proteins are replaced by the arginine-rich protein, protamine, which are responsible for the final compaction of chromatin in the mature sperm head.¹³ The pattern of chromatin condensation is thus highly correlated with the steps of germ cell development, especially during spermiogenesis. Only a limited amount of information is available on the process of spermatogenesis and the organization of chromatin in amphibians, and none is available in *Rana tigerina*, a species of rice field frogs which is indigenous to Thailand. Thus, the purposes of the present study are to classify various steps of the development of male germ cells in *Rana tigerina* based on the pattern of chromatin organization and ultrastructural features.

MATERIALS AND METHODS

Experimental Animals

Rana tigerina, rural rice field frogs commonly found in Thailand, were cultured in cement tanks at the Faculty of Science, Mahidol University. They were maintained in a natural environment having approximate 12 hour light/dark cycle. The ambient temperature was about 25-30 °C, while the relative humidity ranged from 80 to 100%. Pelleted frog feeds were given once daily in the afternoon, and the water in the cement tanks was changed at alternate days. Only sexually mature frogs, generally more than 12 month-olds,¹⁴ were used in the experiment.

Specimen Preparation

Mature male frogs that were more than 12 months old were collected during the breeding season (April-October),¹⁴ and anesthetized by being placed in an ice bath for 5-10 minutes, or until they become immobile. The testes were removed and immediately processed for transmission electron microscopy. The testicular tissues were cut into small pieces about 1 mm³ and

fixed in the solution of 4% glutaraldehyde plus 2% paraformaldehyde in 0.1 M Millonig's buffer (0.23 M NaH₂PO₄·H₂O, 0.19 M NaOH, 0.06 M glucose), pH 7.2, at 4 °C for 2 hours. Then the tissues were washed in three changes of the same buffer in order to remove the fixatives, followed by post fixation in 1% osmium tetroxide in the same buffer for 1 hour. Then, the tissues were washed again in three changes of the same buffer. After fixation, specimens were dehydrated through increasing concentrations of ethyl alcohol at 50%, 70%, 90% and 95%, consecutively, by immersing them for 10 minutes, twice at each ethanol concentration, and at 100%, by immersing them for 20 minutes, 3 times, at 4 °C and 20 minutes, 3 times, at room temperature. Then the specimens were cleared in two changes of propylene oxide, for 15 minutes each, infiltrated in mixtures of propylene oxide and Araldite 502 resin at the ratios of 2:1 for 1 hour, and 1:2 overnight, then in pure Araldite 502 resin for at least 6 hours, and finally polymerized at 30 °C, 45 °C and 60 °C for 24, 48 and 48 hours, respectively.

Light Microscopy

In order to facilitate the classification of various steps of male germ cells, thick sections of about 0.75-1 mm were cut from each blocks of Araldite-embedded tissue with glass knives on a Porter-Blum MT-2 ultramicrotome, mounted on glass slides at 55 °C, and stained with 1% methylene blue in 1% borax in H₂O at 70 °C, for 30 seconds, washed with several changes of distilled water, then dried on a hot plate and covered by glass cover slips using superglue as the mounting medium. The sections were examined and photographed with an Olympus Vanox microscope.

Transmission Electron Microscopy

Thin sections with an interference color of silver to silver-gold (about 60-90 nm thick) were cut with glass knives on a Porter-Blum MT-2 ultramicrotome. The sections were picked up on uncoated 300-mesh copper grids, air dried and stained by floating on saturated aqueous uranyl acetate in the dark for 30 minutes, then rinsed with several changes of distilled water, and the excess water was blotted off with Whatmann filter paper. The sections were further stained by floating on saturated aqueous lead citrate for 30 minutes, rinsed with several changes of CO₂-free distilled water, and the excess water blotted off with Whatman filter paper and air dried. The sections were then examined with a Hitachi transmission electron microscope H-300 at 75 kV.

Scanning Electron Microscopy

Spermatozoa collected from cloaca were fixed in the solution of 4% glutaraldehyde plus 2%

paraformaldehyde in 0.1 M Millonig's buffer, pH 7.2 at 4 °C for 1 hour, the specimen were then washed in three changes of the same buffer, 5 minutes each, followed by post fixation in 1% osmium tetroxide in the same buffer for 30 minutes. Then, the specimen were washed again in three changes of the same buffer. After fixation, specimens were dehydrated through an increasing concentrations of ethyl alcohol at 50%, 70%, 90%, and 95% consecutively, by immersing them for 10 minutes, twice at each ethanol concentration and at 100 % by immersing them for 10 minutes for 3 times, at 4 °C. Specimens were dried in a Hitachi HCP-21 critical-point drying machine, using liquid CO₂ as a transitional medium. They were mounted on aluminum stubs with carbon-paint adhesive, and coated with platinum and palladium in a Hitachi ion sputtering apparatus, E2500. The specimens were examined by a Hitachi S-2500 scanning electron microscope at 15 kV.

Measurement of Chromatin Fibers

The male germ cells of *R. tigerina* were classified into various steps based on the pattern of chromatin organization and other ultrastructural features including the acrosome and the tail formation. The sizes of chromatin fibers in at least 10 cells from each step of the male germ cells were measured from electron microscopic negatives in a Nikon profile projector. Fibers were measured at random by recording the distance between the distinct edges. Catalase crystal with lattice spacing of 87.5 Å (Agar Aids) was photographed at the same magnifications and used as standards for measurement of chromatin fiber sizes. From the variation in sizes and the orientation of the chromatin fibers, the patterns of chromatin organization and condensation was deduced.

RESULTS

Histological Organization of *Rana tigerina* Testis

Each testicular lobule contains several convoluted seminiferous tubules, each of which is surrounded by a thick basement membrane. The seminiferous epithelium consists of 2 groups of cells, i.e., spermatogenic cells and follicular cells (Fig 1A). The interstitial areas are filled with interstitial cells, blood vessels and connective tissues (Fig 1A). The differentiating male germ cells are always found in synchronously developing groups, each surrounded by processes of follicular cells, thus this structure is called a spermatocyst (Fig 1A). Because of this unique organization, the steps of spermatogenic cells could be clearly identified. At the beginning of the spermatogenic process, the spermatocyst consists of

a single large primary spermatogonium enclosed in a layer of follicular cells (Fig 1B). The primary spermatogonium gives rise, by successive mitotic division, to a number of secondary spermatogonia (Fig 1C). These differentiate into six steps of primary spermatocytes (Figs 1B-F) that finally undergo meiotic division to form secondary spermatocytes (Fig 1E). These cells, in turn, undergo a second meiotic division, giving rise to double the number of spermatids (Figs 1G-I). As a result of these divisions, the size of the spermatocyst is increased considerably, and the processes of enveloping follicular cells become highly attenuated (Figs 1A-I). The spermatids are elongated, and oriented in clusters embedded in the cytoplasm of follicular cells (Fig 1I). Thus, it appears that follicular cells of the spermatocysts serve the same sustentacular and nutritive function as the Sertoli cells of mammalian testis.¹⁹ The wall of the spermatocyst ultimately breaks down, leaving the follicular cells and their adhering clusters of spermatids and spermatozoa still attached to the basement membrane of the seminiferous tubule (Fig 1I).

Classification of Spermatogenic Cells

Based on the nuclear size and the pattern and degree of chromatin condensation, and in later stages, the formation of the acrosome and the tails, spermatogenic cells of *Rana tigerina* can be classified into 14 steps.

Primary spermatogonium (Sg1)

This cell contains a large spherical nucleus about 8-10 µm in diameter with mostly euchromatin with very few blocks of heterochromatin in the center. Each nucleus contains one or two prominent nucleoli (Figs 1B, J). The chromatin consists of 2 levels of fibers with about 10 and 30 nm in diameter. The former appear as thin zigzag lines, while the latter appear in cross sections as dense dots (Fig 1L). Small heterochromatin blocks, which are formed by tight aggregation of 30 nm fibers, are few in number and widely scattered throughout the nucleus (Fig 1L). The cytoplasm contains a little developing rough endoplasmic reticulum (Figs 1J, K). Polyribosomes are numerous and evenly distributed throughout the cytoplasm, whereas mitochondria tend to be congregated in one pole of the cell (Fig 1J). Some of these cells are undergoing mitotic division as the two newly divided nuclei remain within the same cytoplasmic mass (Fig 1K).

Secondary spermatogonium (Sg2)

These cells appear in clusters of 2 or 4 cells, still lying close to the basement membrane, and each cluster is surrounded by processes of follicular cells to form a cyst (Fig 1C). The nucleus of Sg2 is round and has a diameter of about 6-7 µm. The nucleoli

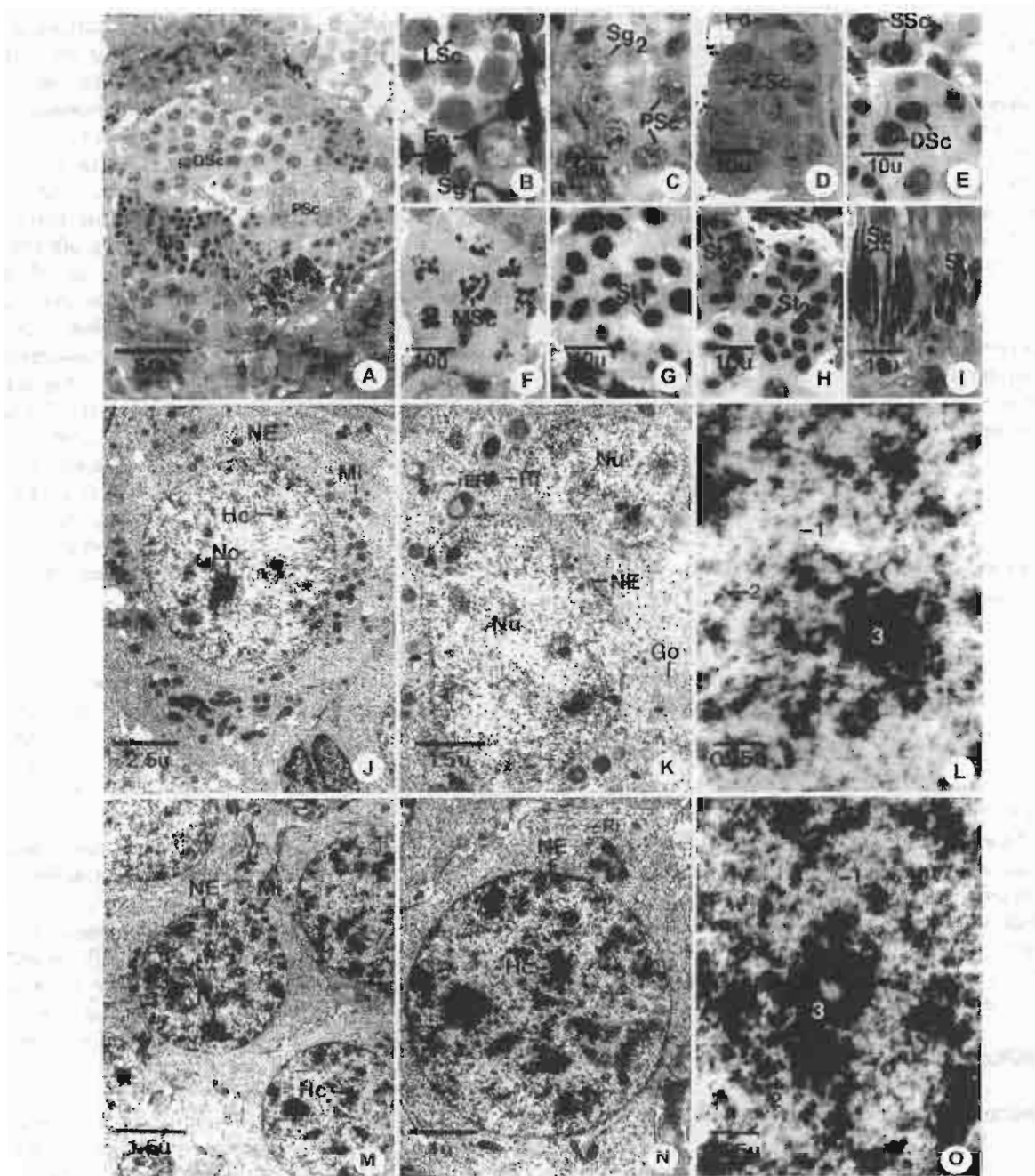


Fig 1.

A-I Semithin sections of a frog's testis showing the histology of seminiferous tubules and the spermatocysts containing clones of synchronously developing male germ cells: primary spermatogonia (Sg1), secondary spermatogonia (Sg2), leptotene spermatocyte (LSc), zygotene spermatocyte (ZSc), pachytene spermatocyte (PSc), diplotene spermatocyte (DSc), metaphase spermatocyte (MSc), secondary spermatocyte (SSc), spermatid I (St1), spermatid II (St2), spermatid III (St3), spermatid IV (St4) and spermatozoa (Sz). Each spermatocyst is surrounded by the processes of follicular cell (Fo). The interstitial area are filled with interstitial Leydig cells (Le). Star (*) indicates the Sertoli cell.

J-L Transmission electron micrographs of primary spermatogonia (Sg1): the nucleus (Nu) contains mostly euchromatin, which consists of 2 levels of fibers, 10 and 30 nm in width (1, 2). Tight aggregations of 30 nm fibers (3) form heterochromatin blocks (Hc). The cytoplasm contains few endoplasmic reticulum (rER), Golgi complex (Go), numerous ribosomes (Ri) and mitochondria (Mi).

M-O Secondary spermatogonia (Sg2). Small heterochromatin blocks (Hc) are increasing in number and scattered throughout the nucleus. Chromatin fibers are organized into 2 levels as in primary spermatogonia. The cytoplasm contains abundant ribosomes (Ri), and mitochondria (Mi).

become more prominent (Figs 1C, 1M). The nucleus contains increasing number of small blocks of heterochromatin compared to Sg1, which are distributed along the inner facet of nuclear envelope as well as in the central region (Fig 1N). In the euchromatic area, chromatin fibers are organized into 2 levels, i.e., 10 nm and 30 nm, like in Sg1 (Fig 1O). Cytoplasm contains abundant polyribosomes, fewer mitochondria than in Sg1, and rough endoplasmic reticuli which is fairly evenly distributed throughout the cytoplasmic mass (Figs 1M, 1N).

Primary spermatocytes

There are 6 steps of primary spermatocytes: leptotene, zygotene, pachytene, diplotene, diakinesis and metaphase steps, each with distinctive patterns of chromatin organization.

Leptotene spermatocyte (LSc)

The cells in this step are grouped in a large cluster of more than four cells per group, each surrounded by cytoplasmic processes of follicular cells (Fig 1B). The LSc is spherical in shape, with a large spherical nucleus about 6-8 mm in diameter (Fig 2A). Most of the chromatin is in the euchromatic form (Fig 2B), and there is no thin rim of condensed chromatin along the nuclear envelope as observed in earlier steps of spermatogenesis. Small loosely packed chromatin blocks are scattered among the evenly dispersed 30 nm fibers (Fig 2B). In the euchromatic area, individual chromatin fibers exhibit two levels of organization, i.e., 30 nm fibers that appear in cross sections as dense dots, and 10 nm fibers that appear as zigzag thin lines (Fig 2C). Within each enlarging chromatin block in the nucleus of late LSc, where chromatin fibers begin to wind together, there is a dense line that may be the initial site of chromatin condensation (Figs 2E, 1F). The nucleolus is still present but not as prominent as in spermatogonia (Figs 1B, 2A). In addition to abundant ribosomes and mitochondria, the cytoplasm also contains small Golgi complexes (Figs 2A, 2D).

Zygotene spermatocyte (ZSc)

This cell has a round nucleus with approximately the same size as LSc. The distinguishing feature of ZSc is the increase in size and density of heterochromatin blocks, some of which are coupled with the synaptonemal complex (Figs 2G, 2H). In contrast to the single dense line found in LSc, each of this tripartite structure has a conspicuous central element separated from the two lateral elements by clear spaces (Fig 2I). Chromatin fibers (30 nm) from sister chromatids are attached to the side of each lateral element of the synaptonemal complex (Fig 2I). The nucleolus completely disappears. Polysomes appear to be less numerous than in spermatogonial cytoplasm (Figs 2G, 2H).

Pachytene spermatocyte (PSc)

The nucleus of this cell is still round and about 6-7 μ m in diameter (Figs 1C, 3A). It is characterized by the presence of long interconnecting blocks or cords of heterochromatin, some of which are attached at the ends to the nuclear envelope (Figs 3A, 3B). Some of these cords are still linked by synaptonemal complex (Figs 3A, 3B). In euchromatic area there are still 2 levels of chromatin fibers. Individual chromatin fibers within the condensed blocks of heterochromatin could be visualized as having 30 nm in size, even though they are tightly packed together (Fig 3C). The number of cells in each cluster increases, and each cluster is still enclosed by cytoplasmic processes of follicular cells (Fig 1C). PSc are the most numerous cell type in the seminiferous tubule and easily observed due to their unique characteristics as mentioned. The cytoplasm also contains ribosomes, mitochondria, and rough endoplasmic reticulum (Fig 3A).

Diplotene spermatocyte (DSc)

The nucleus of this cell has a round to oval shape with slightly smaller size than PSc (about 5-6 mm in diameter). The chromatin blocks become increasingly larger and attached to the nuclear envelope in a cartwheel-spoke pattern (Figs 1E, 3D). Despite the much increased condensation, individual 30 nm chromatin fibers within the tight aggregates of heterochromatin blocks could still be visualized (Fig 3F). There are fewer 10 nm fibers remaining in the euchromatic areas in comparison to PSc (Figs 3E, 3F). DSc are much fewer in number than PSc. The types and quantity of cytoplasmic organelles appear similar to those of PSc (Fig 3D).

Diakinesis-Metaphase spermatocytes (DiSc, MSc)

DiSc is identified by the presence of long and large pieces of chromosomes that are distributed within the whole nucleus (Fig 3G). DiSc rapidly turns into MSc whose chromosomes become aligned in a row along the equatorial region (Fig 3H). The nuclear membrane disintegrates and completely disappears in MSc (Fig 3H). Despite their tight aggregation, the outline of individual 30 nm chromatin fibers in the chromosomes could still be visualized, while the 10 nm chromatin fibers disappear (Fig 3I). The cytoplasm contains only a few organelles, mainly, ribosomes and mitochondria (Fig 3G). Both DiSc and MSc are so few and transient that they are only occasionally observed within the seminiferous tubule. Thus, it could be concluded that throughout the transformation of primary spermatocytes, 30 nm chromatin fibers become increasingly condensed into larger heterochromatin blocks, while still maintaining their individual identity, and the 10 nm fibers are decreasing in quantity until they are entirely absent in MSc (Fig 3I).

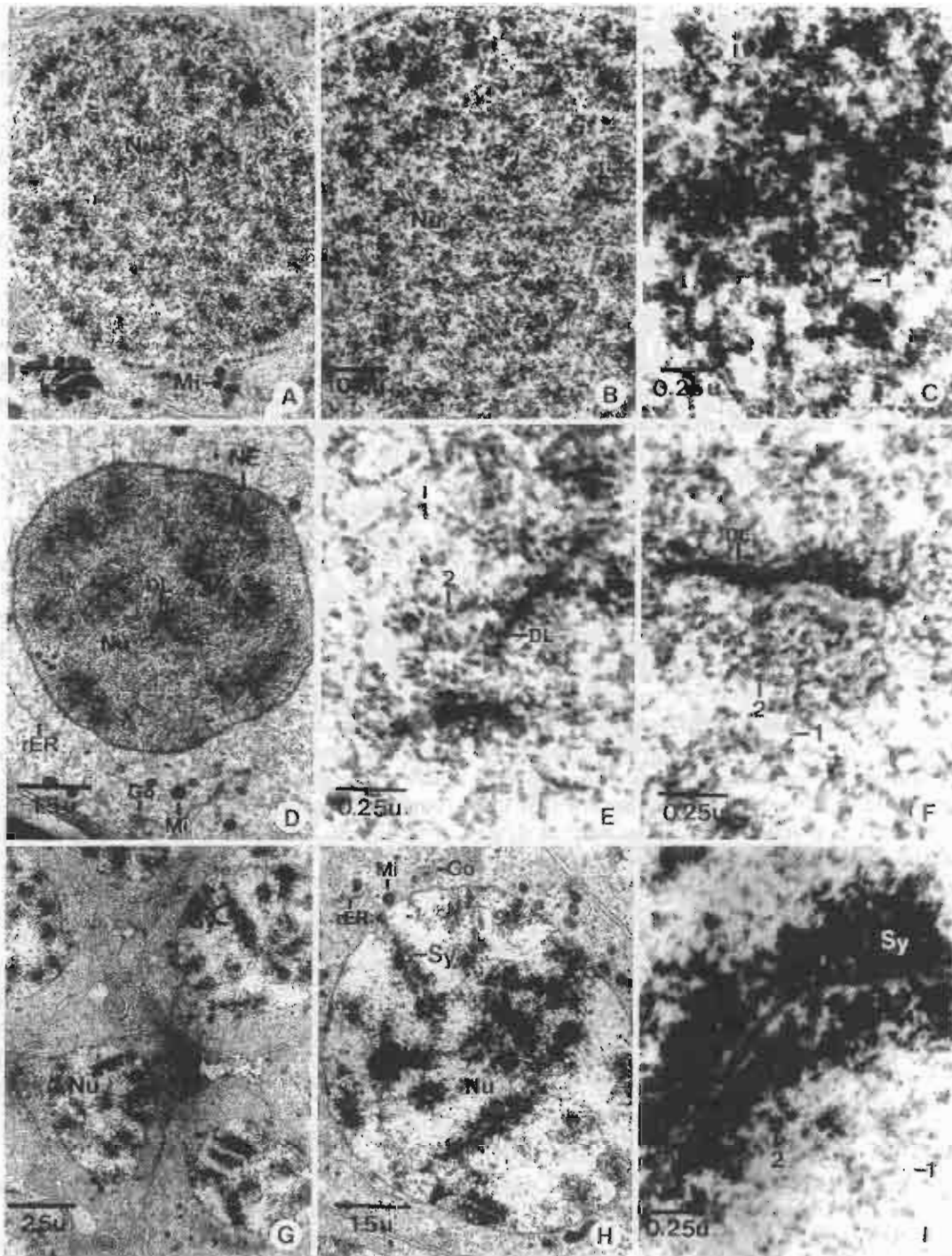
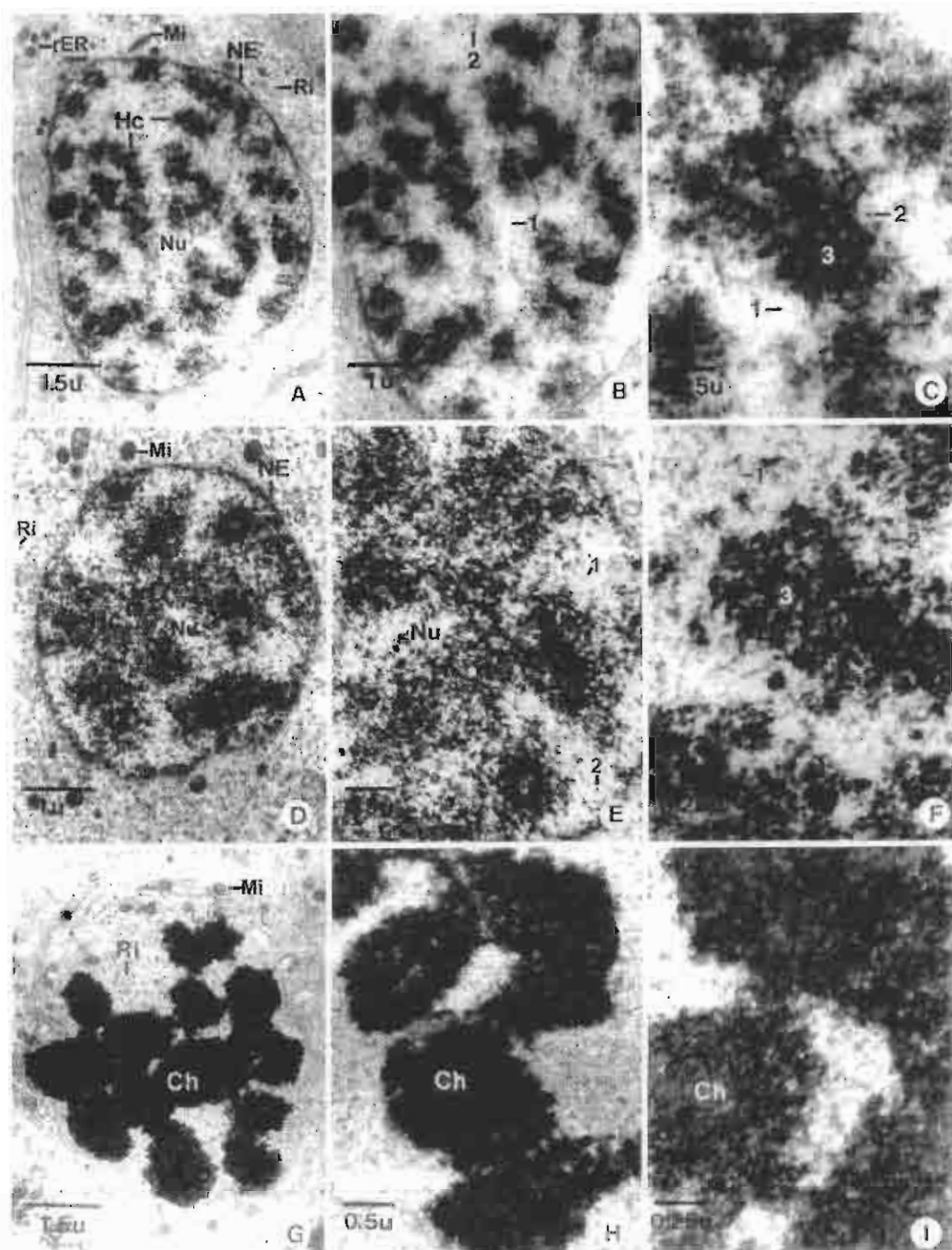


Fig 2.

- A-C Early leptotene spermatocytes (LSc): the nucleus (Nu) has a round shape. It contains 10 nm (1) and 30 nm (2) chromatin fibers. Small blocks of condensed chromatin (arrow) are evenly scattered throughout the nucleus.
- D-F Late leptotene spermatocytes (LSc): the dense line (DL) can be identified as a single long thick line in the nucleus (Nu), where 30 nm (2) chromatin fibers are threaded together and start condensing into a larger heterichromatin block. The cytoplasm contains mitochondria (Mi) and rough endoplasmic reticulum (rER).
- G-I Zygotene spermatocytes (ZSc): in the nucleus (Nu), the synaptonemal complex (Sy) is fully formed and becomes numerous. Chromatin fibers are still organized into 2 levels, i.e., 10 nm (1) and 30 nm (2). The cytoplasm contains mitochondria (Mi), Golgi complex (Go) and rough endoplasmic reticulum (rER). High magnification of the synaptonemal complex is displayed in Fig 1.

**Fig 3.**

- A-C Pachytene spermatocytes (PSc): the nucleus (Nu) exhibits long and thick intertwined heterochromatin blocks or cords (Hc). Chromatin fibers can be identified as 2 levels, and those within the heterochromatin blocks could still be visualized individually as 30 nm fibers (3). The cytoplasm contains mitochondria (Mi), ribosome (Ri) and rough endoplasmic reticulum (rER).
- D-F Diplotene spermatocytes (DSc): the nucleus (Nu) shows long and thick heterochromatin blocks (Hc) aligned along the nuclear envelope (NE) in a cartwheel pattern. Most single chromatin fibers are 30 nm (2) in size while 10 nm fibers (1) are much decreased in quantity. The cytoplasm contains mitochondria (Mi) and ribosomes (Ri).
- G-I Diakinesis-metaphase spermatocytes (DSc-MSc): the nucleus exhibits 30 nm chromatin fibers aggregated together to form long and large chromosomes (Ch) that begin to separate from each other in the diakinesis step (in G), and move to be aligned along the equatorial region in the metaphase step (in H). Only 30 nm fibers are present within the chromosomes, whose outlines could still be visualized (in I). The cytoplasm contains only a few organelles, mainly mitochondria (Mi) and ribosome (Ri).

Secondary spermatocyte (SSc)

The first meiotic division of a primary spermatocyte generates two secondary spermatocytes. It is seldom observed in a histological section, implying that duration of a spermatogenic cell in the secondary spermatocyte step is relatively short. The nucleus of a secondary spermatocyte is round, about 5-6 μm in diameter (Figs 1E, 4A). It contains 4-6 large clumps of heterochromatin blocks along the inner facet of the nuclear envelope, usually with one block in the center (Fig 4A). The 30 nm fibers within the heterochromatin blocks are loosely packed in contrast to those appearing in late spermatocytes (PSc and DSc); and 10 nm fibers become visible again (Figs 4B, 4C). The cytoplasm has similar features to that in the earlier steps, but with an increasing number of vacuoles (Fig 4A).

Classification of Spermiogenic Cells

There are four steps of spermatids, i.e., spermatid I (St1), spermatid II (St2), spermatid III (St3) and spermatid IV (St4), which could be classified on the basis of nuclear sizes and shapes, the patterns of chromatin condensation, and the degree of acrosome formation. The nuclei of successive steps vary from round to oval, and finally to a cylindrical shape, and range in sizes from 3-4 μm in St1 to 2x6 μm in St4.

Spermatid I (St1): These cells are still grouped in cysts that lie close to the lumen (Fig 1G). Each cell is characterized by the presence of a round to oval-shaped nucleus, which is reduced in size to approximately 4-5 μm in diameter (Fig 4D). The nucleus contains loosely coiled 30 nm chromatin fibers that are more evenly spread when compared those in SSc (Figs 4D-4F). The 10 nm fibers appear in the light nucleoplasm between the aggregates of 30 nm fibers (Fig 4F). The cytoplasm is a relatively large mass as the nucleus is reduced in size (Fig 4D). In addition to abundant mitochondria and relatively few ribosomes, the cytoplasm also contains few rough endoplasmic reticulum, a few stacks of flattened vesicles of Golgi complex and small, smooth vesicles closely associated with it (Fig 4D).

Spermatid II (St2): The nucleus of St2 is decreased in size and transforms into an oval shape about 3x4 μm in diameter, as well as becoming eccentrically located within the cell (Figs 1H, 4G). The nucleus contains evenly dispersed 30 nm chromatin fibers, which appear in cross sections as dense granules (Fig 4I). Few small heterochromatin blocks, and 10 nm chromatin fibers are still present (Figs 4H, 4I). In the cytoplasm a large Golgi complex, each consisting of 4-5 stacks of cisternae (Fig 4H), is formed on one side of the nucleus while the opposite side exhibits the development of the flagellum, with an axoneme

outgrowing from the basal body (Fig 4G). Pro-acrosomal vesicles of various sizes are distributed near the Golgi complex. Globular-shaped mitochondria with tubular cristae are widely dispersed throughout the cell (Fig 4G). The acrosome starts to appear as a short thick but flat segment on the nuclear envelope, at the location adjoining the Golgi complex (Fig 4H). The two leaflets of the nuclear envelope lie close together at acrosomal area, whereas they are more widely and irregularly spaced elsewhere. Underneath the nuclear envelope there is an evenly thick, dense, layer of the nuclear lamina (Fig 4I).

Spermatid III (St3): The nucleus of St3 becomes elongated to about 2x4 μm in size (Figs 1H, 5A). It contains 30 nm fibers which are closely packed together and becomes almost uniformly dense (Fig 5A, B), except in pockets of light areas where there appear to be fewer chromatin fibers (Fig 5B). The 10 nm fibers completely disappear (Fig 5C). The acrosome appears as an enlarged thickened plate in close apposition to the nuclear envelope at one pole of the nucleus (Fig 5B). The cytoplasm is relatively clear in comparison with earlier spermatids, and the cytoplasmic organelles become sparse except for the mitochondria, which appear to be concentrated around the tail (Fig 5A). The cytoplasm shows progressive migration to the caudal part of the nucleus and becomes more elongated (Fig 5A). At the caudal end of the nucleus the centrioles, which are surrounded by a striated cylindrical fibrous sheath, start to form the base of the tail axoneme (Fig 5A). The branches of the striated cylindrical fibrous sheath extend laterally from the side of the centrioles (Figs 5A, 5I).

Spermatid IV (St4): Spermatids 4 usually lie close to the lumen of seminiferous tubule, where the heads are usually embedded in the cytoplasm of folliculo-Sertoli cell (Fig 1I). The nucleus is elongated to about 1.5x7 μm in size (Fig 5D, 5E). The chromatin becomes almost completely condensed throughout the nucleus, as 30 nm fibers, become tightly packed; however, the outlines of individual fibers (granules) are still visible (Fig 5F). The cytoplasm is pushed back to the opposite side to where the acrosome is (Figs 5D, 5E). Only the caudal end still possesses a substantial amount of cytoplasm (Fig 5E). The acrosome appears as a flat cap-like structure over the pointed anterior end of the nucleus. Its interior has a homogeneous matrix of medium density (Fig 5D). The striated cylindrical fibrous sheath, which becomes a part of the initial segment of the midpiece, increases in length and is inserted to the caudal end of the nucleus (Fig 5E). The mitochondria start to cluster around the striated cylindrical fibrous sheath of the initial segment (Fig 5E).

Spermatozoa (Sz): The mature spermatozoa are recognized by their highly elongated cylindrical nuclei, with slightly tapered anterior end (Fig 11). Each head is about 9-11 μm in length and 0.5-0.75 μm in width at the mid-section (Fig 5G). The nucleus occupies virtually the entire head region which is surrounded by a smooth plasma membrane. It contains completely opaque chromatin with very few intra-nuclear vacuoles (Fig 5H). The 30 nm chromatin fibers are tightly compact into an electron dense mass, such that the outline of individual 30 nm chromatin fibers could no longer be resolved (Figs 5H, 5I). The anterior portion of the nucleus is smoothly curved and covered by a thin acrosome over a distance of approximately 1-1.5 μm of the anterior region. The inner acrosomal membranes covering the head are closely apposed to the nuclear membrane. The acrosome material appears homogeneous and moderately electron-dense (Fig 5H). A small area of the cytoplasm is present only at the posterior region of the head surrounding the caudal pole of the nucleus and the proximal end of the tail, and slimming down in the midpiece that connects the head and the main part of the tail (Fig 5I). The midpiece contains a pair of centrioles oriented at right angle to each other (Figs 5I, inset), with the distal centriole aligned in continuity with the axoneme of the tail. The centriolar complex as well as the proximal end of the tail's axoneme is surrounded by a striated cylindrical fibrous sheath (Figs 5I, inset). The approximate width of each striated band and the interval between neighboring bands is about 30 nm (Fig 5I). The neck is, therefore, not clearly separated from the midpiece and they together measured approximately 1.7-1.8 μm long from the anterior edge of the proximal centriole to the posterior end of the distal centriole (Fig 5I). The cytoplasm of the midpiece begins to taper at about 1.5-2.5 μm from the base of the nucleus. The mitochondria in the midpiece are non-helical (Figs 5G, inset), and most are arranged longitudinally along the centriolar-axonemal core (Fig 5I). The principal piece of the tail consists of the 9+2 axonemal complex as the core, surrounded by a smooth plasma membrane (Fig 5I). The tail is about 35-40 μm in length; thus the total length of a mature spermatozoon is approximately 40-50 μm (Fig 5G).

DISCUSSION

Classification of Male Germ Cells in the Testis of *Rana tigerina*

The first ultrastructural study of an anuran (*Bufo arenarum*) spermatogenesis was published by Burgos and Fawcett,¹ who reported 8 stages of the male germ cells, but did not make a detailed classification of spermatids. The male germ cells in the testes of *Xenopus*

laevis were classified into 11 stages.¹⁶ By using autoradiographic technique, it was found that the durations of leptotene, zygotene, pachytene, diplotene and metaphase spermatocytes were 4, 6, 12, 1 and 1 days, respectively, and spermiogenesis was completed within 12 days. As for *Rana* species, 11 stages of male germ cells had been identified in *R. esculenta*,¹⁷ which was comparable to *X. laevis*.¹⁶ However, it was noted that the durations of leptotene spermatocyte and spermiogenesis were longer than in *X. laevis*. In the present study of *R. tigerina*, using a more detailed ultrastructural criteria, especially the characteristics of chromatin organization, we could recognize 14 distinct steps of male germ cells. Another interesting finding is that spermatogenesis in *R. tigerina* is occurs within a cyst-like structure, in which germ cells mature in coordinated clusters as in fish.¹⁸ These clusters of germ cells have also been shown in other anuran species and called "spermatocysts".¹ Evidently, individual spermatogonia divide mitotically several times to produce a pool of daughter cells that remain within a common cyst, walled by the processes of follicular cells. Within any particular cyst, successive generations of daughter cells divide synchronously and develop at a similar rate, so that the cyst always contains an increasing cell number in the same step. In *R. temporaria*, spermatogonia undergo eight mitotic divisions, implying that a single spermatogonium could eventually give rise to a cyst containing well over 200 secondary spermatogonia.¹⁸ In *X. laevis* the number of cell divisions within the secondary spermatogonial cysts is reported to vary between four to eight generations.¹⁶ In rats, there are fewer division cycles, and thus a single spermatogonium produces only 24 cells, which subsequently mature into primary spermatocytes.¹⁹ Therefore, the cystic type spermatogenesis could result in mass production of many more gametes than in mammals, and may be an adaptation feature for the external fertilization in fishes and amphibians, where a large quantity of spermatozoa is needed to compensate for the greater difficulty in gamete union.¹⁸

Ultrastructural characteristics of various steps of the male germ cells, as revealed by transmission electron microscopic studies, help to confirm the classification of male germ cells by light microscopy, as well as to understanding of the cellular activities. A primary spermatogonia (Sg1) have a nuclei, constituted mainly of the euchromatin. This results in very clear nucleoplasm and very prominent nuclei. This suggests high transcriptional activity and a high rate of ribosome synthesis. Each cell divides mitotically, giving rise to secondary spermatogonia (Sg2), which are distinguished by the increasing amount of small heterochromatin blocks. These cells, therefore, may

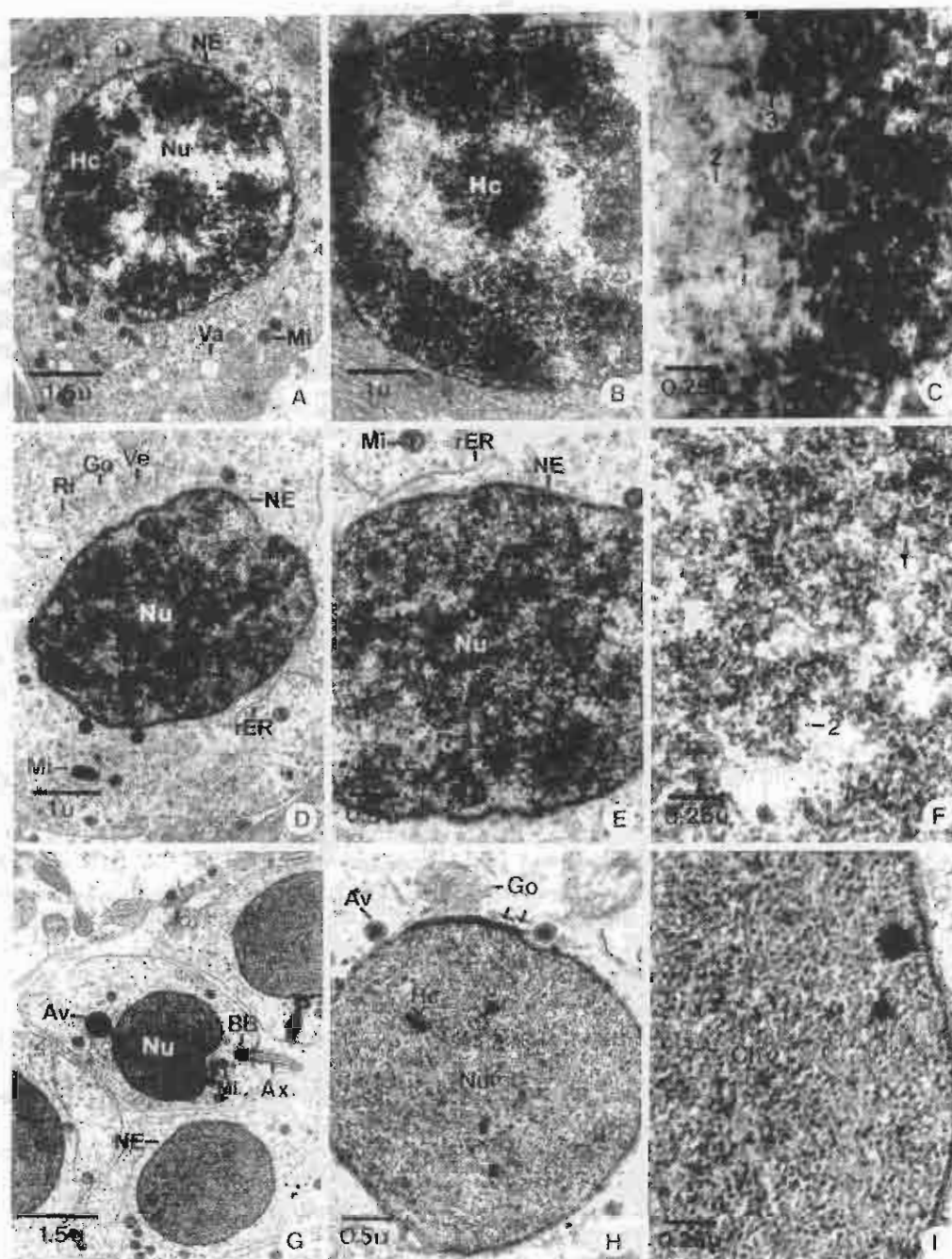


Fig 4.

- A-C: Secondary spermatocyte (SSc): the nucleus (Nu) contains 4-6 blocks of heterochromatin (Hc) that are distributed on the inner facet of the nuclear envelope (NE). Chromatin fibers could be observed at 2 levels, i.e., 10 nm (1) and 30 nm (2). The heterochromatin (3) is formed from loosely bound 30 nm fibers. The cytoplasm contains numerous mitochondria (Mi) and some vacuoles (Va).
- D-F: Spermatid I (S1): the nucleus (Nu) has a round shape, and it contains chromatin appearing as fine granules, which are the cross sections of 30 nm fibers (2), and become loosely packed throughout the nucleus. The cytoplasm contains mitochondria (Mi), relatively few ribosomes (R), rough endoplasmic reticulum (rER) and a few stacks of Golgi complex (Go) with smooth vesicles (Vi) associated with it.
- G-I: Spermatid II (S2): the nucleus (Nu) becomes oval shape, in which 30 nm fibers (2) are loosely but evenly packed together, and dispersed uniformly throughout the nucleus (Nu). The Golgi complex (Go) and acrosomal vesicles (Av) are present in the anterior end of the nucleus and the acrosome appears as a short thickening of the nuclear envelope (arrow), while the developing tail appears as an axoneme (Ax) growing out from the basal body (BB) at the posterior end.